THÈSE

Application of metabolomics for the determination of serum biomarkers aiding the prognosis for septic shock and hepatocellular carcinoma using Mass Spectrometry and ^{1}H NMR spectroscopy based approaches

en vue de l'obtention du grade de

Docteur de l'UNIVERSITE PARIS XIII

Ecole doctorale Galilée

Spécialité : Chimie

Présentée et soutenue publiquement par

Zhicheng LIU

Le 6 février 2017

Directeur de thèse : Pr. Philippe Savarin

Jury

Rapporteurs	Dr. Christophe Junot (CEA, Saclay)
	Pr. Patrick Emond (Université de Tours, Tours)
Examinateurs	Pr. Guowang Xu (DICP, Dalian, Chine)
	Pr. Laurence Le Moyec (Université Evry, Evry)
	Dr. Mohamed Nawfal Triba (Université Paris 13, Bobigny)
	Pr. Philippe Savarin (Université Paris 13, Bobigny)

Acknowledgement

Above all, I would like to express my sincere respects and thanks to my doctorial supervisor, Pr. Philippe Savarin. It was him who brought the possibility of this doctorial work to me and granted me too much help that I will never ever forget. He set an example to me that one should be conscientious and diligent when he is at work and should be kind and patient when he gets along with others. Even though he is the leader of the laboratory, who is always too busy indeed, he is still open to answer my questions, timely and even modestly. I was pretentious before I met Pr. Savarin, however, I realized that I had no reason to be that proud when I witnessed his humility. Thus, for me, Pr. Savarin is not only the tutor who imparts his knowledge but a senior who impacts my personality as well.

I would like to thank Pr. Guowang Xu, the director of our Chinese cooperative laboratory who accepted me in his laboratory and come all the way for my defense. During the one year and a half I passed in Dalian, it was a great honor that I was well accommodated by him with his generosity and geniality. He is a powerful scientific leader who has a keen insight and is always open to discussion. I was very impressed by his expertise and his enthusiasm in work which encourage me to learn from him and to pay more efforts in the following work.

I am really thankful to Dr. Mohamed Triba, Pr. Edith Hantz, Dr. Nadia Bouchemal, Dr. Roland Amathieu, Agnes Victor-Bala and Pr. Marc Lamy La Chapelle in our French laboratory for all of their help and care to me during this thesis work. They are all competent in their own field and have offered me a lot of advises. Moreover, they are so friendly to me that I feel never isolated in a foreign country. Also, I am equally thankful to all the other staffs in the Chinese laboratory, especially to Dr. Peiyuan Yin for all he has done for installing me in Dalian and for his constructive suggestions to my work; to Dr. Yang Liu for teaching me biological knowledge with his patience and amity; and to Yanli Li for all her work.

I need to appreciate to all the fellows in the both laboratories. Especially to Dr. Jieyu Zhao, Dr. Yanni Zhao, Dr. Jia Li, Dr. Junjie Zhang, Dr. Xinyu Liu and Dr. Corentine Goosense for their guidance and advises in the experiences and in the manipulations with the apparatus and software. And to Bohong Wang, Lichao Wang, Zaifang Li, Yongtao Liu, Yang Wang, Jiao Wang, Yang Ouyang, Yanqing Fu, Yuansheng Zhang and Xiangpin Lin for their companion.

I want to thank to Pr. Christophe Junot and Patrick Emond who have accepted to judge this thesis work and to be the reporters. My thanks are equal to Laurence Le Moyec who has accepted to assist in the jury.

I am also thankful to the workers in hospital Jean Verdier where served us all the clinical samples, to Dr. Pierre Nahon and Nathalie Barget for their work.

Finally, I should thank to all my family and my friends who always support and encourage me during my life.

Contents

List of abbreviations

Hepatocellular Carcinoma (HCC)

Nuclear Magnetic Resonance (NMR)
Mass Spectrometry (MS)
Liquid Chromatography-Mass Spectrometry (LC-MS)
Gas Chromatography-Mass Spectrometry (GC-MS)
Capillary Electrophoresis-Mass Spectrometry (CE-MS)
Radio Frequency Ablation (RFA)
Quality Control (QC)
Relative Standard Divergence (RSD)
Principal Component Analysis (PCA)
Partial Least Squares Discriminant Analysis (PLS-DA)
Orthogonal Partial Least Squares Discriminant Analysis (OPLS-DA)
Hierarchical Clustering Analysis (HCA)
Radiofrequency (Rf)
Tetramethylsilane (TMS)
Line-broadening (LB)
Analysis of Variance (ANOVA)
Area Under Receiver Operating Curve (AUROC)
Electron Ionization (EI)
Electrospray Ionization (ESI)
Chemical Ionization (CI)
Atmospheric Pressure Chemical Ionization (APCI)
Fast Atom Bombardment (FAB)
Quadrupole (Q)
Time of Flight (TOF)
Ion Trap (IT)
Fourier Transform-Ion Cyclotron Resonance (FT-ICR)
Systemic Inflammatory Response Syndrome (SIRS)
Multiple Organs Dysfunction Syndrome (MODS)
lipopolysaccharide (LPS)
Cecal Ligation and Puncture (CLP)
C-Reactive Protein (CRP)
Bronchoalvelar Lavage (BAL)
Non-alcoholic Fatty Liver Disease (NAFLD)
Magnetic Resonance Imaging (MRI)
Computed Tomography (CT)
Barcelona Clinical Liver Cancer (BCLC)
Percutaneous Injection (PI)

List of figures

List of tables

General Introduction

Metabolomics, which is also noted as “metabonomics”, is the systematic study involving small biological molecular named “metabolites” [1-3]. It characterizes the variations at the level of metabolites in living organism triggered by the endogenous or exogenous stimulations. Metabolomics plays an important role in the systematic biology, which is also known as “omics”, including genomics, transcriptomics and proteomics [4]. Compared with the other “omics”, which investigate the innate properties and modification in the organism, metabolomics is the terminal of systemic biology that presents the definitive characteristics and even the responses to the environment distinct in the life. Genomics determines the genome of the living bodies. Transcriptomics and proteomics analyses the transcriptome and proteome respectively. These upstream omics tell “what may happen” to the organism, but metabolomics shows “what has happened” to the organism (Figure 1).

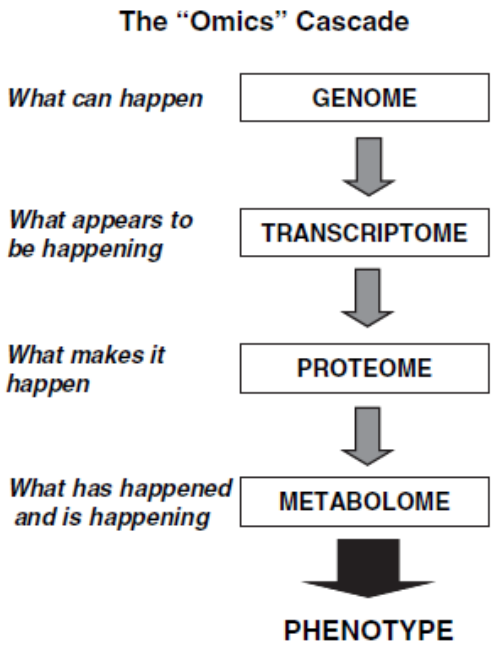

Figure 1. The ‘‘Omics’’ cascade comprises complex datasets that as an entity comprehensively describe the response of biological systems to disease, genetic, and environmental perturbations. The most

powerful database will integrate data from all omics levels. However, of these databases the metabolome is the most predictive of phenotype [5].

Until present, metabolomics has been widely applied in the studies of clinical medicine [6-8], intestinal flora analysis [9], environment [10], botany [11], drug development [12], nutrition [13], food science [14, 15].

In the latest years, diagnosis and treatment measurements are revolved by the presence of the mention “Precision Medicine”[16] which emphasizes the individual clinical care [16]. As metabolomics allows to investigate the whole metabolic profile of biological systems, it provides evidence for the understanding of individual cases. Consequently, in the clinical field, currently, metabolomic is widely applied to improve the diagnosis and prognosis. Metabolomics is sensitive to figure out the metabolic variation, which is correlated to certain lesions in the patients. Detection of significant variations in some specific metabolites leads to the discovery of relevant lesions or diseases. The metabolite indicators are named as the “biomarkers” of diagnosis [17]. As a consequence, seeking for the new reliable biomarkers, which improves the diagnosis of disease, has been one of the main purposes of the application of metabolomics in clinical medicine.

The other primary goal of the application of metabolomics in the field is to predict the outcome of disease. According to the comparison of the metabolic profile in the patients, some metabolites are likely to be sensitive and specific in the discrimination between the patients with and without optimist prognosis. These metabolites are therefore the biomarkers of prognosis that help to understand the severity of disease in each individual, even at the onset of the disease, so that the personalized treatment will be subsequently executed.

However, the individual differences and different reactions and compliances to the therapy among the patients make it still challenging to determine new biomarkers [18]. To this end, mounting studies aim to seek out the reliable biomarkers for clinical diagnosis or prognosis. In this study, we focused on the application of metabolomics to seek out the biomarkers predicting the outcome for septic shock and for hepatocellular carcinoma (HCC).

Metabolomics is usually realized based on two principal analytical methods: nuclear magnetic resonance (NMR) spectroscopy and mass spectrometry (MS) [19]. With NMR spectroscopy, the sample preparation is easier than MS method and the method does no damage to the sample, and it shows a quite good reproducibility. However, its low sensitivity and the narrow measuring concentration range are the disadvantages. MS, which is usually coupled by chromatography or by capillary electrophoresis, shows its excellent sensitivity and its wide dynamic range and a larger metabolome coverage. Actually, the complementarity of the two techniques in metabolomic study has been well revealed [20]. Consequently, one of the objectives of this study is to accomplish the metabolomic studies using both ^{1}H NMR spectroscopy and mass spectrometry.

The project was carried out by the collaboration between the team of "NMR metabolomic" from the Chimie, Structure, Propriétés de Biomatériaux et d'Agents Thérapeutiques (CSPBAT) laboratory of University Paris XIII (Bobigny, France) and the Key Laboratory of Separation Science for Analytical Chemistry from Dalian institute of chemistry physics (DICP, Dalian, China). NMR spectroscopy and MS based metabolomic studies are respectively finalized in the two laboratories. The thesis work was also in close collaboration with Jean Verdier University Hospital (Bondy, Paris, France).

This thesis is composed by four parts: general introduction, methodology, experimental research and conclusions with perspectives. The methodology part is principally divided into two sections: ^{1}H NMR-based metabolomics and MS-based metabolomics.

For the part of experimental research, the first study aims to understand the differences in the metabolic profile of serum between the surviving and non-surviving patients in the early stage of septic shock by liquid chromatography-mass spectrometry (LC-MS) based metabolomics. A non-targeted scan of the metabolic profile for the septic shock patients was applied using LC-MS. According to the

differences at the level of the metabolic profile, septic survivors were distinguished from the septic non-survivors before clinical interventions.

The second study about the determination of biomarkers predicting the mortality for the patients who suffered from septic shock by using ^{1}H NMR spectroscopy. Discriminatory models were revealed to exhibit the differences of serum metabolome between the evolutions of septic shock survivors and non-survivors during the first 12 hours.

The last part of the study presents a work of discovery of serum biomarkers predicting the recurrence for HCC patients before and after radio frequency ablation (RFA) therapy. By comparing the metabolic profile of recurrent HCC patients with those without relapse, we attempted to find out the key metabolites indicating the HCC recurrence before and after the RFA treatment. The study was achieved by gas chromatography-mass spectrometry (GC-MS) based metabolomics.

I. Methodology

Chapter I. Methodology of general metabolomics

1.1.1 Definition

Metabolomics, was first defined by Prof. Nicholson as “the quantitative measurement of the dynamic multiparametric metabolic response of living systems to pathophysiological stimuli genetic modification” [21]. The other definition from the point of view of metabolites (small biological molecules ≤1500 Da) is the study aiming to systematically qualify and quantify metabolites in one biological system (e.g. biological fluid, cells, tissues, etc.) at one point of time [22].

Metabolomics is an important part of “omics” which is a general name for the studies determining and quantifying pools of biological molecules that translate into structures, functions, and dynamics in organisms. It consists of studies such as genomics, transcriptomics, proteomics, metabolomics, etc. Unlike other above mentioned “omics”, metabolomics investigates the small molecules which are the terminal metabolites indicating not only the inner modification in organisms but also the impact issued from the alteration of environment [23].

1.1.2 Development of metabolomics

The definition of “metabolomics” was first introduced for biomedical research in the year of 90s. Until now, it has been applied in kinds of fields [6-15]. It has been well developed in the recent years by increasing studies. Figure 2 shows the evolution of the number of submitted articles of metabolomics in the past decade, which reveals an increasing amount of metabolomic studies. Accordingly, a cascade of researches in this field has been being ongoing, especially in the 21th century. The present study focuses on the application of metabolomic seeking the biomarkers for clinical

diagnosis and prognosis..

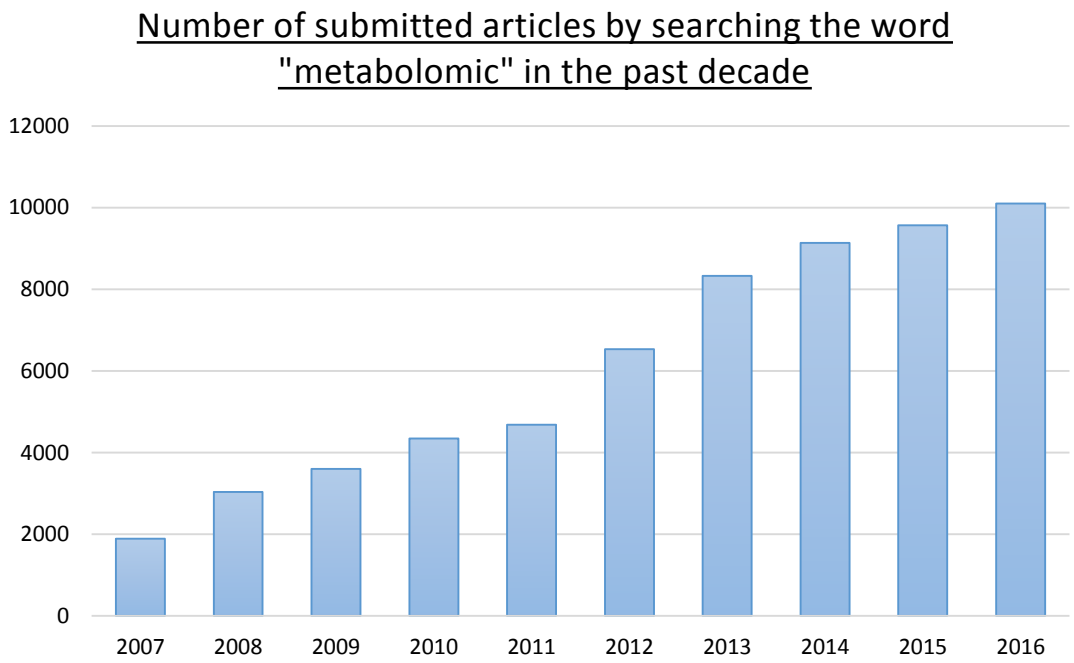

Figure 2. Diagram presenting the number of papers, which include the word “metabolomic” along the past decade according to the statistics by google scholar (https://scholar.google.com/)

1.1.3 Metabolomic experimental Steps

The protocol guiding the experiences of metabolomics has been summarized by former studies [19, 24, 25]. Generally, the main manipulative steps include experimental design, sampling and stockage, preparation of samples, data acquisition, data analyses, result validation, and interpretation of results (Figure 3).

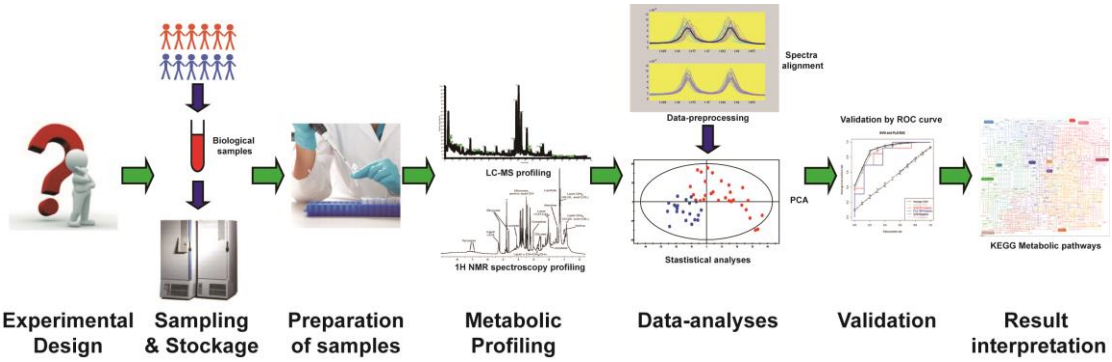

Figure 3. Schematic flow-chart emerging the general process of the metabolomic study.

Experimental design

For metabolomic, the experimental design involves, for example, the selection of sampling time, the selection of spectroscopy experimental method, the method of sample preparation, the choice of statistic process. In a word, the experimental design should coincide with the needs of the solution of the scientific problem [26, 27].

Sampling and storage

It is always required that the sample collection should be representative of population and homogenous [28]. The corresponding measures are to limit the variations among the samples and to collect the samples randomly in the population. That is, biological samples should be collected simultaneously in the same way for the people with similar ages, a proper proportion of gender, similar healthy conditions, etc.

Generally, for bio-samples, solid (tissue, organ, cells, etc.) and liquid samples (serum, plasma, urine, CSF, saliva, etc.) are collected for metabolic analyses.

Serum samples are obtained after removing the spontaneous clot in collected blood. Whereas, plasma samples are prepared by adding an anticoagulant (e.g. EDTA, citrate, lithium heparin, etc.) in the blood and then centrifuging to eliminate the hemocytes and platelets. Compared with the blood sampling, samplings of urine is simpler that no particular treatment is otherwise needed other than rapid package and good storage [25].

To avoid the variation of metabolic profile in the air, the sampling is recommended to be executed rapidly and then the samples should be stored at -80^{o}C before analyses in

order to achieve a metabolism quenching [29-31].

The processes from sample preparation to the biological interpretation will be exposed in the following two chapters.

Chapter II. ^{1}H NMR spectroscopy-based metabolomics

1.2.1. Principle of NMR spectroscopy

A. Theory of Lamor frequency

Nuclear Magnetic Resonance (NMR) is a physical phenomenon in which atomic nuclei, in a magnetic field, absorb and then emit an electromagnetic radiation [32].

When an atomic nucleus possessing unpaired protons and neutrons (such as ^{1}H, ^{13}C, ^{15}N, ^{31}P) is located in an external magnetic B_0, the proton spins with an angular speed and a frequency, v_0, called the Larmor frequency, unique for each isotope [33]. The Larmor frequency is related to the external magnetic field B_0 through the gyromagnetic constant γ.

$$\nu_0 = \gamma B_0 \qquad (1.2.1)$$

The intrinsic magnetic moment of nucleons are also called « spins ». They are oriented parallel (α) or antiparallel (β) to the direction of the magnetic field B_0 (Figure 4a, 4c).

In fact, when an atomic nucleus is submitted to an external magnetic field, the lowest energy is split into two levels of energy: the higher energy, which corresponds to the anti-parallel orientation and the lower energy, which corresponds to the parallel orientation of the magnetic moment (Figure 4b). The energetic difference ΔE is given by:

$$\Delta E = \gamma h B_0 \qquad (1.2.2)$$

where h is the Planck constant. If N is the number of particles in each energy level:

$$\frac{N\alpha}{N_\beta} = \exp\left(\frac{-\Delta E}{kT}\right) = \exp\left(\frac{-\gamma h B_0}{kT}\right) \qquad (1.2.3)$$

where $N_\alpha > N_\beta$ (Boltzmann distribution [34]) and k is the Boltzmann constant. It should be noticed that the difference of energy (ΔE) is fairly small and so is the difference between N_α and N_β.

If the proton is submitted to another alternative magnetic field B_1, a part of the

protons with the lower energy E_α are stimulated and leads to a transition to the level E_β. As the field B_1 is shut down, the excited protons tend to return to the ground state and result in an emission and this emission will be recorded by the receptor and amplified by the amplifier of spectrometer. As to the magnetic moment of the protons, before the excitation with B_1 (may be along x or y axis of figure 4d), the direction of resultant magnetic moment for the protons with lower energy (α) is parallel to B_0 while the resultant magnetic moment for the protons with higher energy (β) is opposite. Given that the number of the protons in the ground state is larger than those in the excited energetic level, the resultant magnetic moment $\mathbf{M}_{resultant}$ is parallel to B_0 (Figure 4c). The direction of **M** is changed by the presence of B_1 and when B_1 is shut down, **M** will relax to the equilibrium state (Figure 4d).

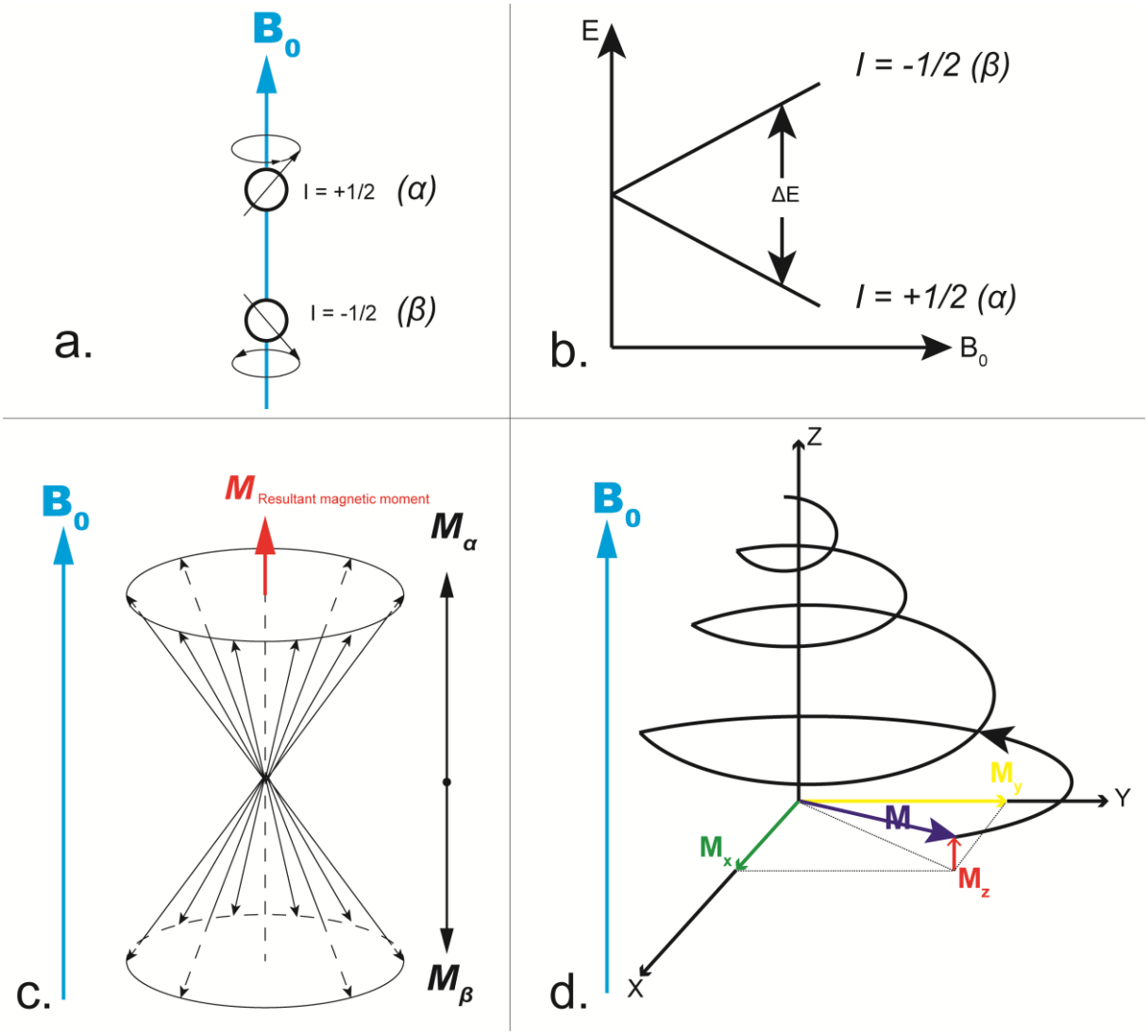

Figure 4. Diagram presenting the principles of spin for the nuclei located in a magnetic field B_0. a: when located in the magnetic field B_0, two types of nucleolus spins are available: spin parallel to the direction of B_0 (I = +1/2, I is the spin characteristics) or spin antiparallel to B_0 (I = -1/2). b: Energy splitting in the presence of an external magnetic field. c: Resultant magnetic moments for all the spins in the B_0 field d : Once nucleus spins receives a radio frequency B1 during a short period, for the excited protons, the direction of their magnetic moment **M** will be firstly changed then comes back to the equilibrium state.

B. Chemical shift and coupling

Due to the current elicited by the electron cloud, the real strength of the external field changes. Formula 1.2.4 exposes the relation between the external field strength (B_0) and the effective field strength (B_{eff}) for the nuclei, where σ is the screening constant.

$$B_{eff} = B_0(1-\sigma) \tag{1.2.4}$$

We introduce the chemical shift δ and generally the chemical shift of tetramethylsilane (TMS) is used as reference for ^{1}H RMN experiences. For one standard substance, its chemical shift is calculated by the equation 1.2.5:

$$\delta = \frac{\nu_{sub} - \nu_{ref}}{\nu_0} \times 10^6 \tag{1.2.5}$$

where ν_{sub} is the frequency of the substance being measured; ν_{ref} is the exact frequency of the TMS, and ν_0 depends on the field strength B_0. As the value of the ratio is small, δ is described by multiplying 10^6.Therefore, δ is presented in ppm.

Spin-spin coupling

It is difficult to identify a substance or even a chemical group only with the help of the chemical shift. This is because the electron cloud of the chemical groups are influenced by its chemical spatial environment, and the interaction among the groups not only alters the original chemical shift of substance but also remolds its multiplicity of the surrounding electron cloud.

The effect is dependent on the interaction between the spins, which are located in the magnetic field.

Always for the example of ^{1}H NMR spectroscopy, a molecular model with 2 adjacent groups of protons H_A and H_B is shown in the Figure 6. The chemical shift of H_A is altered by the interaction between H_A and H_B. And as there exists two directions of spin of HB (Spin = +/- 1/2), two peaks are visible, representing the interaction between H_B and H_A. This effect is called spin-spin coupling. Accordingly, the presence of the number of peaks, which is also called the multiplicity, is due to the combination of the two spin types of the interacted proton. For one group of proton, the multiplicity of peak can be deduced by the triangle of Pascal (taken the example of the two groups of protons H_A and H_B, shown Figure 7). The intensity of each peak corresponds to the possible combinations. It should be noted that the spin-spin coupling is generally detectable within the three bonds distance, however, in molecules such as alkenes and molecules with aromatic cycles, the interaction may be observed within a distance of 5 bonds.

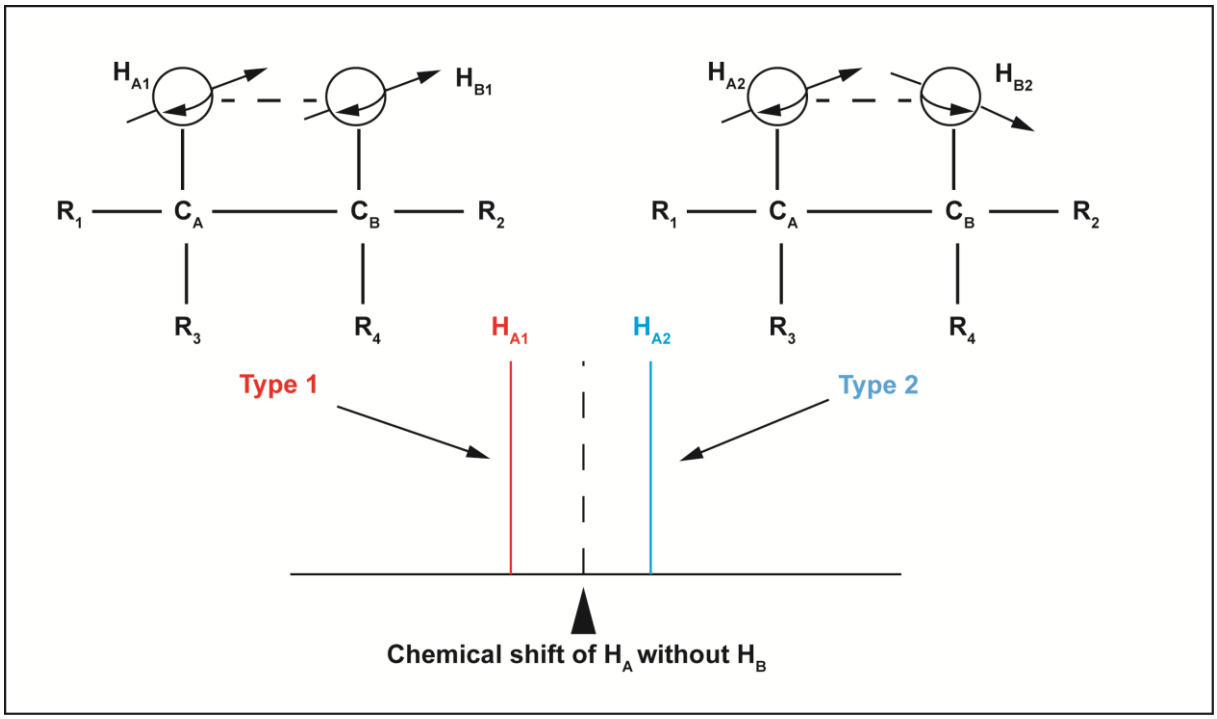

Figure 6. Schematic presentation of the effect of spin-spin coupling. 2 protons labelled H_A and H_B are located on two adjacent carbons C_A and C_B. There are 2 possibilities for H_A spins (parallel H_{A1} or anti-parallel H_{A2}) relative to H_B. The effect leads to a chemical shift between the two kinds of spins H_{A1} and

H_{A2}.

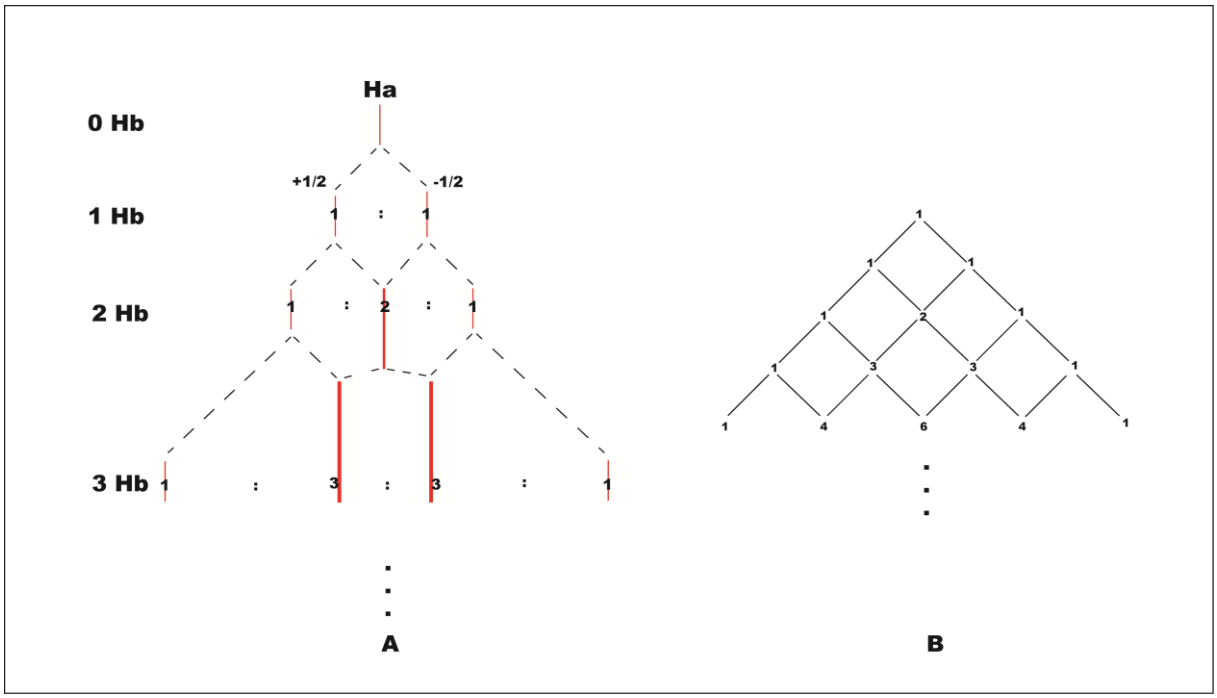

Figure 7. Diagram presenting the combinations of spins. Peaks are presented by the bars in the diagram. The intensity of each peak is presented by the height and thickness of the bar. The ratio of intensity among the peaks is marked on the bars. (A) The law of the combination corresponds to the triangle of Pascal (B).

C. General NMR data pre-processing

1) Appodization

Once the acquisition of spectrum is done during the Free induction Decay (FID) [35], the spectrum is beforehand subjected to be multiplied by the factor $e^{-t\pi}$, named line-broadening (LB, in Hz), which is also called appodization, prior to the transformation of Fourier. One goal is to enhance the ratio signal/noise in the spectrum. The other objective is to narrow the peak stretches.

2) Fourier Transform (FT)

The FT is the central step in NMR data processing, which transforms the time domain signal into a frequency domain signal. After the treatment of FT, acquired signals are converted into bell-shaped peaks whose airs represent the quantification of corresponding compounds.

1.2.2 Description of NMR spectrometer

The main parts of the NMR spectrometry include sample changer, superconducting magnet, probe (containing transmitter and signal receptor), amplifier and signal processing monitor [36], the schematic diagram is presented in Figure 5.

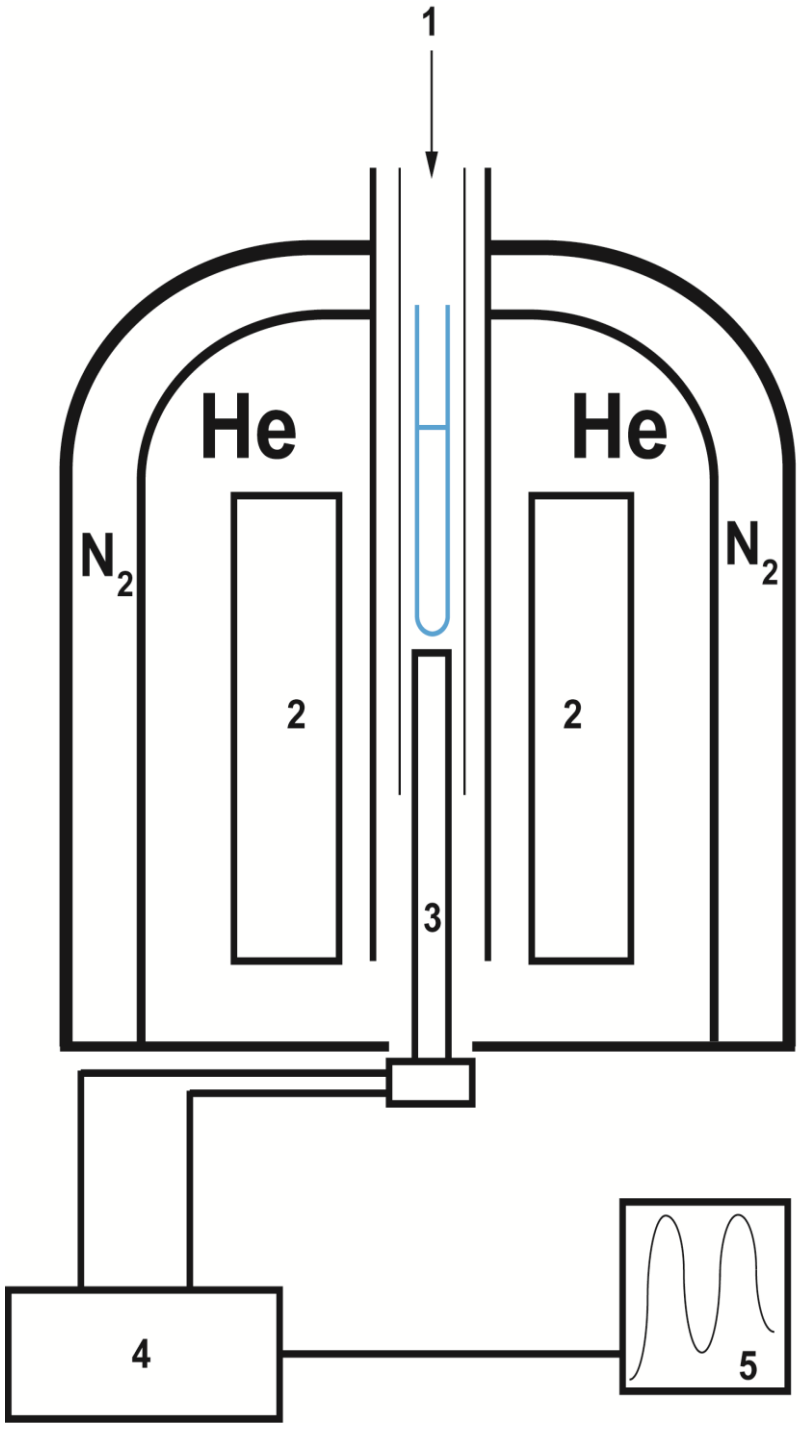

Figure 5. Schematic diagram of the main components of the NMR spectrometer. 1: injection port; 2: superconducting magnet; 3: probe; 4: amplifier; 5: monitor.

1/ Sample changer

It is the entrance of the sample which allows to perform a series of experiments automatically according to an edited experimental sequence. Concerning the

metabolomic studies, typically, the biological sample is prone to evolve due to the enzymatic reactions. Aiming at this problem, the sample changer used for sequential metabolic studies is thermostated at low temperature (4°C).

2/Superconducting magnet

It is produced by the induction coil. The coil is immersed in the liquid helium with its temperature at 4K to preserve the superconductivity. Meanwhile, liquid nitrogen is filled at the outer layer of the liquid helium. It helps to isolate the environment of the superconductor.

3/Probe

It is the core component of the instrument, in terms of exciting the nuclear spins, and detecting the NMR signal. The sample is inserted into the probe to perform the NMR experiment. The probe contains the radiofrequency (Rf) coils, tuned at specific frequencies for specific nuclei in a given magnetic field. The probe also contains the necessary hardware to control the sample temperature.

4 and 5/Signal amplifier and monitor

The received signals are accumulated by the amplifier and Fourier transform is subsequently performed.

1.2.3. Experimental steps of NMR-based metabolomics

A. Sample preparation

In the part of NMR-based metabolomic of this thesis work, serum samples were analyzed with a 500MHz NMR spectrometry (Bruker, Avance III). The samples were prepared before the acquisition of spectrum. As the samples were kept in the freezer at -80^{o}C before the experiences, they were first thawed on the ice. Afterwards, 450 µL of each sera sample was added in the NMR tube. 50 µL of D_2O was also added into the tube.

B. Water suppression using pre-saturation pulses during data acquisition

As metabolomics analyzes samples from bio-systems, which usually contain a considerable quantity of water. The signal of H_20 are aimed to be removed during the acquisition for its high intensity and large peak masking other signals with low concentrations which are close to it. A low power pulse at the solvent frequency and is applied during the preparation delay. This low power pulse excites the water proton signal such that no signal can fully accumulate and be measured. Indeed, the method cannot remove completely the signal of water, as the peak of water remains large in our experiences, specifically, further suppression of the region of chemical shift for the peak of water will be introduced in the part “correction of baseline and region suppression”.

C. Phasing

To have the peaks of the spectrum as more symmetric as possible, the phasing process after the transform is always necessary. The available software in our laboratory for the correction of phase include NMR pipe (https://www.ibbr.umd.edu/nmrpipe/), Topspin (Bruker, Germany) and Chenomix (Chenomix, Canada). We denote both the factors by “phase 0” and “phase 1” respectively. Generally, in our works, the phase for all the spectra was corrected only by the phase 0. The uniform criterion was to balance the two extremes of the spectrum superior or equal to 0.

D. Correction of baseline and region suppression

The appropriate definition of baseline for the NMR spectrum is basic for the following analyses. This is because the ultimate assignment and quantification are all dependent. Especially, in metabolomic studies, the assignment for the peaks representing metabolites with low concentration but significant is definitely due to the establishment of baseline. For the qualification of each peak, their intensity should be integrated from the baseline to the top of the peak. In the current study, the regions of chemical shift (ppm) such as (-1, 0) and (8.5, 10) were suppressed since there were

no signals in the regions. The region (4.8, 5.2) has also been removed because of the present of the peak H_20. And the region (3.7 4) was otherwise rejected in the study of septic shock because the presence of large peaks in the region corresponds to the arterial perfusion by starch, in the emergency rescue, which are not belonging to the metabolome of patients.

C. Calibration and alignment

The variation of magnetic field, pH, salt concentration, temperature or other instrument-related variables need to be considered [37]. The calibration is the first general step of the alignment Introduced standard substance such as trimethylsiylpropionic acid (TSP) or dimethylsilalpentanesulfonic acid (DSS) for being the referred peak. Nevertheless, these organic compounds have a good affinity to some serum proteins (e.g. Albumin) [38]. Consequently, the doublet of lactate (1.32^{d}), the doublet of α-glucose (5.23^{d}) and the singlet of formate (8.5^{s}) in the spectra can be used as the reference to calibrate the spectra.

Further, once the spectrum is calibrated at the chemical shift of the referred peak, discrepancy of the signals of others peaks may still exist among the multiple acquisitions. Hence, other peaks are aligned by referring to the average or by the median of all the spectra.

D. Peak assignment

With a certain condition of pH and experimental temperature, most peaks in the NMR spectra are identifiable by referring their chemical shift and multiplicity. Moreover, ^{1}H NMR 2D experiments, assignment results from other previous studies and established database (e.g. human metabolome database, HMDB, http://www.hmdb.ca) are helpful for the identification of the substance. In our study, the software Chenomx (Chenomx Inc., Alberta, Canada) was also applied for the assignment. One of the spectrum recorded with the serum samples of one septic shock patient is taken as an example (shown figure 8), table 1 shows the assignment obtained by the Chenomx software.

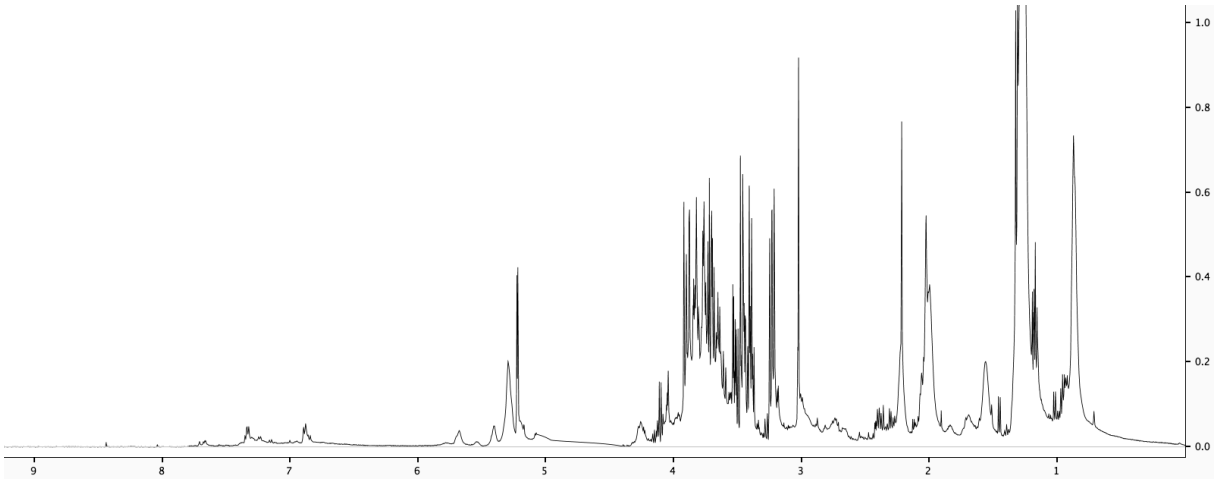

Figure 8. One of the ^{1}H NMR spectrum recorded with the serum samples of patients suffering from septic shock. (NMR Spectrometer: Bruker Avance III 500MHz)

0.85^{m} 1.5^{m}	VLDL, LDL, lipids
0.82^{d} 0.95^{d}	2-Hydroxyisovalerate
0.89^{t} 1.64^{m} 1.73^{m}	2-HB
0.93^{t} 0.99^{d}	Isoleucine
0.95^{dd} 1.70^{m}	Leucine
0.97^{d} 1.03^{d}	Valine
1.06^{d}	3-Hydroxyisobutyrate
1.19^{d} 4.15^{m}	3-HB
1.30^{s}	3-Hydroxy-3-methylglutarate
1.13^{d}	Isobutryrate
1.16^{d}	Isopropanol
1.22^{d}	Methylmalonate
1.32^{d} 4.11^{q}	Lactate
1.40^{m}	Glycocholate
1.46^{d}	Alanine
1.875^{m} 1.70^{m}	Lysine

1.91^{s}	Acetate
1.98^{m} 3.32^{m}	Proline
1.99^{s}	Acetamide
2.02^{s}	Glycoproteine
2.12^{m} 2.32^{m}	Glutamate
2.09^{m} 2.41^{m}	Glutamine
2.2^{s}	Acetoacetate
2.36^{s}	Pyruvate
2.39^{s}	Succinate
2.52^{d} 2.68^{d}	Citrate
2.71^{s}	Dimethylamine
2.89^{s}	Trimethylaimine
2.90^{s}	N,N-dimethylglycine
3.05t	Proline
3.25^{s}	Creatine
3.03^{s} 3.92^{s}	Creatinine
3.14^{s} 4.04^{s}	Dimethysulfone
?3.18^{s}	Acetyl-carnitine/Choline
?3.19^{s} 4.11^{ddd}	Choline
3.23^{t} 3.72^{m} 3.82^{m} 4.64^{d} 5.23^{d}	Glucose
3.25^{s}	TMAO/Betaine
3.27^{t}	Glucose-6-phosphate
3.34^{s}	Caffeine
3.55s	Glycine
3.65^{dd} 3.55^{dd}	Glycerol
4.05^{t}	Myo-insitol
5.175^{d}	Mannose
5.79^{s}	Urea
6.52s	Fumarate

6.88^{d} 7.18^{d}	Tyrosine
7.32^{d} 7.36^{d}	Phenylalanine
7.77^{d}	Tyrosine
7.67^{s} 7.02^{s}	1-MH
7.70^{s}	dTTP
8.5^{s}	Formate

Table 1. Assignment of the example spectra recorded with one septic shock patient sample, using Chenomx software. s: singlet; d: double; dd: doublet of doublet; t: triplet; q: quartet; m: multiplet.

E. Spectra bucketing

The spectra bucketing corresponds to the definition of variables. The spectrum is actually divided by each 0.001ppm chemical shift. For an acquisition from -1 to 11ppm, 11000 intervals called “buckets” are consequently obtained. The bucket is composed by the value of its chemical shift and the corresponding recorded intensity. For the spectra pre-treated by the above processes, all their buckets are gathered and a dataset is thereby created. The integrated dataset is afterward defined as the matrix X for the analytical software where its lines representing for each recording of spectrum and its column representing for each bucket.

Other experimental steps in NMR-based metabolomics such as data pre-treatment, statistical analyses, result validation and biological interpretations will be concretely discussed in chapter IV.

Chapter III Mass spectrometry based metabolomics

1.3.1 Principle of mass spectrometer

The mass spectrometry (MS) is an instrument which serves to test the molecular mass and the structure of substance. The identification of the compounds is achieved by analyzing the ion fragments ionized from the substance.

After the ionization, the ion fragments are volatilized to gas phase and then separated in the light of the ratio of mass to charge (M/Z) [39].

Basically, a mass spectrometer possesses an ion source to produce gas phase ions, one or several mass analyzers to separate the ions according to their mass, a detector to count the ions, and a monitor with its accessories [40]. Figure 13 has schematically presented the main elements of the mass spectrometer.

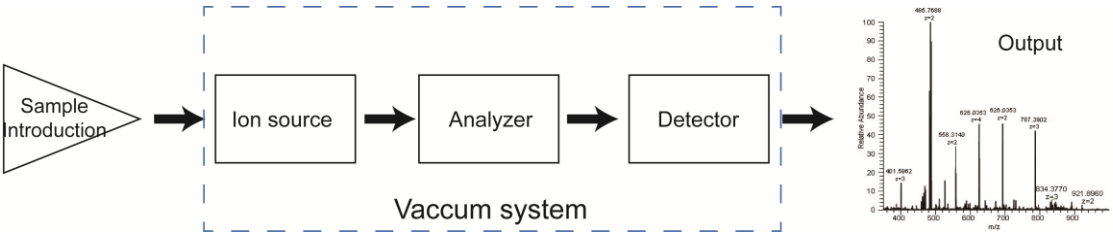

Figure 13. Schematic diagram presenting the main components of the mass spectrometer. The vacuum for the ion source, analyzer and detector is maintained by the pumps. The output of the spectrum is presented on the connected computer.

Ionization and fragmentation

There are various methods of ionization, which can be roughly divided into two types: hard ionization and soft ionization.

In the part of the research of HCC recurrence, an electron ionization (EI) was applied. EI is a hard ionization which uses the energetic electrons to impact directly the

molecule. The principle of the formation of molecular ion in the EI is expressed by the following equation:

$$M + e^- \rightarrow M^+ + 2e^- \quad (1.3.1)$$

where M is the ionized molecule to be ionized and M+ is the molecular ion after the electronic reaction.

After the impact, energy belonging to e^- is transmitted to the molecular ion M+, results in further fragmentations. The secondary fragmentations may be ionic or neutral. In the part of metabolomic study on HCC recurrence research, as well as many other past metabolomic studies using the tandem of gas chromatography and mass spectrometry, the EI source is applied.

An electrospray ionization (ESI) was employed to combine to ultra-performance liquid chromatography for studying the septic shock mortality.

Compared with the hard ionization method, the ESI source is classified as a soft-ionization since less energy is sent up to the molecule, and the molecule is then disrupted into positively charged molecular ion and electron in the ion source. The molecular ion is then further fragmented.

As to its application in the combination of LC-MS, the liquid of sample (whose pH is usually adjusted) is smashed into micro droplets (1-2µm) by a high voltage. The molecule wrapped in the droplets is then ionized by the effect of Coulomb explosion, which is issued from the evaporation by the pneumatic nebulization and the inhomogeneous distribution of charges between inside and outside of the droplets. The ions are detected in the form of cations such as $[M+H]^+$, $[M+Na]^+$ and $[M+nH]^+$ in the positive mode and detected as $[M-H]^-$ in the negative mode.

Other rifely used ion sources which are connected to the MS include chemical ionization (CI) [41], fast atom bombardment (FAB) [42], atmosphere pressure chemical ionization (APCI) [43] and matrix assisted laser desorption ionization (MALDI) [44].

Analyzer

The analyzer may serve for collision, selection and analysis of the ions. After the injection of the ions from the ion source, the ions are subjected to the analyzer and

their kinetic energy is provided by the force of electric and magnetic field forces. The ions are separated by their different radius of rotation based on its m/z. There are various types of MS analyzer such quadrupole (Q) [45], time of flight (TOF) [46], ion trap (IT) [47], orbitrap [48], and Fourier transform ion cyclotron resonance (FT-ICR) [49]. In this thesis work, the tandem of analyzers linear trap quadrupoles-orbitrap (LTQ-orbitrap) and quadrupole were applied for the analyses in LC-MS and GC-MS respectively.

- Quadrupole (Q)

As shown in Figure 14 below, the quadrupole analyzer is composed by the four electrodes in which there are two connected pairs of rods. All the rods are connected with one direct current (DC) source and an alternative current source which is generated by a radiofrequency. At one certain time point, between one pair of rods there is an electric field with a voltage ($=V_{DC}+V_{RF}\cos(\omega t)$) and between the other pair the field intensity is meanwhile adverse ($=-V_{DC}-V_{RF}\cos(\omega t)$). With an EI source which is widely used in the GC-MS, only positive ions are injected into the quadrupole. The ion is therefore attracted by the rod with negative field and repelled by the positive one. Due to the alternative filed intensity, the ion will go through the analyzer with an oscillation. The ion selection and separation depend on its ratio m/z. With the presence of the introduced DC, non-selected ions will hit the rod (shown in the figure by the “unstable trajectory”) and those ions within the range of detection are allowed to pass through the analyzer. The amplitude of the oscillation corresponds to the ratio m/z, too. This is because the ions with smaller m/z will be accelerated faster than big ones, and therefore lead to a larger amplitude which is perpendicular to the central axis of the quadrupole. Thus, ions with smaller m/z spend longer time than ones with bigger m/z on passing the analyzer, which is the feature of the ion separation.

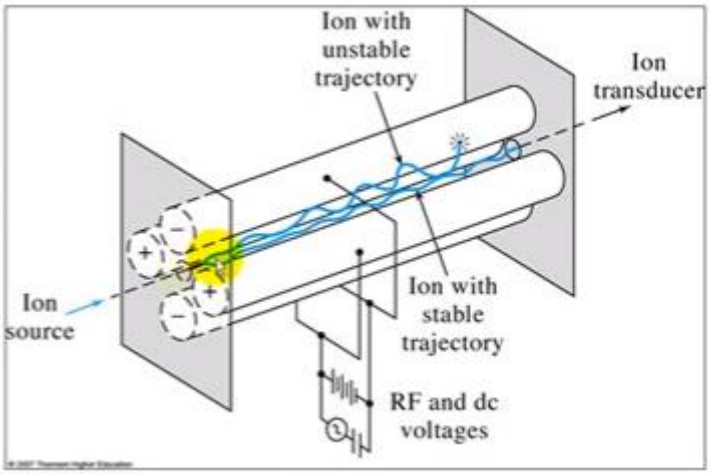

Figure 14. Schematic diagram exhibiting the structure of the quadrupole and the passing path of ion in the analyzer.

Additionally, applications of a tandem of triple quadrupoles are widespread for targeted metabolomics. In the QQQ-MS, the first Q serves as a mass filter and it submits the screened ions into the second Q with an acceleration. The Q2 is like a container of collision where the selected ions are collided with neutral gas molecule and a collision-induced dissociation (CID) is elicited for the fragmentation of the ions [50]. The fragments of the precursor ions are eventually transmitted into the Q3 and their masses are scanned. With the mass information of the precursors and their product ions, a better understanding of the structure of an undefined molecule and also a good quantification will be achieved.

- Orbitrap

The orbitrap is a spindle-like MS analyzer which allows to trap ions orbiting around the trap axis with their specific orbitals in the analyzer. Ions are trapped in the analyzer, and an outer alternative electric filed makes the ions orbit around and oscillate along the trap axis. The frequency of the orbit depends on the mass-charge ratio, which is presented by the formula 1.3.2.

$$\omega = \sqrt{(z/m) \bullet k} \qquad (1.3.2)$$

where ω is the angular velocity of the oscillation, z/m is the mass-charge ration and k is field curvature. Hence, the ions are separated and recognized in the light of their different frequency.

The advantages of the orbitrap includes its high resolution (accurate until 0.0001Da) and low mass error. A cutaway view of orbitrap mass analyzer is shown in Figure 15.

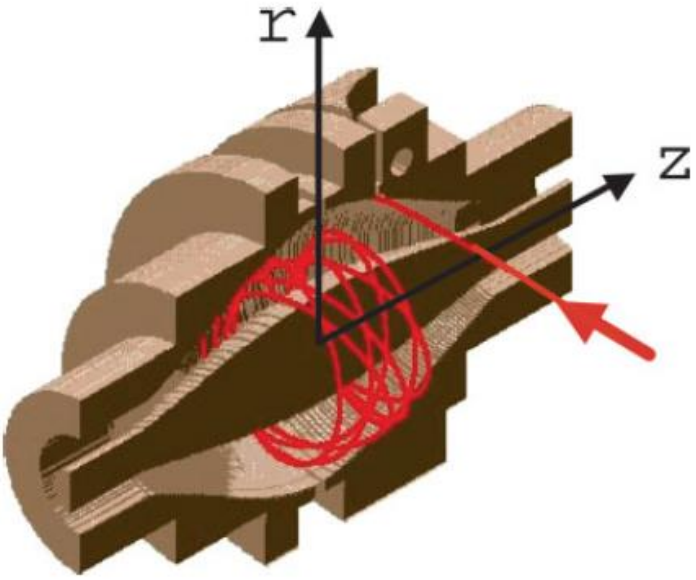

Figure 15. A cutaway view of orbitrap mass analyzer. Ions are injected into the orbitrap at the point indicated by the red arrow. The ions are injected with a velocity perpendicular to the long axis of orbitrap (the Z axis), where they begin coherent axial oscillations within (By Hu. et al. 2005) [51].

Detector

After the ions pass the analyzer, the signals of the ions are recorded and accumulated by the detector. Indeed, the reception and the recording of signals are by the sequence of different mass-charge ratio. As the ions are separately captured, their resultant weak currents are recorded and stimulated by an amplifier. For example, the electron multiplier [52] is frequently applied as the amplifier which is generally composed by a pair of metal plate. The secondary emission to the opposite plate is possible after the first hit on one of the plates, which is favored by the existence of potential difference between the two plates. The repeated alternative movement of the charged particle in the amplifier makes it possible to record the signal from the same particle. Other used detectors include Faraday cups and ion-to-photon detectors [53].

1.3.2 Tandem mass spectrometry (MS/MS) or tandem MS to chromatography techniques

MS/MS[54]

The tandem mass spectrometry, also noted as MS/MS or MS^2 is commonly used in the metabolomic studies for the qualification of the ion peaks or for determining the structure of the unknown compounds.

As regard to the principle of the MS/MS, briefly, the ions are firstly selected and separated in the first MS by their m/z. Then, further dissociation of the ions takes place in the second MS [50]. Eventually, the experience provides information not only the mass-to-charge ratio of both the precursor ion and the product ion, but also the position of fracture in the initial ion.

In the case that only one mass spectrometry is applied, the assignment of the MS peaks is primarily realized by referring the obtained value of m/z to the exact mass of the ion. However, this is not reliable for the existence of isomers. Through the application of MS/MS technique, the qualification should be more convincible if the product ions of the observed ion can be also matched to those which are obtained by the standard substance or to some data base of note. On the other hand, the difference of m/z between the precursor and product ion allows to speculate the position of the fractured bond in the precursor ion, and therefore to speculate the configuration of the unknown substance.

Chromatography–MS

In the studies of metabolomics, as the analyte is usually a mixture of extensive molecules, if the bio-samples are analyzed directly by the MS, the repetition of fragment ions from different molecules makes it hard to interpret the MS peaks. Hence, a tandem of chromatography with MS is appreciated, which allows to beforehand separate the analyte in the light of the property of its elements [55]. The isolated components are eluted in gradient and then ionized in the ion source.

Concretely, the analyte is packed by the carrier, which may be gas or liquid, flows through the chromatographic column. The chromatographic column plays a role as a stationary phase which is able to absorb the analyte in the mobile phase by a certain percentage of quantity of the analyte. The coefficient of distribution (*K*) of the component in both the stationary and mobile phase is a constant at equilibrium (formula 1.3.3). The absorbed fractions are gradually washed off and detected respectively by the detector. Meanwhile, the time of retention (R_t), which is calculated by the formula 1.3.4, is recorded for each component. A flow through the chromatographic column about a mixture of two substance is taken as an example, shown Figure 16.

K = Cs/Cm (1.3.3)

$$Rt = t_0 + t_0 K \frac{V_s}{V_m} \quad (1.3.4)$$

where C_s and C_m are the concentrations in the stationary phase and mobile phase of the absorbed solute; the V_s and V_m are the volumes retained by the two phases respectively. t_0 is the dead time [56].

The gas chromatography-mass spectrometry and the liquid chromatography-mass spectrometry are widely used for carrying out metabolomic studies.

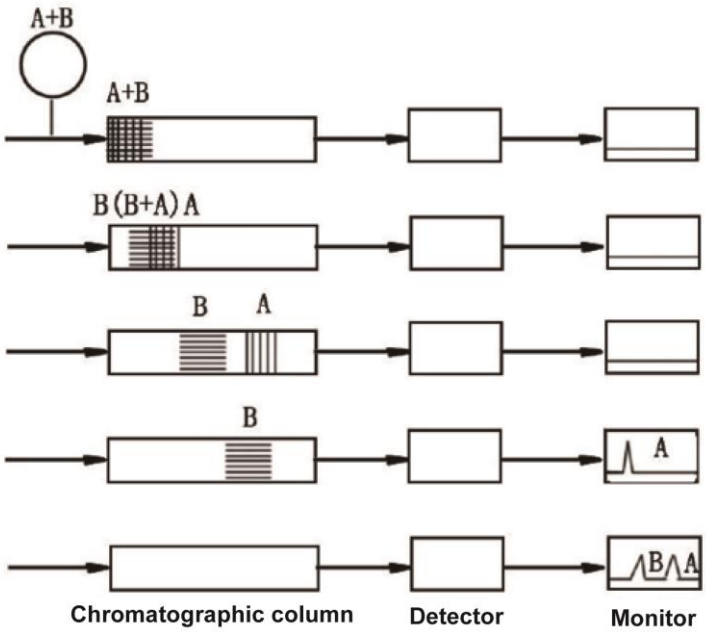

Figure 16. Schematic diagram showing a flow of a mixture of two components A and B through the chromatographic column. A and B are separately eluted and recorded by the detector. After the transform of signal, the corresponding peaks of A and B are present on the monitor.

- Gas chromatography

The gas chromatography uses a carrier gas which wraps the analyte and runs through the column. It separates the mixture with the components that are easy to be vaporized. The tandem of GC-MS can be applied in the analyses with solid, liquid, and gaseous samples [57].

The applied carrier gas needs to be pure and stable. This is because the MS is sensitive to detect the impurities and the reaction between the carrier gas and the stationary phase should be stemmed. Gas such as hydrogen, nitrogen, and inert gases are used as the carrier gas.

An EI ion source is commonly used for the GC-tandem MS. The reactive electrons are produced by the heated cathode. The separation of the components depends mostly on the temperature programming of the column and the flow speed of the carrier gas. The mass selective detector (MSD) is usually used as the detectors of the GC-MS [58]. In order to improve the vaporability, thermostability and even the sensitivity of the compounds in the analyte, which is beforehand treated by a derivatization. The active hydrogens, in the groups such as –OH, -COOH, -SH, -NH_2, etc., are substituted by the

groups with lower polarity. In the view of need, the derivatization strategies can be chosen among the methods such as silanization, acylation, halogenate, etc. [59]

The transmission of particle is at the atmosphere in the chromatography part but is vacuum for the MS part. For the non-targeted metabolomic analyses, the full scan field ranges usually between 50 to 600 m/z. And, the selective ion monitoring (SIM) method is applied for the targeted analyses which requires the set of the scan range of m/z in the several periods of retention time. As the EI source is mostly employed, only the positive mode is available, and the precursor molecular ion is not detectable. Hereby, the qualification of the peaks depends on the specific fragments. The relative quantification of component is done by the determination of the peak area. In the present work, the SHIMADZU GC-MS 2010 plus was utilized.

- Liquid chromatography [60]

Liquid chromatography is the other tandem method to the MS. Unlike the GC-MS, liquid mobile phase is applied as the carrier of analytes. The mobile phase is a mixture of two solutions with distinct polarities: one polar solution (e.g. H_20+0.1% formic acid) and one solution with low polarity (e.g. acetonitrile). The percentage of each solution is adjusted along the separation to preserve as more metabolites whose polarities are in a large range as possible.

The choice of the chromatographic column is principally dependent on the polarity of the metabolites of interest. Generally, reversed-phase (RP) column such as C8 and C18 column [61] is suitable for the separation of molecule with medium and low polarity while a hydrophilic interaction chromatography (HILIC) column [62] is predominant for the separation of polar or ionic compounds.

LC-MS has been taken advantage in metabolomic studies since it allows to obtain a large coverage of metabolites in bio-systems and to achieve an exact molecular mass for the metabolites with a high sensitivity and resolution. It is possible to analyze and to detect both positive and negative ions. Besides, a combination between the application of RP column and HILIC column helps to obtain more metabolites of interest.

During this study, an ultra-performance liquid chromatography (UPLC)-MS is applied. The column is filled with particles inferior to 2µm, which increases linear velocity with a high pressure. Compared with the high-performance liquid chromatography (HPLC) technology using fillings of 3.0 to 4.6µm, the UPLC leads to a better resolution, sensitivity and a faster analytical speed [63]. A HSS (high strength silica) T3 column (Waters, Milford, MA, USA) which is a RP column has been applied. It is actually a modified C18 column which performs a better separation in polar molecule and in a larger pH range than C18 column. Using such a column in untargeted metabolomic analyses, we have achieved not only a good retention of nonpolar molecule such as kinds of lipids but also a good retention of polar metabolites such as amino acids.

Other than tandem chromatography-MS, the combination between capillary electrophoresis (CE) and MS is also well applied for metabolomic studies. The major aimed metabolites by the technique are the polar metabolites [64, 65].

1.3.3 Processes of mass spectrometry-based metabolomics

The process of execute the mass spectrometry based metabolomics is mostly similar to the process of NMR spectroscopy-based metabolomic which has been exposed in the last chapter. However, some operations in the steps distinguish from those in the precedent method. The remarkable feature of the MS based metabolomics is therefore introduced as following:

Sample preparation

The sample preparation begins from the removal of proteins. Solution of extractant such as methanol, acetonitrile is added to the biofluid. After a centrifugation, the proteins are precipitated while the supernatant is drawn and lyophilized. Indeed, the metabolites to be analyzed are dissolved in the supernatant liquid. In this thesis work, methanol water solution (volume ratio 1:4) was used as the extractant. However, it should be underlined that for lipidomics studies (important branch of metabolomics, not included in this study) [66], which focus on the analyses in the extensive kinds of

lipids, the extractant is different from the mentioned compounds, solution with less polarity is applied for the dissolution of the lipids.

The freeze-dried samples should be redissolved before the instrumental analyses. For LC-MS the solution can be consistent with the extractant. For GC-MS studies, derivatization reagent is added into the lyophilized samples, and the sample analyses are performed after the extraction of the supernatant after the derivatization reactions.

The preparation of quality control (QC) samples are demanded at the same time of the preparation of the real samples. The QC samples are collected usually by the mixture and a subpackage of all the real samples. The method of extraction should be in accord with that in real samples.

Moreover, one or several internal standard references are also added into the samples during the preparation. The internal standard substance does not exist in the analyte and it serves to a better quantification with their known concentration.

Spectra acquisition and peak assignment

In the sequence of analyses, the QC samples are inserted after an equal amount of real samples. They are used to affirm the stability of the instrument and to acquire complementary product ion information [26].

Unlike the spectrum of NMR spectroscopy, the spectrum of MS within the scan scope of m/z is not necessarily continuous. A mass spectrum is presented by bars accompanied by a determined mass. Each peak represents a molecular ion or an ion fragment which are corresponding to certain metabolites. However, in the experiences of chromatography tandem to MS, the total ion current (TIC) chromatogram is continuous which describes the integrated intensity across the entire range of masses being detected at every point of retention time in the analysis. Figure 17 shows a comparison between the mass spectrum and a TIC chromatogram.

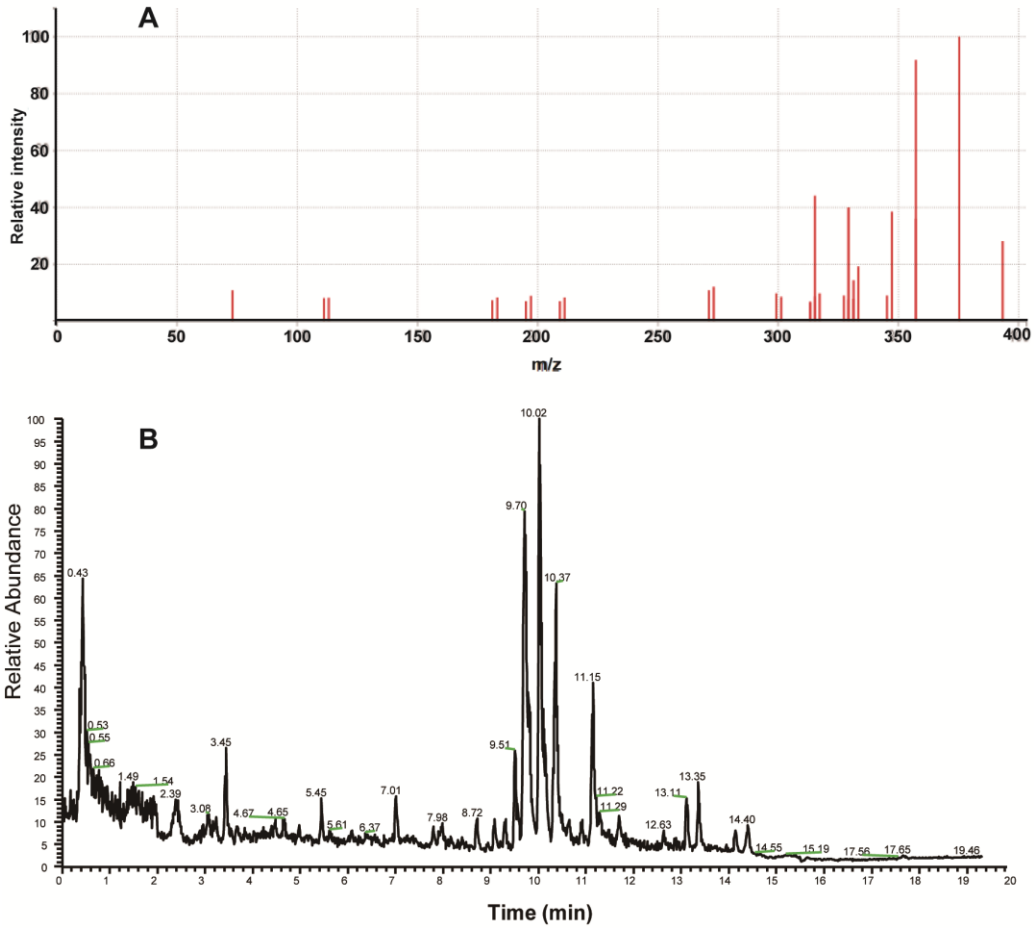

Figure 17. Comparison between the mass spectrum and a TIC chromatogram. A: MS/MS spectrum of UDCA (ursodeoxycholic acid), taken from HMDB (www.hmdb.ca) the abscissa is for the m/z and the ordinate is for the relative intensity; B: One of the TIC chromatograms obtained by the serum metabolic profiling in the septic shock patients. The abscissa is not m/z but the retention time obtained by UPLC-ESI-Orbitrap-MS. UDCA was one of the detected metabolites in the experience (negative mode, [M-H]=391.2831 RT=9.27min) but not visible in the TIC diagram.

With the help of the chromatography, the qualification of the ion peaks can be both determined by the m/z and by the retention time. The data base such as HMDB and metlin (https://metlin.scripps.edu/index.php) can be also helpful for the assignment of the peaks. In the case that more than one isomer is possibly present, the further confirmation of the qualification can be done by matching the results of MS/MS or the spectra of corresponding standard substance.

Data pre-processing

The ion peak area is usually recorded for the quantification of each peak. For the data obtained from GC-MS analyses, a deconvolution should be first operated on the data. Apart from this, peak matching and alignment are followed, which are accomplished by the software such as SIEVE, Markview for LC-MS and Leco ChromaTOF for GC-MS. Afterwards, the assessment of the stability of QC samples is necessary to confirm the reliability of the recorded peaks. In order to avoid some exogenous substance in each test, the peaks are eliminated if the null peak area is present in more than 20% samples. Afterwards, RSD of each peak of QC samples is calculated and those peaks with a RSD superior to 30% are also removed for their poor stability. Equally, only the remained ion peaks after the screening are further analyzed in the real samples. A PCA analysis including all the QC and real samples is also useful to view the dispersion between the samples. A focalization of QC samples in the PCA score plot should normally found for they are in fact equivalent. Figure 18. has shown an example of the PCA exhibiting the QC samples and the real samples.

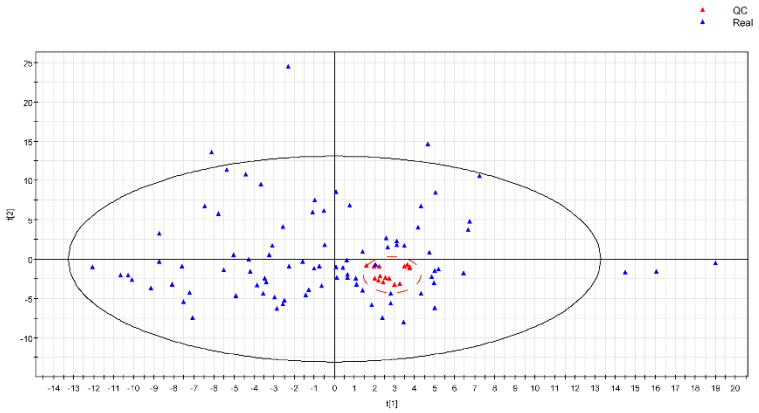

Figure 18. A score plot of PCA obtained by analyses of GC-MS on all the samples of HCC patients. The red triangles are the QC samples and the blue triangles represent the real samples.

Introduced methods of normalization are equally applicable for the MS peaks normalization. Besides, the normalization can be otherwise implemented by referring to the internal reference. We chose the internal reference that shows the lowest RSD in the QC samples as the reference of normalization. The normalization is performed

by the ratio of intensity of each peak to the detected intensity of standard reference in every real sample.

Once the data is processed, the statistical analyses methods as well as result validation and biological interpretation which are similar to those applied with NMR-based approach will be exposed in the next chapter.

Chapter IV. Similar experimental steps and comparison between NMR and MS-based metabolomics

For both NMR and MS-based metabolomics, methods of data pre-treatment encompassing the spectra normalization, the variable scaling are similar. Similarity can be also found for the methods of statistical analyses as well as the result validation and biological interpretation. First part of this chapter summarizes the similar experimental steps for both the techniques-based metabolomics. A brief comparison between the two techniques is concluded at the end of the chapter.

1.4.1 Methods of data pre-treatment

A. Normalization

The normalization of spectrum is a method attenuating macroscopically the dilution effect. Except for the experimental errors, a common source of non-induced variance issues from the large dynamic range of metabolite concentrations in the studied samples, which gives rise to unequal variance of residuals [67]. But, the variability of one certain metabolite is often analyzed by its mean concentration, the heterogeneous changes in different samples elicit errors in the results. On the other hand, for the analyses in the biofluid, urine for example, another important influencing factor is the inequivalent intake of water among different subjects. Thus, a normalization of the peaks for each spectrum in the whole dataset is needed.

Numbers of normalization methods are available, among which, the integrated peak area normalization, quotient normalization and quantile normalization are the most employed.

1) Integral peak area normalization

Integral peak area normalization is simple for we only need to sum up the total peak area of one spectrum and then integrate the area for each peak and calculate its

proportion to the total. However, this method is prone to be biased as the intense peaks occupy a large proportion in the total area and the spectrum is extremely sensitive to their variation. In this case, small but significant peaks in a bucket are possible to be unequally normalized.

2) Quotient normalization

Compared with integral normalization, the quotient normalization is more frequently suggested in the data pre-treatment of metabolomics. This is because it is less hampered by extreme amounts of metabolites than the above. And, normalization in samples with low metabolic variations is more exact [68]. The algorithm is as following:

1. Perform an integral normalization for all the test spectrum
2. Calculate the median spectrum (usually we choose the median spectrum)
3. Calculate the quotients of all variables included in test spectrum to those in the reference spectrum
4. Calculate the median of the obtained variable quotients
5. Divide all the variables of the test spectrum by this median

3) Quantile normalization

The quantile normalization is frequently performed by the following steps [69, 70]:

1. List and assign each of the variables to a column and metabolites to a row (for mass, for NMR, each row represents a sample).
2. Each column is sorted by intensity from the lowest to the highest.
3. Determine the arithmetical mean of each row according to sorted rank.
4. Substitute the mean value for each intensity value in the row.
5. Restore the original order of the assigned mean values to determine the normalized relative intensity.

Hence, quantile normalization is a normalization method based on the ranking of the variables. It reduces the non-biological systematic errors.

B. Variable Scaling

The scaling, is the normalization of the variables. Given that the analyzed variables correspond to the metabolites, in the case that several metabolites are fairly concentrated, the variation of these metabolites or the corresponding variables will be over highlighted. The consequence will be that significant variation in the low concentration metabolites will be overlooked. To avoid this bias, it is necessary to balance the weight of all the variables, and the variable scaling should be done. In metabolomic studies the mostly frequently applied scaling methods include Auto-scaling (or "UV-scaling"), Pareto scaling and range scaling. Their algorithms and their characteristics are shown in table 2 [71]. Figure 11(a-d) takes one example and shows the achieved scaling by three different methods. Accordingly, we observe that after the scaling, the intensities of the variables have been all centered and thereby a new normal-like redistribution is performed for the variables.

Method	**Formula**	**Goal**	**Advantage**	**Disadvantage**
Auto-scaling	$\tilde{x}_{ij} = \frac{x_{ij} - \overline{x}_i}{s_i}$	Compare metabolites based on correlations	All metabolites become equally important	Inflation of the measurement errors
Pareto-scaling	$\tilde{x}_{ij} = \frac{x_{ij} - \overline{x}_i}{\sqrt{s_i}}$	Reduce the relative importance of large values, but keep data structure partially intact	Stays closer to the original measurement than auto-scaling	Sensitive to large fold changes
Range-scaling	$\tilde{x}_{ij} = \frac{x_{ij} - \overline{x}_i}{\left(x_{i_{\max}} - x_{i_{\min}} \right)}$	Compare metabolites relative to the biological response range	All metabolites become equally important. Scaling is related to biology	Inflation of the measurement errors and sensitive to outliers

Table 2. Different frequently used scaling methods and their characteristics.

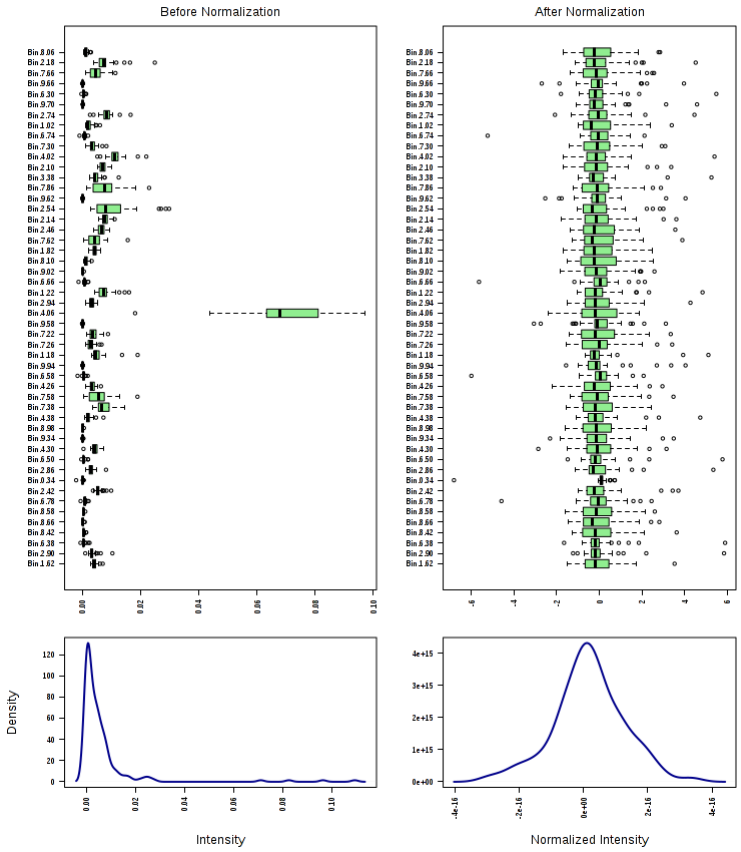
Before Normalization
After Normalization
Density
Intensity
Normalized Intensity

a.

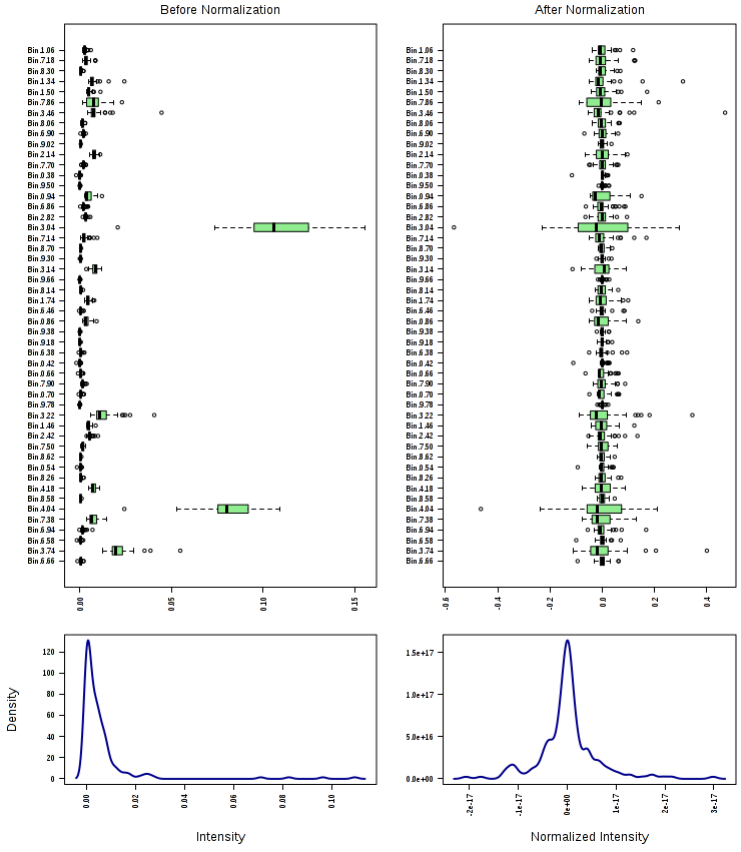
Before Normalization
After Normalization
Density
Intensity
Normalized Intensity

b

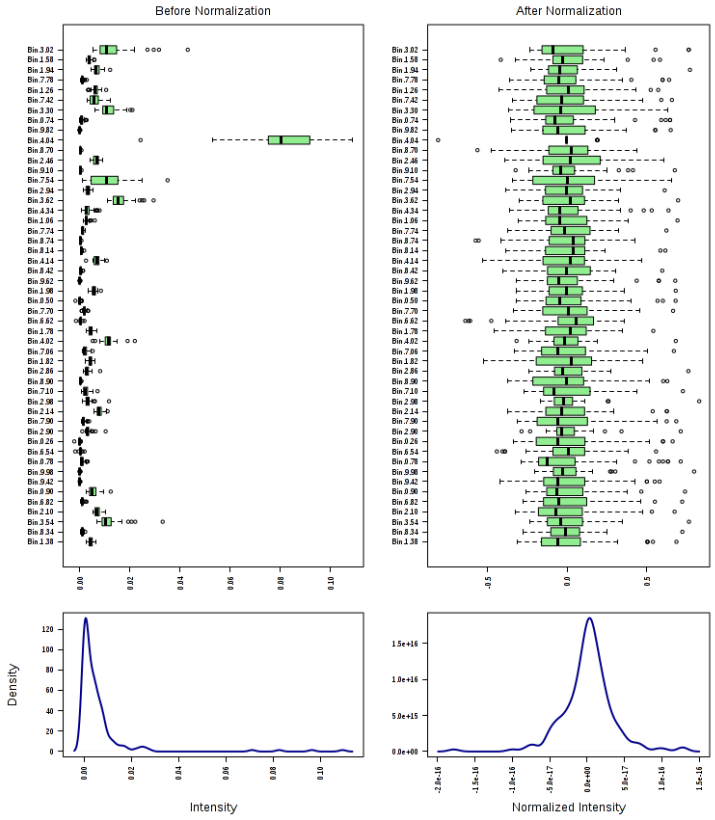

c

Figure 9. Schematic diagram presenting the effect of three different scaling methods. a: the Auto-scaling; b: the Pareto-scaling, c: range-scaling. Abscissa axis: intensity of the variable, ordinate axis: density of the variable. The example data of 1H NMR urine metabolomic study from Metaboanalyst 3.0 (metaboanalyst.ca) is used to exhibit the comparison between the scaling methods.

1.4.2 Data statistical analyses

There are usually a large number of samples and variables for metabolomic analyses. Hence, statistical analyses are employed for the visualization and interpretation of metabolomic variations.

There are two main aspects of statistical analysis in the metabolomics: univariate analyses and multivariate analyses. The choice between the two strategies depends on the initial experimental design. In general, multivariate analyses are prior for the non-targeted spectroscopic analyses because they usually consist of large numbers of variables with their considerable correlation between them. Univariate analyses are

important for the targeted analyses, which focus on the quantification of some known feature metabolites. In NMR spectroscopy based metabolomic studies, however, the application of multivariate analyses is dominant since each detected metabolite may correspond to not only one peak, which is a traced by numbers of variables. In spite of that, by calculating the mean intensity of involved peaks, univariate analyses have been equally shown to be feasible in NMR spectroscopy based metabolomics [72].

A. Univariate analyses

1) Student T test

In metabolomic studies, student T-test is usually used to determinate the difference between two means from two compared groups. The null hypothesis of the test H_0 is that there is no difference of mean between the two sets of data. The null hypothesis should be rejected if the probability of the H_0 is inferior to the threshold of confidence, and the H_1 "there exists significant difference of mean between the two groups of samples" is accepted.

Its formula is shown as below:

$$t = \frac{\bar{X}_1 - \bar{X}_2}{s_p \cdot \sqrt{\frac{1}{n_1} + \frac{1}{n_2}}}$$

where

$$s_p = \sqrt{\frac{(n_1 - 1)s_{X_1}^2 + (n_2 - 1)s_{X_2}^2}{n_1 + n_2 - 2}} \qquad (1.4.1)$$

In the formula, $\overline{X_1}$ and $\overline{X_2}$ are the mean of the two groups of samples; n1 and n2 are the numbers of samples for the two groups respectively and (n-1) represent the degree of freedom for each group. The S_{X1} and S_{X2} are the standard deviation for the two groups and Sp is the pooled standard deviation.

There are preconditions includes:

(1) the samplings should be randomized

(2) each studied group should be independent to others;

(3) the distribution of the studied variables should follow or almost follow the normal distribution in the population;

(4) the variance of variable among different population should be equivalent.

In metabolomic analyses, T test is frequently used to verify whether one metabolite is significantly varied in the comparison between two studied groups of subjects. The threshold $p < 0.05$ is usually regarded as the criterion that difference of concentration of the metabolite is significant.

2) T' test

The T' test is the derivative test from student T-test. It is used when the variances of the two compared groups are not equivalent.

3) Binomial test

If the distribution of the variables does not follow the normal distribution, the student T-test or T' test are not available. In this case, nonparametric tests [73] are employable to understand whether the two groups are significantly different. There are types of nonparametric tests, in which the binomial test [74] is frequently used in metabolomic analyses. In the test, the variable is only possible with two values (e.g. control group vs. experience group). In our studies, the binomial test is realized in the SPSS software (IBM, Chicago, USA) [75], whose initial hypothesis and final decision are analogous to that in T-test. As an example, when the amount of sample is relatively small, to figure out if the concentration of one metabolite is significantly different between healthy controls and patients, the binomial test is proposed.

4) ANOVA

ANOVA, short for Analysis of Variance is another statistical test providing whether the means of two or more than two groups are equal. [76]. It is similar to the student T-test when only two groups are analyzed.

For the studied variable(s), in fact, their variations exist between inter- and intra-

groups. The null hypothesis is similar to that in T-test: we suppose initially that there is no difference of mean among the groups, and refuse finally the hypothesis if the intergroup mean difference is much larger than that in the intragroup. For the metabolomic study, ANOVA is therefore predominant when there are more than two studied groups.

B. Multivariate analyses

1) *Unsupervised methods*

a. Hierarchical cluster analysis

There are numbers of algorithms in cluster analysis [77], in which the subjects and the analytes are first grouped to subsets and analyzed separately. The advantage is that it shows clearly both quantitative relationship and correlation among the analytes and the samples. In metabolomic studies, hierarchical cluster analysis (HCA) [78] is the frequently applied to discover the metabolite discriminators. Figure 12 presents an example of heat map which complies with the HCA algorithm.

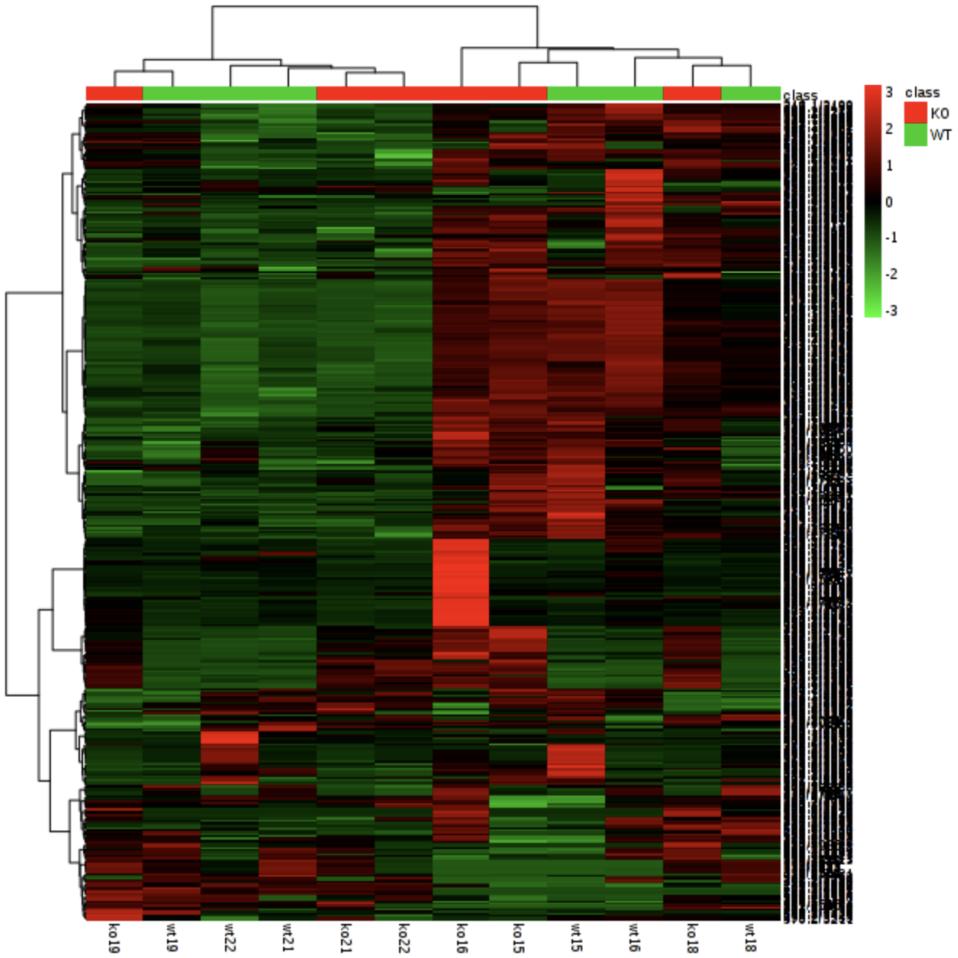

Figure 10. An example of heat map concerning the comparison between the mice with genotype knockout (KO) and wild type (WT). The green color stands for the downregulation of analyte while the red color represents the up-regulating. The correlations among the variables are shown by the connecting lines [79]. (Example taken from www.metaboloanalyst.ca)

b. Principal component analysis (PCA)

Principal component analysis is a multivariate technique that analyzes a data in which observations are described by several correlated quantitative variables [80, 81] . The aim of the analysis is to find out a transformation that transforms an original set of correlated variables to a new set of uncorrelated variables, called principal components [82]. The input data set is noted as a matrix X. A linear combination T of X is sought, noted as:

$$T = X \bullet p + E \qquad (1.4.2)$$

where p is the weight of X and E is the residue. In the space of T, the first component T1 is the first column of T matrix that represents the largest variation among the variables. The components are obtained in order of decreasing importance, and the aim is to reduce the dimension of the variables. The second component is perpendicular to T1 and T3 is perpendicular to the plane formed by T1 and T2, and so on. Consequently, the data is usually represented by two or three dimensions.

The two analyses HCA and PCA belong to unsupervised learning methods in which the data is not labelled.

2)*Supervised methods*

a) PLS-DA

Compared with the unsupervised methods, supervised multivariate methods introduce extraneously a matrix of response Y, which is related to the classification. Partial least squares discriminant analysis (PLS-DA), is derived from PLS regression (PLS-R) [83], which finds the linear relationship between Y and X:

$$\mathbf{Y} = f(\mathbf{X}) + \mathbf{E} \qquad (1.4.3)$$

b) OPLS-DA

Orthogonal partial least squares – discriminant analysis (OPLS-DA) is an extension of PLS-DA. It allows to remove the systematic variation of matrix X which are not correlated with Y, which helps to make the model simpler to be interpreted. With a similar regression algorithm as PLS-DA, a single component is used to predict the class while the other components describe the orthogonal variation with respect to this first predictive component [84].

Important parameters in the PLS/OPLS-DA:

- R^2 and Q^2

R^2X and R^2Y record the fraction of explained variance of X and of Y respectively by each calculated component. Q^2 represents the predictability of the model [85]. The closer to 1, the better ability of prediction is for Q^2.

- VIP

The variable importance in projection (VIP) is the weight of each variable in the model. In the part of MS-based metabolomic study the VIP was used to define the most important metabolite discriminator for different groups. It also can be used to select variables in order to filter the noise and other uncorrelated variables [86].

- AUROC

The area under receiver operating characteristic curve (AUROC), is a graphical plot that displays the performance of a binary classifier system as its discrimination threshold is varied [87]. The ROC curve is characterized by the sensitivity (axis y) and specificity (1-specificity for the axis x) of the classification. Taking example of clinical applications of ROC curve, the sensitivity of a diagnostic test is the proportion of patients for whom the outcome is positive that are correctly identified by the test. The specificity is the proportion of patients for whom the outcome is negative that are correctly identified by the test.

Method of multi-levels model

In the study aiming to investigate the evolution of septic shock, we have employed the multi-levels models on the patients who provided two points of samplings [88], which aims to analyze the samples belonging to the same subject in the multivariate analysis. The method allows to remove the variation of inter-individual, which is often calculated as the principal difference between the samples in the model of multivariate analysis, shown Figure 11. Hence, we use this method to determinate the metabolic differences between the two samplings for each patient, providing us the information of the effect of the clinical intervention and the individual feedback.

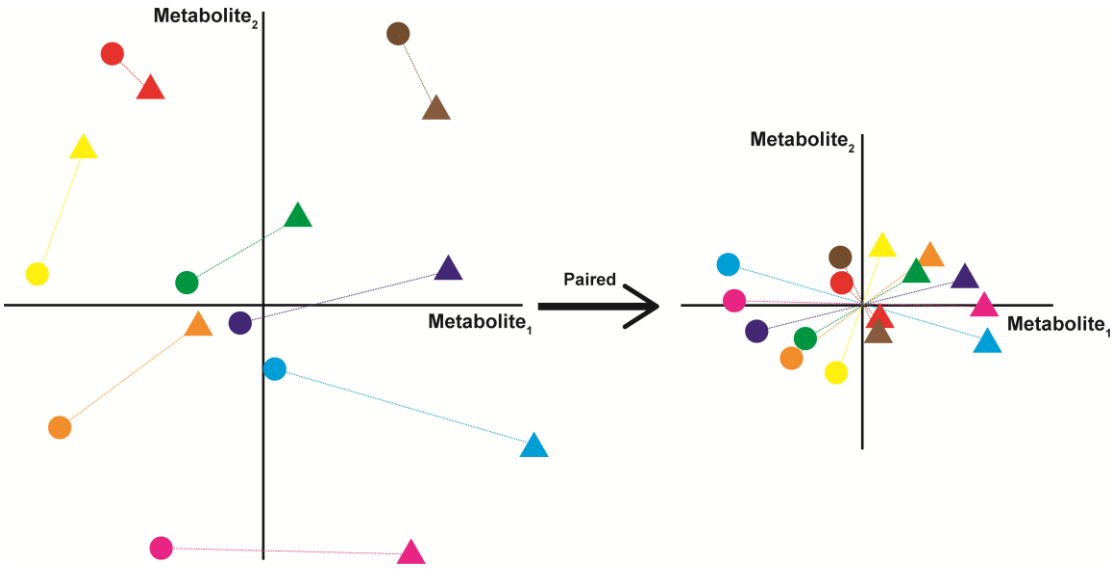

Figure 11. Principle of the multi-levels model presented in a space of two metabolites. The dots and the triangles represent two different samplings. Each color represents the same subject. Before the paired method conversion, it seems that the main distinction issues from the differences between the subjects but not between the different samplings for each subject; after the rearrangement by the paired method, the mean points of the two samplings are placed to the coordinate origin and an obvious discrimination between the two samplings is thereby displayed.

1.4.3 Result validation

The validation of the results is rifely required in the metabolomic studies since the obtained discriminatory models or metabolites are generally significant for the studied population only when they are applicable to predict the new specimens. Actually, univariate and multivariate analyses are applied to verify the reliability of obtained with new samples or with internal validation by sample permutation.

In many studies, the samples are divided into two parts: training set and test set. The samples in the training set are used to establish a discriminatory model, which monitors the differences between the samples in different groups. Afterwards, the samples of in the test set are projected into the founded model to verify the predictive ability of the model [89]. On the other aspect, as multivariate analyses such as PLS-DA and OPLS-DA are frequently used in the data analysis, among large numbers of variable

dimensions it is usually possible to find out a dimension which separates well the compared groups even though the differences between the groups are not significant. The effect called “over-fitting” is therefore not acceptable [90]. Further, the SIMCA-P software is widely used in nowadays to perform PLS/OPLS discriminatory models. However, in our previous study we demonstrated that the obtained results from the software might be at random because the algorithm is dependent to the order of the samples [91]. In conclusion, validation of the findings is important to ensure that the findings are not bias. In our studies, we primarily used two sorts of validations: internal validations by the samples in the training set and external validations by the samples in the test set.

A. Permutation validation

The permutation validation confirms that the discriminatory model is not over-fitting. Figure 12 shows an example of permutation validation (obtained in the SIMCA-PA software). The abscissa is the correlation between the permutated variable and the original variable. The ordinate corresponds to the calculated R^2 and Q^2. The blue line stands for the linear regression of Q2 with the permutation of Y, and the green line represents the similar evolution of R^2. Theoretically, the two value should achieve the maximum when the permutated Y equals exactly that in the training model. Hence, the slope of both the two lines should be positive [92, 93].

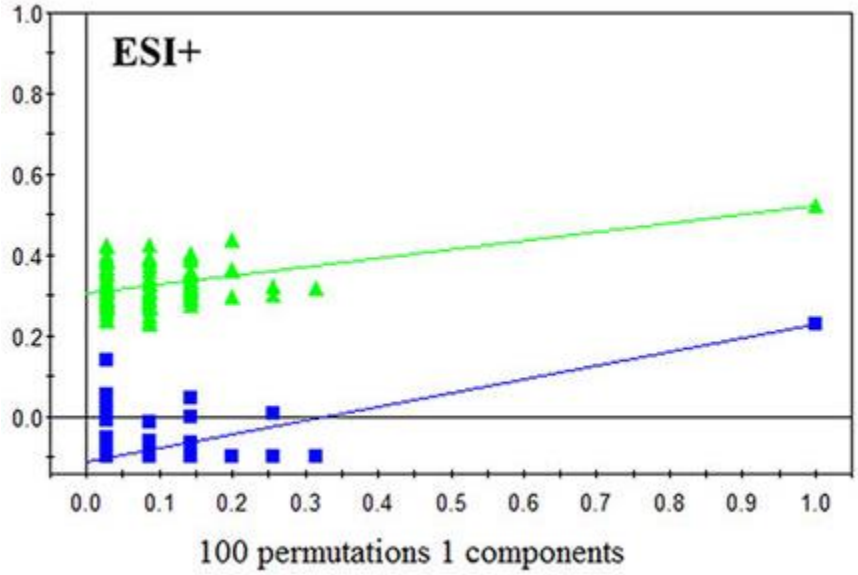

Figure 12. Example of permutation and cross validation in SIMCA-P. [94]

B. Validation by the test set

One strategy of validation by the test set is to reproject the samples which are not included in the training set to the established discriminator model. The prediction is valid if the model performs still a good separation in the test samples. Another strategy which is ensure the significance of several determined discriminatory metabolites by calculate their area under receiver operating curve (AUROC) [95]. After the quantification of the targeted metabolites is obtained, AUROC of the metabolites can be calculated to verify the sensitivity and specificity of the metabolites for being a potential biomarker. The value of AUROC range from 0.5 to 1, where 0.5 means there is no separation and 1 means the separation between the groups is perfect.

Further, if there are various significant metabolites found with excellent performances in the discriminatory model. A combinational biomarker can be generated by a regression analysis with the defined metabolites. The validation by AUROC can be simply executed with the combinational biomarker in the test set.

1.4.4 Biological interpretation

The detection of the significant variations in the metabolites enables to deduce the variation of the involved metabolic pathways. Typically, for the clinical application of metabolomics, the understanding of deregulation of the metabolic pathways is important which provides evidence to improve the diagnosis, prognosis and as well as the treatment protocol. Frequently used database of metabolic pathways include "KEGG pathway" (http://www.kegg.jp/kegg/pathway.html) and "HMDB pathway" (http://www.hmdb.ca/pathways) [96-98]. The database not only reveals the attribution of metabolic pathway for the metabolites, but it provides information of related proteins and genes as well. Furthermore, the metabolomic results inspire the complementary experiences with other omics platforms. Accordingly, the parallel observation in the genome or proteome improves the understanding of the origin of the variation of metabolites. Besides, some online software such as "Metaboanalyst 3.0" (www.metaboanalyst.ca) [99] and "Biocyc" (http://biocyc.org) [100] are available to induce the metabolic and signaling pathways which are correlated with the determined discriminators. Some commercial bioinformatics solutions (e.g IPA https://www.qiagenbioinformatics.com/products/ingenuity-pathway-analysis/ and MetaCore https://portal.genego.com/) provide useful features for performing molecular pathway and network analyses. Most of them integrate information from different omics approaches and focus on providing solutions that facilitate a deeper insight into the role of the metabolites in the molecular mechanisms of patho-physiological processes [101].

1.4.5 Comparison and combination between NMR-based and MS-based metabolomics.

Both NMR and MS, which are the two principal techniques in metabolomics, have been used for the determination of clinical biomarkers in this study.

A comparison between the two approaches concerning their application in metabolomics shows that MS provides a wider coverage of metabolites than NMR does. The reason should be that MS brings a better sensitivity. Metabolome is usually analyzed in ^{1}H NMR-based metabolomics with limits of detection on the order of 10μM [102]. A study of Nicolson et al. has eventually determined about 55 metabolomics in human plasma by different sequences using a 750MHz NMR spectrometer [103]. The number of defined metabolites increased to 70 in another study using GC-MS during only one analysis in the plasma of sheep [104], given that more metabolites are possible to be identified with LC-MS. Even though using a cryoprobe helps to improve the sensitivity and resolution for NMR, the high cost limits its use. Indeed, especially for untargeted metabolic profiling, the coverage of metabolites is crucial to find out as more significant variations as possible in the metabolome.

However, the quantification of NMR-based method is more reliable since the reproducibility is better and the acquisition is less influenced by the salinity of the sample [102]. Alterations may be present among the results obtained from MS instruments within different tandems and from the bias of alignment and peak matching which are performed with the software for a same sample [105]. Besides, NMR-based method needs a simpler preparation of samples and also do less damage to the samples.

Studies using the combination of both NMR and MS-based methods have been performed, which showed that the two methods were well complementary. Apparently, the coverage of metabolites is improved by using both of the two techniques and it was shown that the combination of the data sets from the two methods is promising for metabolomic studies [106, 107]. Using the combination of the two techniques helps to develop a high-throughput metabolomic method of tissue extraction [108]. Another study showed that using the two methods together helps to fast identify unknown metabolites [109].

II. Metabolomic studies of sepsis and septic shock

2.1 Introduction of sepsis and septic shock

Sepsis is defined as a systemic inflammatory response syndrome (SIRS) which is caused by infections [110, 111]. It's diagnosed by the symptoms such as abnormal body temperature, rapid breathing, elevated heart rate, confusion and edema [112, 113]. As sepsis develops, severe sepsis is characterized by the advent of organ dysfunction or tissue hypoperfusion [114]. Septic shock is the most severe stage which is accompanied by multiple organ dysfunction syndrome (MODS) [115] and a continuous intractable low blood tension [116, 117]. The evolution of sepsis is shown in Figure 19 [117]. Furthermore, complications such as bleeding [118], coagulation and thrombus [119, 120], necrosis [121] are also frequently present along the sepsis which aggravate the case. Sepsis is usually caused by bacterial infection and it is also possible to be caused by the invasion of fungi or virus [122]. Of which, kinds of gram-positive and gram-negative bacteria were found to be mainly related [123].

In recent years, although improvement of effective antibiotic therapies are applied in the treatment [124], and the early goal-directed therapy is also widely suggested [125, 126], but the mortality of sepsis, or especially septic shock, remains high (up to 30% - 50%) [127, 128] because of complexities and the lack of evidence in the early prognosis with the frequently used biomarkers (e.g. CRP, IL-6, PCT, etc.)[129, 130] or clinical score assessments (e.g. SOFA), in this context, new methods for the diagnosis and for predicting the outcome of sepsis in the early stage are eagerly required.

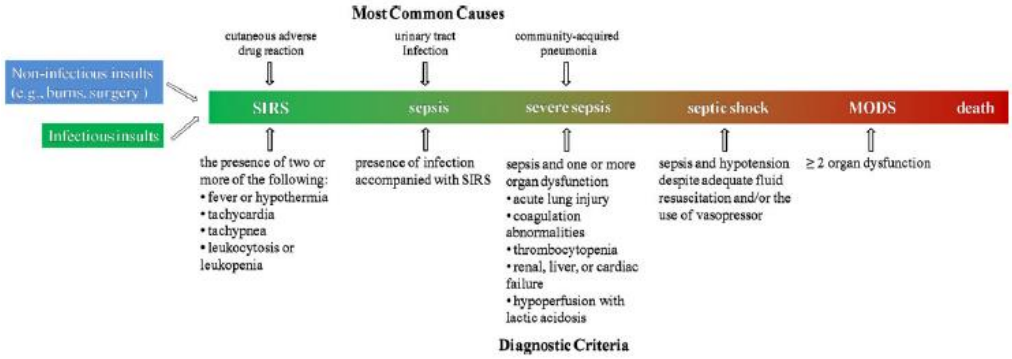

Figure 19. Schematic diagram expressing the evolution of sepsis [117].

With the help of metabolomic studies, it is possible to monitor the metabolic variation in the organism. Hence, large amount of studies have been performed for finding out the metabolic characteristics in septic subjects or severe subjects and for seeking new biomarkers. In this work of thesis, we mainly focus on the prediction of mortality of septic shock, meanwhile, it is equally vital to understand the metabolic variation in the earlier stages.

2.2. State of art for metabolomics studies about sepsis and septic shock

2.2.1 Early diagnosis

In the past, gram-negative bacteria induced lipopolysaccharide (LPS) toxin release is considered as the main cause of sepsis [131]. LPS results in modulating related genes and proteins such as high-mobility group box-1 (HMGB-1) [132], LBP (LPS binding protein), soluble CD14 [133, 134], C-reactive protein (CRP) [135], tumor necrosis factor α (TNFα) [136] and interleukin [137, 138], etc., which involve in the signaling of systemic inflammatory response. However, as mentioned in the introduction, sepsis may be also elicited by gram-positive bacteria. In order to understand the metabolic distinct between the different origins of infection, Hoerr et al. revealed that

differences in metabolic profile exist between gram-positive and gram-negative induced infections in mouse model. The main discriminators were detected as kinds of amino acids, urea, and Krebs cycle involved metabolites [139].

Metabolomic approach is applicable to deduce the stage of sepsis as a LC-MS based metabolomic study has shown discrimination of metabolic profile among the different stage of sepsis [140].

Using ^{1}H NMR-based metabolomic analyses with lung tissue, BAL fluid and serum respectively, Izquierdo-Garcia et al. realized new models which consists of discriminatory metabolites such as alanine, creatinine and myoinositol differing septic rats from healthy ones [141]. In human patients, with the help of the similar approach, another work using serum concerning sepsis early diagnosis was performed by Mickiewicz et al. In their work, metabolic differences were compared not only between septic and control subjects but also between the septic and SIRS patients. Accordingly, it's shown that it was feasible to achieve discriminations among the three group of patients with high specificity and sensitivity [142]. On the other hand, urine samples analyzed by GC-MS also showed separation among controls, late and early onset of neonatal sepsis [143]. Besides, targeted metabolomics study involving 186 analytes emerged important discriminations between SIRS without infection patients and septic ones. In the study, fatty acid (C10:1) and PCaaC32:0 showed good reliability to characterize sepsis compared with SIRS [144].

2.2.2 Prognosis

Sepsis, especially severe sepsis and septic shock trigger a high mortality rate in the patients. Accordingly, there is always an urgent needs of accurate prognosis in the early stage. As the variation of metabolic profile is sensible to the evaluation of the disease severity, metabolomics is therefore a useful tool to predict the outcome of sepsis.

In the study of Lin et al, cecal ligation and puncture (CLP) was operated for imitating sepsis in rodents [145]. They predicted thereby the prognosis of sepsis by comparing

the metabolic profile according to NMR spectroscopy of the surviving rats and the non-survivors. It was found in their work that elevated level of lactate, alanine, acetoacetate, acetate and hydroxybutyrate were witnessed in the non-surviving rats. Meanwhile, the decreased metabolite was formate [146]. Similar work which was performed by the (high performance liquid chromatography) HPLC-MS has revealed that considerable variations were further found in the serum fatty acids such as oleic and linoleic acid [147].

The prediction of outcome in the human patients is extensively focused by the researchers. With the NMR-based metabolomic study on urine from severe sepsis or septic shock patients, patients with positive prognosis were separable from the ones with negative prognosis. The major discriminators included some amino acids, glucose and ethanol [148].

Recently, combination of multiple platform is favored in the prognosis of sepsis. Indeed, with the help of various techniques, the findings will be ensured. By integrating metabolomic analyses and inflammatory mediator profiling, death in sepsis was well predicted, they found that the combination of metabolites and inflammatory mediators show a better sensitivity and specificity in the prediction than the classical clinical evolution systems (e.g. SOFA, APACHE) [149]. Furthermore, applying together metabolomics and proteomics also showed an excellent improvement of prognosis by Langley et al [150]. They reported that the defect of fatty acids and their related carnitine variations were the first obvious characteristics of adverse outcome in sepsis. Some energy-related metabolites such as lactate, citrate, malate and gluconeogenic amino were generally increased in the serum of non-survivors. Their findings were generally in accord with other studies except that they did not find differences in the metabolic profiles between different origins infected sepsis (among S. pneumonia, S. aureus, or E. coli infections).

2.2.3 Other metabolomic studies concerning sepsis

Sepsis-induced dysfunction of organ is one of the main aggravated factors of the

disease [151, 110, 152-156]. Hence, various studies focused on determining the metabolic variations of dysfunction of different organs. For example, research of sepsis-induced acute lung injury exhibited a remarkable increase of glutathione, adenosine, phosphatidylserine in septic patients compared with the healthy controls, which indicated the increased oxidant stress, loss of ATP homeostasis and apoptosis respectively; and a decrease level of sphingomyelin which reflected the disruption of endothelial barrier function [157]. For the case sepsis-induced liver dysfunction, targeted metabolome in rats were analyzed by Racknagel et al. Increasing levels of bile acids were discovered in the septic patients with liver dysfunction than those in controls [158]. Sepsis involved heart and kidney injury were also studied by metabolomics, as to the findings, abnormal concentration of carnitine and its derivatives were correlated to the acute kidney injury (AKI) [159], and the affected Krebs cycle enzymes by the sepsis was considered as the main factor of heart failure [160].

Other metabolomic studies on sepsis includes the one of Stinger et al., who explained in their studies that metabolomic studies on whole blood (WB) might be less lengthy and might retain more information including blood cells. According to their work, most metabolites leads to a higher concentration of metabolites than those in the serum; 18 vital metabolites were uniquely detected in the WB. Their work remind us using the WB might be in priority for studying sepsis [161].

2.3 Experimental research: Determination of metabolic differences between the septic shock survivors and non-survivors

As it has been introduced in the beginning of the chapter, to date, the mortality rate in the septic shock patients still remains high, thus, there is always an urgent need of effective prognostic method. Hence, we attempt to investigate the metabolic differences between the septic shock survivors and non-survivors by using the metabolomic approach. We expected to better understand the clinical features in the cases with poor outcome, according to our results, which might give reason to execute specific treatments.

We are aware that more information can be obtained by using both NMR spectroscopy and MS metabolomics. Thus, the two methods were experienced to finalize the experimental research. Our first study aims to use LC-MS to find out the metabolic differences between the septic shock survivors and non-survivors before clinical interventions.

Before the performance of the study, the choice of studied cohort and the selection of the samples are crucial within the experimental design. The cohort of subjects is screened in order to homogenize the samples.

As it was well known that the age was related to the survival rate of sepsis [162], and the majority of patients were aged more than 55 years old. Consequently, a few patients younger than 30 years were primarily excluded. The patients with cancer were also excluded in the analyses. This is because extensive metabolic pathways are prone to be modified by the tumor-related signaling [163]. Patients with cirrhosis or chronic kidney diseases were also removed since the injury in the liver and kidney by the two complications hinders the immune defense [164]. Also, the two factors were reported to impact the survival by the previous studies [165, 166]. Indeed, the patients affected by blood diseases were not included because the innate distinct in the blood might influence the discriminatory analyses.

Sera metabolomics has been proven effective in the previous studies. Of note, sera metabolome is informative. Serum is also easy to be collected and stored. Compared with other biofluids, the stability and integrity of sera are preeminent [167]. Hence, serum is focused as the prime subject in the thesis works of metabolomics.

As regard to the determination of metabolic differences between the septic survivors and non-survivors. The samplings at the admission of hospitalization were in priority to be used for the metabolomic study, for the metabolic profiles are least intervened by the clinical treatment. Besides, the investigation in the samplings before treatments seems the most significant to display the internal variations which are triggered by the disease. As a consequence, the first study predicting the mortality of septic shock by the metabolome variations was done with the samples at H0 (drawn before clinical interventions).

2.3.1 Study 1: Application of LC-MS-based metabolomics method in differentiating septic survivors from non-survivors.

According to the findings in the first study, we were informed that the metabolic profiles of the septic shock survivors were well distinguished from those of the non-survivors. In the following step, we considered to understand if there also exists differences of evolutions of the case in the metabolome between the survived and dead septic shock patients. Also, a NMR-based metabolomic study may confirm our findings of the LC-MS-based study and may provide complementary information of metabolome variations predicting the septic shock mortality. Consequently, the second study on the determination of metabolite biomarkers for predicting septic shock mortality was performed with 1H NMR spectroscopy in our French laboratory.

2.3.2. Study 2: 1H NMR spectroscopy based metabolomic study predicting the mortality of septic shock in the early stage and during its evolution

^{1}H NMR spectroscopy based metabolomic study predicting the mortality of septic shock in the early stage and during its evolution

Zhicheng LIU[1], Roland AMATHIEU[1,2], Mohamed TRIBA[1], Nadia BOUCHEMAL[1], Xiangping Lin[1], Laurence LE MOYEC[3], Philippe Savarin[1]

1. Sorbonne Paris Cité, Laboratoire de Chimie, Structures et Propriétés de Biomateriaux et d'Agents Therapeutiques, UMR 7244, University Paris 13 Bobigny, France

2. Intensive Care Unit Jean Verdier Teaching Hospital, AP-H, Bondy, France

3. University of Evry Val d'Essonne, UBIAE, INSERM U902, Evry, France

Abstract

Septic shock is the most severe phase of sepsis, leading a high mortality. However, the prognosis of septic shock remains difficult for the present. In the current study, to investigate the differences of metabolic profile between the septic shock survivors and the non-survivors, we set up models separating the two group of patients using NMR based metabolomic. We report that the metabolic differences are found both before the clinical treatment and during 24 hours after the hospitalization. Further, the up-regulating metabolites such as glucose, lactate, creatinine in the separations between survivors and non-survivors are exposed to be decreased in the survivors during 24 hours after the hospitalization. Our separating models also show better predictions of mortality than the clinical scores. The results determine that the NMR based metabolomic is useful for the prediction of mortality of septic shock.

Key words: ^{1}H Nuclear Magnetic Resonance spectroscopy, metabolomics, septic shock, discriminatory model, biomarkers.

Introduction

Septic shock is the most severe phase of sepsis [1, 2]. It is intractable as it is usually accompanied by types of complications such as hypotension and multiple organ dysfunctions syndrome (MODS) [3]. The common strategies of treatment for septic shock include the antibiotic therapy and the compressive infusion. In recent years, the early goal-directed therapy (EGDT) which improves curative effect is recommended to be applied [4, 5]. However, the early personalized prognosis and diagnosis remain challenging because of the complicated etiology and pathogenesis. Evaluation with some biomarkers (e.g. TNF-alpha, IL-6 and PCT, etc.) and with clinical scores such as sequential organ failure assessment (SOFA) [6] have been applied for the prognostic, their reliabilities are not satisfactory [7]. Thus, there is still an urgent task to find new methods the early prognosis and diagnosis.

Recently, studies have shown that the metabolomics is employable for early diagnosis and for predicting clinical prognosis. As regard to the researches in sepsis, in the comparison between the septic patients and healthy subjects, potential biomarkers have been announced with their good performance characterizing sepsis. Mickiewicz et al. reported that they were able to distinguish the differences between systemic inflammatory response syndrome (SIRS) [8]. Some other works have shown discriminations of metabolic profile of septic patients in the early stage of sepsis in the condition of the outcome. In our previous pilot study, we have also applied the liquid-chromatography – mass spectrometry (LC-MS) based metabolomic to expose important differences in the metabolic prolife between the septic shock survivors and non-survivors before clinical intervention. Most of these studies were designed to be performed by using the samples at a single time point. However, empirically, good outcome of the illness also depends on positive compliance to the treatment and a good understanding of individual feedback should be therefore the foundation of personalized therapy. Consequently, in the present study we proceed to discover the discrimination of metabolic profile between the septic shock survivors and non-

survivors both before and during the treatment by using ^{1}H NMR spectroscopy metabolomics.

Materials and Methods

Patients and samples collection

All human serum samples were collected by the Jean Verdier Hospital, Paris, written informed consent was obtained from all subjects or their surrogate decision maker. Patients according with specific published criteria for septic shock at admission to the intensive care unit (ICU) were enrolled in this study. The samplings were fulfilled from January 2009 to December 2011. The screening standard included following factors: (1) younger than 30 years old; (2) hematonosis; (3) cancer and other metabolic-related diseases; (4) cirrhosis or chronic kidney disease. We included definitely 29 patients who died within 7 days after admission to the ICU and 21 alive patients in our study. All the samplings were obtained before clinical therapies on the patients under fasting condition. Serum were subsequently stored at -80^{o}C before experiments.

The serum samples were drawn under fasting conditions and were subsequently stored at -80^{o}C.

Sample preparation

450 µL of unfreezed samples were pipetted into a NMR tube of 5mm diameter together with 50µL of D2O. Prepared samples were then submitted to the NMR spectroscopy (Advance III, Bruker, Germany) Spectra were acquired at 297K (Other parameters). The ^{1}H NMR spectra were recorded by the Carr-Purcell-Meiboom-Gill (CPMG) sequence [9]. The spin-spin relaxation delay was during 18ms with 128 transients in one record. For several samples, the 2D NMR experiments by the total correlation spectroscopy (TOCSY) sequence were achieved to affirm the quantification with the 1D spectra. The mixing time was 80ms with 32 transients in one record.

Data processing

After the spectra were acquired for all the samples, they were manually phased and their linear baseline were unified based on the NMRPipe Software[10]. All free induction decays (FIDs) were multiplied by a 0.3 Hz exponential line broadening factor prior to Fourier Transformation. The spectral region was restricted between -1 to 10ppm with 11000 divisions of 0.01ppm. The region of water (4.6-5.5ppm) was excluded in order to avoid the impact of its massive intense on other signals. Peaks from 3.7 to 4.4ppm were also removed since peaks in the section represented the infusion of the starch, which aided to heighten the blood tension in the patients. The spectra were then normalized by the algorithm of quotient [11]. All the peaks were centered by the method of auto-scaling. The peaks were adequately identified by the Human metabolome database (HMDB, www.hmdb.ca) NMR library and by the Chenomx software (Chenomx Inc, Canada).

Multivariate analyses

All the multivariate analyses were achieved in-house using the Matlab software (version 2012b, Massachusetts, USA), based on the code of Trygg and Wold. A principal component analysis (PCA) for all the recorded spectra data was first used to detect outliers which may contain abnormally acquired peaks. Orthogonal projection to latent structure-discriminant analysis (OPLS-DA) was applied to establish the discriminatory models between different groups of patients. The models were validated by the cross-validation method [12].

Results

Sample distribution

116 samples from 56 patients were obtained in which 49 enrolled samples were drawn at the admission of hospitalization before clinical interventions (samples H0) in a part of the patients and 57 samples were obtained 24 hours after the hospitalization with

uniform anti-biotic treatments (samples H24). 76 samples were H0-H24 paired from the same patients (38 pairs) in which 23 pairs were from the survived patients and 15 pairs were from non-survived patients.

Identification of peaks

One of the recorded spectra was taken as an example, shown in Figure 1 with the labels of identified peaks. All the defined peaks were otherwise listed in the table 1 (Page 25) with their chemical shift and multiplicity.

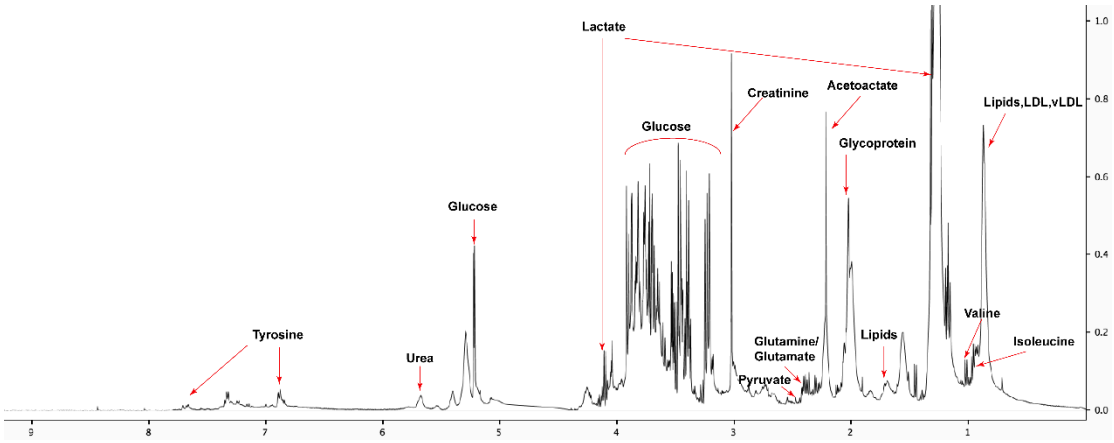

Figure1. One of the spectrum obtained in the patients of septic shock with a 500MHz 1H NMR Spectroscopy (Avance III, Bruker).

Discriminatory analyses separating septic non-survivors from survivors with samples drawn before treatments.

For the sampling H0, a model based on OPLS-DA was performed with 28 samples drawn from septic non-survivors and 21 from survivors. Shown in Figure 2, an obvious separation between the two groups of patients was observed in the score plot (Figure 2a) with the Q^2 = 0.58, a cross-validation including 500 permutations presented that the model was not over-fitting (Figure S-1). On the basis of the findings in the loading plot (Figure 2b), the most correlative peaks corresponding to the discriminatory metabolites were found and numerated. They were also cited in table 2 with their chemical shift, multiplicity and correlation. Positive correlation means the concentration of the metabolite was up-regulated in the non-survivors, and negative

correlation represented a down-regulation of the metabolite in the non-survivors. Accordingly, it was shown that levels of amino acids such as alanine, lysine, glutamate and tyrosine increased in the non-survivors. Increasing concentrations were also found in several energy metabolism-related metabolites such as 3-hydroxybutryrate, lactate creatinine. Meanwhile, metabolites involved in the tricarboxylic acid (TCA) cycle such as glucose, pyruvate, citrate and fumarate were also observed to be up-regulated in the non-survivor. Other significant up-regulating metabolites were found in choline and urea. On the contrary, glycoprotein was the only one decreased metabolite in the findings. The results showed that there existed differences between the survivors and the non-survivors before clinical intervention.

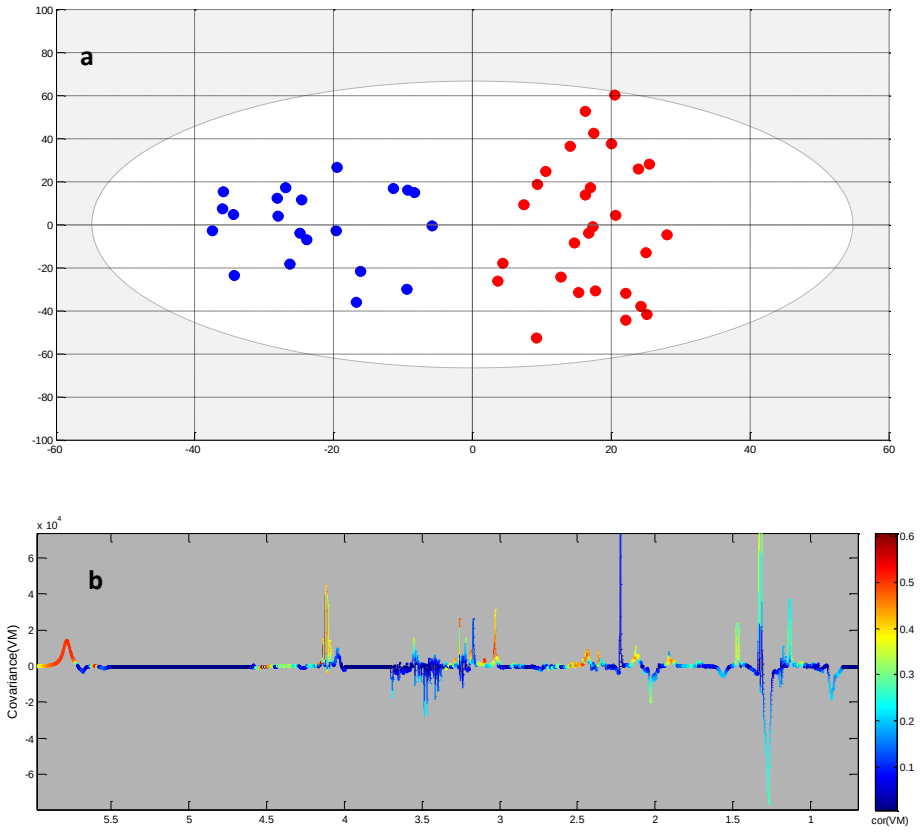

Figure 2. OPLS-DA of the discriminatory model between the septic shock survivors and non-survivors at H0. a. Score plot, blue dots represent the survivors and the red dots represent the non-survivors; b. loading plot. The color indicates the correlation between the marked peak and the classification of the sample. The closer to red the color is, the more important the correlation is. Positive peaks implies an up-regulation of the represented metabolite in the non-survivors and the negative peaks present a

diminution of the represented metabolite in the non-survivors.

Peaks	Correlation	Identification
1.06^{d}	0.39	3-Hydroxybutyrate
1.32^{d}, 4.11^{q}	0.4	Lactate
1.46^{d}	0.35	Alanine
2.02^{s}	-0.32	Glycoprotein
2.13^{m}, 2.32^{m}	0.34	Glutamate
2.37^{s}	0.43	Pyruvate
2.52^{d}, 2.69^{d}	0.44	Citrate
3.03^{s}, 3.92^{s}	0.41	Creatinine
3.19^{s}	0.49	Choline
3.23^{t},3.72^{m},3.82^{m},4.64^{d},5.23^{d}	0.48	α-Glucose
3.29^{s}	0.44	Unknown
4.21^{d}	0.34	Unknown
5.79^{s}	0.5	Urea
6.52^{s}	0.31	Fumarate
6.88^{d},7.18^{d}	0.48	Tyrosine
7.31^{m}, 7.41^{m}	0.41	Unknown
8.32^{s}	0.37	Unknown

Table 1. Discriminatory metabolites in the separation between the septic shock survivors and non-survivors at H0. s: singlet; d: doublet; t: triplet; q: quadruplet; m: multiplet.

Discriminatory analysis of the evolution of septic shock from H0 to H24 for septic shock survivors and non-survivors

For the patients having both their samples H0 and H24, a clear separation between the samples H0 and H24 was observed in the H0-H24 paired model, based on the method of multi levels [13]. On the basis of the "within model", which determines the evolution from H0 to H24, the evolution of septic shock from H0 to H24 for each patient was investigated and differences of the evolution of septic shock between the survivors and the non-survivors were taken in account in a new OPLS-DA model. H0 samples only from septic shock survivors and from non-survivors were separated from those from the H24 samples. The Q^2 for the separation in the survivors was 0.45, the primary discriminators were listed in the Table 2. Accordingly, a universe increment has been found in various amino acids from H0 to H24 for the non-surviving patients. However, a reversed variation was found in the amino acids such as valine, glutamate, glutamine and glycine for the evolution from H0 to H24 for the septic survivors. Opposite variations have been also detected in citrate and glycoprotein according to a comparison of evolution between the survivors and non-survivors.

Chmical shift	Assignment	Correlation1	Correlation2	Validation1	Variation2
0.88m	VLDL, LDL	0.72	NS	↓	-
0.97d 1.03d	Valine	NS	0.35	-	↓
1.06d	3-Hydroxyisovalerate	0.69	0.31	↓	↓
1.14d	isobutyrate	0.61	0.57	↓	↓
1.23s	CH3 lipids	0.67	NS	↓	-
1.32d 4.11q	Lactate	NS	0.38	-	↓
1.46d	Alanine	-0.48	NS	↑	-
1.58m	Lipids CH2	-0.39	NS	↑	-
1.7m	Lysine	-0.51	NS	↑	-
1.91s	Acetate	0.35	0.53	↓	↓
2.03s	Glycoprotein	0.44	-0.35	↓	↑
2.12m 2.32m	Glutamate	-0.48	0.34	↑	↓
2.07m 2.43m	Glutamine	-0.47	0.51	↑	↓
2.37s	Pyruvate	NS	0.29	-	↓
2.55d 2.62d	Citrate	-0.61	0.48	↑	↓
3.02s	Creatinine	-0.57	NS	↑	-
3.1s	Malonate	0.63	0.55	↓	↓
3.14s	Dimethylsulfone	0.72	NS	↓	-
3.19s	Choline	0.64	0.65	↓	↓
3.23t 3.72m 3.82m	alpha-Glucose	0.47	NS	↓	-
3.55s	Glycine	-0.34	0.64	↑	↓
3.65dd	Glycerol	0.56	0.45	↓	↓
4.05t	Myo-insitol	0.41	0.47	↓	↓
4.37s	Unknown	0.69	0.49	↓	↓
6.88d 7.8d	Tyrosine	-0.43	NS	↑	-
7.04s	1-MH	-0.44	NS	↑	-
7.32d	Phenylalanine	-0.39	NS	↑	-

Table 2. Discriminatory metabolites with their correlations in the separation between paired H0 and H24 samples. Correlation 1: correlation of the metabolite to the discriminatory model for the non-survivors; Correlation 2: correlation of the metabolite to the discriminatory model for the survivors. Variation1: direction of variation of concentration for the metabolite from H0 to H24 for the non-survivors; direction of variation of concentration for the metabolite from H0 to H24 for the survivors. ↑: increased concentration of the metabolite at H24 compared with H0; ↓: decreased concentration of the metabolite at H24 compared with H0. s: singlet, d: doublet, t: triplet, q: quadruplet, m: multiplet. NS: difference not significant.

Discriminatory analysis separating the samples H0 from H12 only for septic shock survivors

Another OPLS-DA model separating the H0 and H12 samples was carried out only among the septic shock survivors, aiming to understand the evolution of the disease in the subjects with optimist prognosis. For each included subject, his H0 and H12 samples were paired. The Q^2 was calculated with 2 components, and equal to 0.44. The validation proved that the model was not over-fitting. According to the score plot

of the model, a good separation between the two groups was obtained (Figure 3a). The principal metabolites which correlated to the discrimination between the two groups were shown in the loading plot (Figure 3b) and Table 3. Interestingly, for these patients, the involved metabolites were similar to the findings in the previous models but with an adverse trend of variation. In other words, generally, the serum level of energetic metabolites such as glucose, lactate and pyruvate; choline and several amino acids down-regulated in H12 samples, when it was compared with that in H0 samples. It also proved that the determined discriminators were related to the prognosis of septic shock.

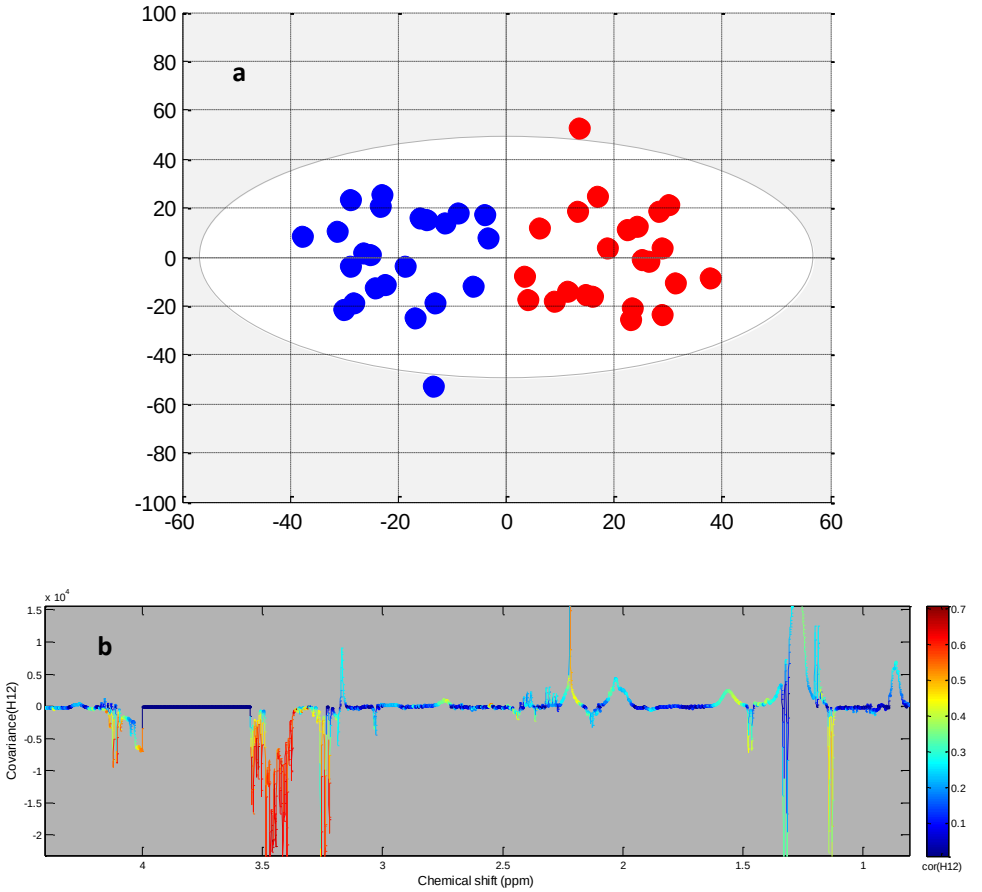

Figure 3. OPLS-DA of the paired discriminatory model comparing the H0 samples from the H12 samples for the survived septic shock patients.

Peak	Correlation	Identification
0.85^{m}, 1.27^{m}, 2.02^{m}	0.3	lipids, LDL, vLDL
1.14^{d}	-0.4	Isobutyrate
1.32^{d} 4.12^{q}	-0.42	Lactate
1.47^{d}	-0.41	Alanine
2.22^{s}	0.42	Acetoacetate
2.36^{s}	-0.39	Pyruvate
2.09^{m} 2.41^{m}	-0.39	Glutamine
3.23^{t},3.72^{m},3.82^{m},4.64^{d},5.23^{d}	-0.6	α-Glucose
4.21^{d}	-0.34	Unknown
6.89^{d} 7.18^{s}	-0.46	Tyrosine
8.13^{s}	0.48	Adenine

Table 3. Discriminatory metabolites in the paired model distinguishing the H0 samples from the H12 samples for the septic shock survivors.

Discussion

Septic shock remains a leading cause of death in the ICU nowadays. This should be due to the difficulties of the prediction of outcome in the early stage. Further, the septic shock patients are generally treated by the uniform therapy protocol, however, the individual differences such as the gravity of disease on the onset and the different responses to the clinical intervention should affect the final outcome. Therefore, in the present study, we have investigated differences of metabolic profile evolution from the admission into ICU to one day after the admission between the survivors and the non-

survivors. On the basis of our results, we exposed that metabolic differences might exist both before and during the clinical therapy between the septic shock survivors and non-survivors. Discriminators such as lactate, creatinine, glucose and glutamate were present in the two separation, they were all up-regulated in the non-survivors.

According to the comparison of evolution H0 to H24 between survivors and non-survivors, opposite variations in the metabolites such as several amino acids, citrate and glycoprotein were found. An increased level of various amino acids and citrate in the non-survivors at H24, compared with H0, showed a more severe case of septic shock as the same result had been exhibited with the separation between the survivors and non-survivors before clinical intervention. Besides, the decrement of glycoprotein from H0 to H24 for the non-surviving patients was accord with the finding obtained in the survivors vs. non-survivors model at H0. On the contrary, decreased levels of amino acids such as glutamate, glutamine and glycine, as well as citrate were found in the H0 to H24 evolution for the survivors and an increased concentration of glycoprotein was obtained at H24 compared with H0 for the survivors, which affirm that the defined significant discriminators were responsible for the death before and even after clinical intervention.

Also, we report that the above discriminators decreased in the survivors from H0 to H12, this finding confirmed that the blood level of the discovered discriminators were correlated with bad prognosis of septic shock. Namely, the higher the level of these molecule was, the poorer the outcome was during the first twelve hours after hospitalization.

It has been reported that sepsis related systemic inflammatory responses (SIRS) elicited insulin resistance (IR). Local activation of immunological response is induced by the reactions to the endotoxin released by the infectious bacteria. The reactions suppress insulin receptor subtract-1 and therefore attenuate insulin receptor signaling. As the level of blood sugar is directly modulated by insulin, in the current study, the present of glycemia in the septic non-survivors might provide evidence of a more severe inflammation in the non-survivors before clinical interventions. The effect was also proved to be related with poor outcome in the model 2 and 4. On the contrary,

for the model separating H0 and H24 samples for the survivors, the level of glucose decreased at H24, which showed an optimist evolution of case.

Lactate is another one of the common indicators of bad outcome in all the achieved models, its level in the serum reflects the severity of hypoxia and disorder of the energy supply. Correspondingly, pyruvate, which is an important materiel for the TCA cycle, was also found to be elevated in the more severe septic shock cases. Interestingly, although considerable amount of pyruvate was transferred to lactate due to the low oxygen press in the blood, increases of two TCA cycle-related metabolites (fumarate and citrate) were still present in the non-survivors. One reason might be that the increased level of various amino acids induced anaplerotic reactions and enhanced the concentration of the related TCA cycle metabolites. The results were similar to those in several other works and equally revealed in our previous study. Furthermore, it has been known that mitochondria were injured by the over-production of NO and free residues during the sepsis [14, 15]. Thus, the disorder of the respiratory chain might be another reason for the accumulation of TCA cycle related metabolites and for the conversion from pyruvate to lactate.

Glycoprotein is mostly located on the membrane of cells, the diminution of its level in the non-survivors might indicate the existence of cell injuring. Further, it has been well known that the waste of muscle tissue and a sever protein breakdown, which might be another issue of the suppress of glycoprotein, is present in the case. Likewise, it was declared by Wang et al. that the ratio lactate/albumin was an independent marker of multi-organ dysfunctions (MODs) and death [16].

Meanwhile, as it is known, the up-regulating creatinine indicates the waste of muscle tissue. Thus, both the augment of the amino acids and creatinine could be a proof of the breakdown of glycoprotein. Other significant discriminators between the survivors and the non-survivors included choline and urea. Choline was known to be bond with the reaction of cell signaling responding the inflammation [17]. A mounting of urea could be a signal of the more severe kidney injury [18].

It has been widely reported that the clinical scores evaluating the severity of sepsis was not accurate. In the current study, we exhibit that the NMR metabolomics based

discriminatory models experience a better prediction of mortality than the two clinical scores (AUROCSOFA=0.63 and AUROCAPSII = 0.76). Our results may help to improve the early characterization of severe cases in the septic shock patients, which may be an evidence for the personalized treatment.

Conclusion

In this study, we reveal metabolic differences between the survivors and non-survivors both before and different evolutions during the 24 first hours after hospitalization of septic shock between the survivors and non-survivors. The deregulation of some amino acids and some energy-related metabolites such as glucose, lactate and creatinine account for the discrimination between the septic survivors and the non-survivors. We note that the consistence of the variation in such metabolites was found in the separation of patients before and after clinical intervention. The comparison between the AUROC of our model and the prediction of mortality by the SOFA or APSII score showed that our models are more reliable to predict the outcome of septic shock. Our findings illustrate that the ^{1}H NMR based metabolomics is helpful to improve the prognosis of septic shock.

References

1. Bone RC, Balk RA, Cerra FB, Dellinger RP, Fein AM, Knaus WA et al. DEFINITIONS FOR SEPSIS AND ORGAN FAILURE AND GUIDELINES FOR THE USE OF INNOVATIVE THERAPIES IN SEPSIS. Chest. 1992;101(6):1644-55.

2. Levy MM, Fink MP, Marshall JC, Abraham E, Angus D, Cook D et al. 2001 SCCM/ESICM/ACCP/ATS/SIS International Sepsis Definitions Conference. Crit Care Med. 2003;31(4):1250-6.

3. Balk RA. Pathogenesis and management of multiple organ dysfunction or failure in severe sepsis and septic shock. Crit Care Clin. 2000;16(2):337-+.

4. Rivers E, Nguyen B, Havstad S, Ressler J, Muzzin A, Knoblich B et al. Early goal-directed therapy in the treatment of severe sepsis and septic shock. New Engl J Med. 2001;345(19):1368-77.

5. Dellinger RP, Levy MM, Carlet JM, Bion J, Parker MM, Jaeschke R et al. Surviving Sepsis Campaign: International guidelines for management of severe sepsis and septic shock: 2008. Crit Care Med. 2008;36(1):296-327.

6. Vincent JL, de Mendonca A, Cantraine F, Moreno R, Takala J, Suter PM et al. Use of the SOFA score to assess the incidence of organ dysfunction/failure in intensive care units: Results of a multicenter, prospective study. Crit Care Med. 1998;26(11):1793-800.

7. Lee WJ, Woo SH, Kim DH, Seol SH, Park SK, Choi SP et al. Are prognostic scores and biomarkers such as procalcitonin the appropriate prognostic precursors for elderly patients with sepsis in the emergency department? Aging Clin Exp Res. 2016;28(5):917-24.

8. Mickiewicz B, Vogel HJ, Wong HR, Winston BW. Metabolomics as a novel approach for early diagnosis of pediatric septic shock and its mortality. Am J Respir Crit Care Med. 2013;187(9):967-76.

9. Foxall PJ, Spraul M, Farrant RD, Lindon LC, Neild GH, Nicholson JK. 750 MHz 1H-NMR spectroscopy of human blood plasma. J Pharm Biomed Anal. 1993;11(4-5):267-76.

10. Delaglio F, Grzesiek S, Vuister GW, Zhu G, Pfeifer J, Bax A. NMRPipe: a multidimensional spectral processing system based on UNIX pipes. J Biomol Nmr. 1995;6(3):277-93.

11. Dieterle F, Ross A, Schlotterbeck G, Senn H. Probabilistic quotient normalization as robust method to account for dilution of complex biological mixtures. Application in 1H NMR metabonomics. Anal Chem. 2006;78(13):4281-90.

12. Westerhuis JA, Hoefsloot HCJ, Smit S, Vis DJ, Smilde AK, van Velzen EJJ et al. Assessment of PLSDA cross validation. Metabolomics. 2008;4(1):81-9.

13. Westerhuis JA, van Velzen EJ, Hoefsloot HC, Smilde AK. Multivariate paired data analysis: multilevel PLSDA versus OPLSDA. Metabolomics. 2010;6(1):119-28.

14. Kim S-C, Pierro A, Zamparelli M, Spitz L, Eaton S. Fatty acid oxidation in neonatal hepatocytes: effects of sepsis and glutamine. Nutrition. 2002;18(4):298-300.

15. Nava E, Palmer R, Moncada S. Inhibition of nitric oxide synthesis in septic shock: how much is beneficial? The Lancet. 1991;338(8782-8783):1555-7.

16. Wang B, Chen G, Cao Y, Xue J, Li J, Wu Y. Correlation of lactate/albumin ratio level to organ failure and mortality in severe sepsis and septic shock. J Crit Care. 2015;30(2):271-5.

17. Parrish WR, Rosas-Ballina M, Gallowitsch-Puerta M, Ochani M, Ochani K, Yang LH et al. Modulation of TNF release by choline requires alpha7 subunit nicotinic acetylcholine receptor-mediated signaling. Mol Med. 2008;14(9-10):567-74.

18. Waikar SS, Liu KD, Chertow GM. Diagnosis, epidemiology and outcomes of acute kidney injury. Clin J Am Soc Nephrol. 2008;3(3):844-61.

2.3.3 Conclusion to the first part of experimental research

Septic shock is the most severe case of sepsis inducing always a high mortality. However, the mechanism of the evolution from septic shock to death for the patients eventually died of septic shock is still not clear. From a point of view of metabolomics, the alterations in the metabolic profile might reveal the related varied pathways in the non-survivors compared with the survivors.

In this first part of thesis work, the goal is to predict septic shock mortality by both NMR and MS-based metabolomics. The separation between the septic shock survivors and non-survivors was found before clinical intervention according to the analyses of metabolic profiles of the patients, using the above two techniques. Beyond the coincide metabolites detected by the two methods, metabolites such as kinds of fatty acids, bile acids were only detected with the MS-based approach whilie the NMR-based analyses determined glucose and glycoprotein which were not detectable in our LC-MS experiences. Further, on the basis of the results involving the evolution of septic shock metabolome during the first 24 hours after the admission into the ICU, differences of evolution from H0 to H24 between the survivors and the non-survivors have been revealed. Notably, the deregulation of energy-related metabolism and a comprehensive up-regulation of the amino acids, as well as the decline of glycoprotein are found to be specific in the non-survivors. Moreover, using both MS and NMR based metabolomics shows a power to acquire a reamarkable coverage of metabolites and they are mutally complementary.

III. Metabolomic studies of hepatocellular carcinoma (HCC)

3.1 Introduction of hepatocellular carcinoma

Hepatocellular carcinoma is the fifth most malignant common type of cancer, and is the most common type of liver cancer [168]. According to the previous report, the incidence of HCC is more than 3 cases in 100000 people, and the number is increasing in recent years [169]. More than 80% of the HCC cases were reported caused by the hepatitis virus (hepatitis B or C) infection or virus-induced cirrhosis [170]. Other possible inducing factors includes hepatic injury caused by frequent alcohol abuse [171] or other kinds of intoxication [172], and by obesity induced non-alcoholic fatty liver disease (NAFLD) [173, 174], etc.

The HCC is diagnosed by some physical symptoms (such as malaise, anorexia, wasting, right upper quadrant abdominal pain, and distension). And confirmed by the clinical imaging (such as ultrasound, IMR, CT, etc.). The increasing blood concentration of α-fetoprotein AFP is well referred as the signal of the development of HCC [175]. The Barcelona clinical Liver Cancer (BCLC) staging is proposed as the grading standard of HCC [176]. The staging system estimates the tumor stage (the Milan criteria is frequently referred [176]), liver function status, physical status and cancer symptoms. The main treatments of HCC includes the liver transplantation [177], surgical resection [178], percutaneous injection (PI) [179], radiotherapy and radio frequency ablation (RFA) [180]. Among which, the first two strategies were reported with slightly better outcome than the others, but they are easier to introduce additional surgical trauma [181]. And, HCC is not sensitive to chemotherapies because of its abnormal apoptosis [182].

Early screening, especially the follow-up in the patients affected by cirrhosis or hepatitis by imaging tests has been rifely recommended as a crucial improvement for the outcome. Yet, due to the liver compensatory function and the insufficient of the

molecular biomarker like AFP, the early diagnosis of HCC remains challenging and HCC is still one of the most lethal cancers. The mortality was recently noted till more than 50% [183]. Furthermore, like other cancers, the primary threats for the survival of HCC are the metastasis and recurrence. Until present, there is always a lack of evidence to predict the two risks in the perioperative period. Hence, to sum up, the discovery of predicting biomarkers is an urgent demand for both the diagnosis and prognosis of HCC.

3.2 State of arts for metabolomic studies of HCC

3.2.1. Metabolomics aiding the diagnosis of HCC

Even though the detection of HCC by the clinical imaging techniques is reliable for the diagnostic of HCC. For the people “in high risk” of suffering from HCC, such as cirrhosis or hepatitis patients, or even the hepatitis B virus carriers, the early screening is important. This is because the development from cirrhosis or from hepatitis to HCC is common. Besides, the misdiagnosis in the early stage may happen by the confusion of the hypervascular nodules or by the concealment of the cirrhotic fibers [184]. The chemical examination that determines the blood level of AFP was regarded as useful for the diagnosis of HCC. However, it has been previously reported that AFP was not as specific as the biomarker of HCC. As metabolomics is powerful in the discovery of novel biomarkers, the search for new biomarkers of HCC has become an important task in many metabolomic studies.

Various metabolomic studies based on the analyses on serum has been performed. In one of the precedent works from our laboratory (Dalian, China) metabolomic study aiming to find out the biomarkers of diagnosis of HCC has been performed in the model of rats and then tested in the model of human patients. In the study, non-targeted method using LC-MS revealed that 3 metabolites (taurocholic acid, lysophosphoethanolamine 16:0, and lysophosphatidylcholine 22:5) were potential to

affirm the rats with HCC against the control rats. Additionally, they were equally useful to distinguish different HCC stages in the rats. The following test study of the effect of the 3 metabolites in human patients showed that the defined markers were effective for the discrimination between small HCC and cirrhosis. They were ulteriorly found to be significant separating HCC patients from the patients with chronic liver disease [185].

Similar work was done by Liu et al, who used RPLC-MS, HILIC-MS and NMR approaches for the HCC discovery in human patients. According to their findings, variations of the metabolites such as β-hydroxybutyrate, oxaloacetate, short chain fatty acids, bile acids, carnitines and lysoPCs between healthy volunteers and HCC patients were found. The altered metabolites indicated disorders in the pathways such as ketogenesis, TCA cycle, lipid genesis, and bile acids in HCC patients. Further, HCC patients were also found separable from the cirrhotic patients. Precisely, levels of glycerol, β-hydroxybutyrate, and acetylcarnitine were adjacent between cirrhotic patients and healthy controls while their levels were elevated in HCC cases. Opposite distinction was found in tyrosine, phytosphingosine, PC 4:0 and LPC 16:0 [186]. The findings in deregulation of lipids were supported by analogic reports by Fages, Zhou and Nahon as well [187-189]. Not only with serum samples, but also urine samples were found useful to distinguish the HCC from benign tumor or healthy controls. The abnormal levels of bile acids are confirmed in the patients of HCC [190].

Furthermore, another our precedent work exhibited the metabolic variation of the HCC tumor compared with the peripheral tissues. Determined varied pathways such as glycolysis, gluconeogenesis, and beta-oxidation with the suppressed TCA cycle were account for the separation [191]. In all the above studies, the sensitivity and the specificity of the defined metabolite discriminators performed better than AFP in diagnosing HCC. In brief, both NMR and MS based-metabolomics are useful to improve the HCC diagnosis.

3.2.2. Improvement of HCC prognosis by metabolomics

Recurrence and metastasis of HCC are the two major threats after the treatment removing HCC tumor. This may be due to unsatisfying deletion of cancer cells, micro-vascular invasion and incorrect postoperative conditioning. However, their mechanisms are not clear until present. Consequently, an appropriate prognosis in the early stage of HCC is always needed for guiding the following therapy and recovery policy. But, the scarce of biomarkers predicting the HCC metastasis or recurrence makes it still problematic. Thus, seek for the biomarkers predicting the metastasis or recurrence has been another important goals in some metabolomic studies.

Prediction of HCC recurrence using metabolomics

According to the GC-MS analysis on urine from HCC patients, Ye et al. showed it possible to tell differences between early recurrent and non-recurrent HCC patients. Samples before and after surgical operation were collected and tested. As to results, the principally varied metabolic pathways in the perioperative period involve purine and pyrimidine metabolism, various amino acids and glyoxylate metabolism [192]. Another work concerning the HCC recurrence was performed with the LC-MS platform by Zhou et al. In the non-targeted metabolomic study on serum samples, comparison of metabolic profiles between early recurrent HCC and late recurrent HCC with or without vascular invasion showed an apparent separation among the samples. Apart from methionine and two aromatic amino acids, lipids such as bile acids, steroids and fatty acids [193].

Prediction of HCC metastasis using metabolomics

Metabolomic characteristics of HCC metastasis-induced lung cancer was studied by Wang et al. using NMR based metabolomics. The established model was based on the operation on the rats. By comparing among controls, HCC rats with and without metastasis, it was proposed that the alterations in the pathways of glycolysis, glycine and choline were related to the HCC metastasis [194].

Interestingly, the factors revealed which linked to the recurrence were similar to those in the separation between HCC and other cases. The fact might indicate that the

marker metabolites for HCC development, e.g. the bile acids and glycine and serine pathway were deregulated, were also associated to the prediction of the outcome of HCC. Especially, the up-regulated glycine, serine pathway and bile acids were universally observed in the diagnosis and prognosis of HCC. Thus, quantification of the relevant molecules in the patients with high risk of being affected by HCC and in HCC patients can be referred for the diagnosis and prognosis of HCC.

3.2.3. Other metabolomic studies on HCC patients with/without hepatitis

Both chronic hepatitis B and C are the principal causes of HCC [195, 196]. Other than the two major inducements, alcohol abuse and obesity should also account for the important issues [197, 198]. However, the mechanism of development of viral HCC differs from that of non-viral HCC, and so does the corresponding clinical treatments. For example, it was recommended by the guideline that treating viral HCC should start from the therapy for the hepatitis [168]. In order to make clear the impact of the inducing factors in HCC, metabolomic studies which investigate the metabolic characteristics in different type of HCC were carried on.

Actually, the metabolic differences between viral and non-viral HCC had been well known, thus, our previous study studying the influence of the RFA therapy on HCC patients were achieved separately among HCC patients with or without hepatitis virus [199].

According to the contribution of Gao et al., metabolic differences among patients suffering from HCC, cirrhosis, and hepatitis B were well shown. As being discussed, the elevated TCA cycle related metabolites were specific for HCC compared with the HBV patients. Besides, the up-regulated lipogensis was proven once again true in the comparison between other types of liver diseases and HCC [200]. Another study focusing on determining the metabolic profile of HCC patients with hepatitis B distinguished well the HCC patients with HBV from those without viral infection. On the basis of the findings, even though metabolic variations like increased fatty acids in HBV-related HCC patients were in accord with those in the previous studies, which

concern the comparison between HCC and cirrhotic patients, some adverse alterations were reported this time such as less concentrated glycolysis and TCA cycle-related metabolites, blood amino acids including serine and glycine. This might be partially explained by the demand of energy and amino acids in the presence of malignant tumor. The other reason might be due to the activity of hepatitis virus which depletes more energy and amino acids [201].

Similar work aiming to investigate the metabolic features in HCC patients induced by HCV was carried out by Fitan et al. Samples from the whole preoperative period were analyzed and they witnessed that unlike the findings with HBV-related HCC, the HCC patients affected by HCV-induced cirrhosis got elevated amino acids and lipids levels than the HCV cirrhosis patients without HCC [202]. The divergence of results might imply that even the metabolic profiles of HCC patients vary when they are affected by different type of hepatitis virus.

Among the metabolomic studies on non-viral HCC, alcohol-induced HCC models were simulated in the nude mice in the study of Li et al. By comparing with the controls, it was found that amino acids such as leucine, phenylalanine and tryptophan were down-regulated in the alcohol-induced HCC, so were LPEs and LPCs. Meanwhile, mounting PCs were otherwise observed. In the study, the profiles of metabolites of cases of liver injury were also compared with those of the controls. Interestingly, the defined discriminator metabolites for the separation HCC/control were also significant for the model separating liver injury from healthy subjects [203].

Both genetic and metabolic specificities in HCC patients with NAFLD were investigated by Clark et al. The observed metabolite discriminators separating the NAFLD from HCC patients were generally consistent with the findings in the alcohol-related HCC. Concretely, declines of tryptophan, phenylalanine and LPCs were again found in the HCC cases when compared with the patients suffering from NAFLD. Other defined metabolites included ketoglutarate, creatine, taurine which increased and arachidonic acid, lysine and citrulline which decreased in the HCC patients [204]. Additionally, the relevant HCC metabolomic studies have been summarized in table 3.

Summary of recent metabolomic studies in the field of HCC

Author and year	Biological specimens	Technological Platform used	Decreased or increased metabolites in the patients compared to the control group
Gao H (2009)	serum	NMR	Acetate, pyruvate, glutamine, glycerol, tyrosine, phenylalanine alpha-ketoglutarate, 1-methylhistidine LDL, VLDL, valine, acetoacetate, choline, taurine, "unsaturated lipid"
Fitian AI (2014)	serum	GC/MS UPLC/MS-MS	HCC vs. cirrhosis: 12-hydroxyeicosatetraenoic acid (12-HETE), 15-HETE, sphingosine, γ-glutamyl oxidative stress-associated metabolites, xanthine, amino acids, serine, glycine , aspartate , a-cylcarnitines HCC vs. controls: Azelate, Taurochenodeoxycholate (TCDCA) Taurocholate (TCA), Taurolithocholate 3-sulfate, Grycocholate (GCA) Tauroursodeoxycholate (TDCA) Grycochenodeoxycholate (GDCA) Undecanedioate Sebacate (decanedioate)
Yang Y(2007)	liver	NMR	High-grade HCC vs. low-grade HCC tumors: lactate, leucine glutamine, glutamate, glycine and alanine, choline and phosphorylethanolamine (PE) glucose,PC, GPC, triglycerides and glycogen
Yin P(2009)	serum	HPLCESITOFMS	TCA, GCA, bilirubin, TCDCA, GCDCA, carnitine, acetylcarnitine Hypoxanthine, phytosphingosine, dihydrosphingosine, LPC(18:2), LPC(18:3), LPC(16:1), LPC(18:0), taurine, 6-methyl-nicotinic acid
Chen T(2011)	serum /urine	UPLCESIQTOFMS and GCTOFMS	**Serum:** carnitine, GCDCA, GCA, cysteine, 2-oxoglutarate, lactate, pyruvate, inosine, erythronate, **Urine:** GCA, dopamine, adenosine, xanthine, phenylalanine, dihydrouracil, hypotaurine, threonine, *N* acetylneuraminic acid Serum: glycerol, glycine, serine, aspartate,citrulline, tryptophan, lysine, glucosamine, phenylalanine, β-alanine, glycerate, arabinose, creatinine, phosphate, O-Phospho-l-serine Urine: normetanephrine, Cysteine, TMAO, adenine, cysteic acid, 6-aminohexanoate, creatine
Patterson AD(2011)	plasma	UPLCESIQTOFMS	glycodeoxycholate, deoxycholate 3-sulfate, bilirubin,fetal bile acids 7α-hydroxy-3-oxochol-4-en-24-oic acid and 3-oxochol-4,6-dien-24-oil LPC(20:4), LPC(22:6)LPC(14:0), LPC(16:0), LPC(20:2), LPC(18:0) LPC(18:1), LPC(18:2), LPC(20:5), LPC(18:3), LPC(20:3)
Wang B(2012)	serum	UPLCESIQTOFMS	GCDCA , Canavaninosuccinate, phenylalanine, PC(16:0/22:6, LPC(16:0), LPC(18:0), PC(18:0/18:2), PC(16:0)/20:4)
Ressom HW (2012)	serum	UPLCESIQTOFMS	lysophosphatidylcholine (lysoPC 17:0) glycochenodeoxycholic acid 3-sulfate (3-sulfo-GCDCA), glycocholic acid (GCA), glycodeoxycholic acid (GDCA), taurocholic acid (TCA), and taurochenodeoxycholate (TCDCA)
Xiao JF	serum	UPLCESIQTOFMS	PhePhe TCDCA, GDCA, 3β, 6β-dihydroxy-5β-cholan-24-oic acid, oleyol carnitine
Zhang A	urine	UPLCESIQTOFMS GCA	GCA
Nahon P(2012)	serum	NMR	Glutamate, acetate ,N-acetyl glycoprotein Glutamine
Budhu A(2013)	liver	GCMS	monounsaturated palmitic acid
Beyoğlu D(2013)	liver	GCMS	glucose, glycerol 3- and 2-phosphate, malate, alanine, myo-inositol, and linoleic acid glycolysis, attenuated mitochondrial oxidation, and arachidonic acid synthesis
Chen F(2011)	serum	UPLCESITQMS	1-Methyladenosine
Shariff MI, (2011)	urine	NMR	Creatine, Carnitine Glycine, TMAO, Hippurate, Citrate, Creatinine
Wu H(2009)	urine	GCMS	xylitol and urea elevated.
Yang J(2004)	urine	HPLC	pseudouridine, 1-methyladenosine, xanthosine, 1-methylinosine, 1- and 2-methylguanosine, *N*4-acetylcytidine, adenosine
Chen J(2009)	urine	HILIC RPLC MS	Hypoxanthine, Proline betain, Acetyl carnitine, Carnitine, Phenylacetylglutamine Carnitine C9:1, Carnitine C10:3, Butylcarnitine

Red color: increased metabolite
Blue color: decreased metabolite

Table 3. A summary of metabolomic-based HCC studies [205].

3.3. Experimental research: Comparison of the metabolomic profiles in the patients suffering from hepatitis C-related hepatocellular Carcinoma with and without recurrence.

The second part of the thesis work concerns the prediction of recurrence in small HCC patients. It is known that small HCCs (≤5 cm or up to 3 lesions ≤3cm) lead a better outcome than big ones [206]. And, for the small HCCs, the RFA treatment is recommended since it is effective and brings less operational wound to the patients. Even though, the HCC recurrence and metastasis remain the principal threats for the outcome. It was reported that the rate of HCC recurrence was up to 70% for 3 years and 80% for 5 years after the treatment [207, 208].

Biomarkers such as AFP, MAGEs and CK_{19} were currently accepted to predict the HCC recurrence [209]. But, the altered metabolic pathway correlated to the relapse of HCC is still not clear. Thus, finding out novel metabolite biomarkers predicting the recurrence is always required.

As introduced before, many metabolomic studies have been performed to achieve the goal, and some potential metabolite biomarkers were discovered with their remarkable sensibility and specificity. For example, in one of the past studies of the Chinese laboratory, LC-MS was applied to determine the metabolic characteristics in early and late HCC recurrent patients. Various lipids were found significant in the discrimination between early recurrent and late recurrent HCC patient [193]. For the current study of HCC recurrence, we attempted to make clear of the variations in the pathways such as glycolysis and TCA cycle in the recurrent subjects. GC-MS is qualified to detect and well quantify such metabolites, it was therefore chosen to be applied.

Additionally, different types of HCC like viral-HCC and non-viral HCC should be distinguished in the treatment and prognosis. The metabolic differences between viral-HCC and non-viral HCC have also been well emerged in one of our past studies [199]. However, to our known, these differences were not viewed in the past metabolomic studies which aim to determine the biomarkers of relapse. Besides, more

than one sampling before and after clinical interventions may help to understand the feedbacks to the treatment. Thus, in the current work, we intend to find out potential biomarkers in viral and non-viral HCC respectively, with two samplings in pre- and post-operative periods.

3.3.1 Study 3: Determination of metabolite biomarker candidate for recurrence of hepatocellular carcinoma in the hepatitis C virus-related HCC patients

Determination of metabolite biomarker candidate for recurrence of hepatocellular carcinoma in the hepatitis C virus-related HCC patients

Zhicheng Liu[1,2], Pierre Nahon[3,4], Zaifang Li[1], Peiyuan Yin[1], Yanli Li[1] Roland Amathieu[2,5], Nathalie Ganne-Carrié[3], Marianne Ziol[6,7], Nicolas Sellier[8], Olivier Seror[8], Laurence Le Moyec[9], Philippe Savarin[2*] and Guowang Xu[1*]

1. CAS Key Laboratory of Separation Science for Analytical Chemistry, Dalian Institute of Chemical Physics, Chinese Academy of Sciences, 457 Zhongshan Road, Dalian 116023, China
2. Université Paris 13, Sorbonne Paris Cité, Laboratoire de Chimie, Structures et Propriétés de Biomateriaux et d'Agents Therapeutiques, UMR 7244, F-93017 Bobigny, Bobigny 93000, France
3. Hepatology service, Jean Verdier Teaching Hospital, AP-HP, Bondy 93140, France
4. INSERM U1162, Génomique Fonctionnelle des Tumeurs solides, INSERM U1162, , Paris, France
5. Intensive Care Unit, Jean Verdier Teaching Hospital, AP-HP, Bondy 93140, France
6. APHP, service d'Anatomie Pathologique, Hôpital Jean Verdier; BB-0033-00027. Centre de Ressources Biologiques Maladies du foie. Groupe Hospitalier Paris-Seine-Saint-Denis,France
7. BB-0033-00027. Centre de Ressources Biologiques Maladies du foie, Groupe hospitalier Paris-Seine-Saint-Denis, Bondy, France
8. APHP, service de Radiologie, Hôpital Jean Verdier, Bondy, France

9. Université d'Evry Val d'Essonne, UBIAE, EA7362, Evry, France

* Corresponding author:

Prof. Dr. Philippe Savarin, Université Paris 13, Sorbonne Paris Cité, Laboratoire de Chimie, Structures et Propriétés de Biomateriaux et d'Agents Therapeutiques, UMR 7244, F-93017 Bobigny, Bobigny 93000, France. E-mail: philippe.savarin@gmail.com.

Prof. Dr. Guowang Xu, CAS Key Laboratory of Separation Science for Analytical Chemistry, Dalian Institute of Chemical Physics, Chinese Academy of Sciences, Dalian 116023, China. Tel. /fax: 0086-411-84379530. xugw@dicp.ac.cn

Abstract

Hepatitis C virus (HCV) infection leads to a high risk of converting to hepatocellular carcinoma (HCC). Radio frequency ablation (RFA) has been proved effective for early stage of small HCC. Whereas, the HCC relapse is still the primary threat for the outcome after the therapy. In the present study, with the comparison between recurrent and non-recurrent patients, we aim to understand the characteristics of metabolic profile variation for HCC recurrence before and after RFA therapy by applying gas chromatography-mass spectrometry (GC-MS) based metabolomics. Significant variations were observed in the pathways such as glycerolipid, TCA cycle, fatty acids and amino acids between recurrent and non-recurrent patients. We report that the variation trend of the involved pathways are not coincided except for the fatty acids before and after RFA treatment. Using a random forest (RF) test and a validation with other samples in the validation set, the combination biomarker by glutamate and aspartate showed a good performance in predicting the HCC recurrence before RFA treatment while the combination of glycerol and proline was determined for predicting recurrence in HCV-related HCC patients after RFA treatment.

Key words: HCC, HCV, recurrence, gas chromatography metabolomics, combinational biomarker.

Introduction

Hepatocellular Carcinoma (HCC) is one of the most common cancers in the world (1). Despite of improvement of survival in recent years (2,3), the high worldwide incidence and malignancy-associated death rate is still challenging, due to the high rate of recurrence and the difficulties of prognosis. In the present, surgical resection, liver transplantation, percutaneous injection (PI) and radio frequency ablation (RFA) are the primary means of curative therapies for HCC. It has been reported that the first two above leaded a slight higher 5-year overall survival than RFA (4). However, RFA takes priority when the HCC is diagnosed at early stage or when the tumor size is small, since this approach shows its safety, relative simplicity and low operative wound to the patients (5). As for the risk factors for HCC, it has been claimed that more than 80% cases of HCC are associated with viral hepatitis, which induces chronic cirrhosis bringing a high risk of HCC (2).

As to the hepatitis C-related HCC, the prevalence is always mounting worldwide in recent years. Especially, in the countries such as the Japan, Egypt and some African countries, hepatitis C virus (HCV) infection has been the overwhelming cause promoting HCC (6). It has been suggested that HCV contributed to HCC by directly modulating pathways that promote malignant translation of hepatocytes (7). HCC may be induced indirectly via HCV involved chronic inflammation, cell death, proliferation, and cirrhosis. It was reported that HCC risk increases to 17-fold in HCV-infected patients compared to HCV-negative subjects (8) However, direct-acting antiviral treatment has been recently reported to be associated with a higher risk of HCC recurrence, which makes the therapy to the HCV-related HCC cases more complicated (9).

Early screening and diagnosis of HCC are recommended in the high-risk patients (10), and known to be essential to improve the outcome. To this end, beyond the traditional marker alpha fetoprotein (AFP), which was demonstrated to be possibly inaccurate, various new biomarkers have been applied in the clinical assessments to execute early screening and prediction of the outcome (2). Besides, it has been shown that the metabolomics is employable in the early diagnosis and prognosis (11,12). Our previous metabolomic studies have revealed the differences of metabolic profiles existing between HCC patients and healthy controls or cirrhotic patients (13-15), and liquid chromatography-mass spectrometry (LC-MS) can be used to discriminate HCC early recurrence from late recurrence (16). Similar studies were also reported by other researchers (17-22). However, in most of those previous HCC studies, the distinct of the development of HCC between hepatitis virus-infected patients and non-viral patients was not taken in consideration. In one of our previous studies, we have demonstrated that the metabolic profiles from viral HCC patients were distinguished from those of non-viral HCC patients (23). To go further, in the present study, we attempt to compare the metabolic profile between the recurrent and non-recurrent HCV-related HCC patients, before and after their RFA treatment, so as to seek out potential metabolite biomarker candidate predicting the HCC relapse.

Materials and methods

Sample collection

All the serum samples were collected by the Jean Verdier Hospital, Bondy, France (F93140). They were from the same cohort of HCC as our previous study (23). The patients diagnosed as HCV infection-related HCC according to the criteria from January 2002 to December 2012 were included.

21 enrolled patients were encompassed in the training set and 25 patients were comprised in the validation test. For all the patients concerned, a follow-up visit had been achieved until present day. The recurrence of HCC in the recurrent patients was detected less than 2 years after the RFA treatment. Along the follow-up visit, the first sampling had taken place before the RFA therapy within 14 days, noted as BT while the AT were the samples drawn two months after the RFA therapy.

Chemicals

The derivatization reagents, pyridine, N-methyl-N-(trimethylsilyl)-trifluoroacetamide (MSTFA) and the internal standard L-Norvaline were purchased from Sigma-Aldrich China Inc. (Shanghai, China). The dichloromethane was bought from Merck (Darmstadt, Germany). The ultrapure water was obtained by Milli-Q water purification system (Millipore, USA). Other chemicals used for reference substance were listed in the supplementary information (S1).

Sample preparation

The samples in the training set and the validation set were stepwise analyzed. All of them were initially stored at -80^{o}C until the sample preparation, which was proceeded on ice. An equal aliquot was extracted from each serum sample in order to make up a pool of samples, from which 16 quality control (QC) samples in the training set and 9 QC samples in the validation set were afterward subpacked. For the real samples, a volume of 100 μL was extracted from each sample into the eppendorf tube where 400 μL methanol solution (methanol: H2O = 4:1) was then added to precipitate proteins. 440 μL liquid supernatant from each tube was finally drawn after the centrifugation at the condition of 4 ^{o}C and 15 000 x g for 15 minutes. All those extracted samples were

then freeze-dried.

During the redissolution process, 100 μL of methoxyamine solution (20 mg/mL in pyridine) was added to each sample. The samples were thereafter taken to the water bath for derivatization reaction during 1.5 hour. The following step was the reaction in the water bath with 80 μL of MSTFA added during one hour. After centrifugation, the supernatant was transferred to the mass spectrometry for the following GC-MS analysis. The samples in the validation set were similarly prepared but 10μL of L-Norvaline was otherwise added into the samples to be the internal standard.

GC-MS analysis

Shimadzu GC-MS 2010 was used for the metabolic profiling of each sample. A capillary column (30m x 250μm x 0.25μm) and an electron ionization (EI) source were employed. The carrier gas was helium with a flow rate of 1.2 mL/min through the chromatography column. The split ratio was set to 10:1. For the training set, the gradient temperature program was set as follows: 70 ^{o}C at the beginning (during 3 minutes), then gradually increased to 220 ^{o}C by an increase of 4 ^{o}C/min, and then heat up to 300 ^{o}C with the gradient at 8 ^{o}C/min, held for 10 minutes. The voltage of the detector was at 1.1 kV. The temperature of the injection port and the transfer line was kept at 280 ^{o}C. The temperature of the ion source was 230^{o}C. The scan field was set between 33 to 600 m/z.

For the validation set, all the similarly prepared samples were analyzed in the same apparatus as that used with the training set samples. The metabolite discriminators defined by the training set (aspartate, glutamate, proline and glycerol) as well as the internal standard L-norvaline were analyzed in selective ion monitoring (SIM) mode. The characteristic ions with m/z = 70, 72, 84, 142, 142, 144, 160, 205, 232, 246 for the

five targeted metabolites were obtained by analyses on their standards and assigned by referring to the database, presented later, according to their mass-to-charge ratio (m/z) and their retention time, shown in the Table S-1. The retention time ranges corresponding to the above ions have been displayed in the Table S-2. The gradient temperature program was different from that in the training set: started by 70^{o}C in the first 3 minutes, the temperature was increased to 180^{o}C by 5^{o}C/min, then went up to 310^{o}C by 20^{o}C/min, retained for 5 minutes. The even time was set to 0.2s.

Several blank samples (without containing in the vial) were tested before the sample analysis for wiping off the residues remaining in the column. Before the analysis of the real samples, several QC samples were beforehand analyzed to confirm the stability of the instrument. Every injection took 1 μL of droplet from all the sample. 1 QC sample was inserted after every 6 real samples in the sequence of analysis to monitor the reproducibility and stability of the method. When spectra of all the samples were recorded, a light diesel sample was subsequently analyzed for acquiring the retention index (RI).

Data processing

The pretreatment such as the deconvolution, the peaks matching, the retention time alignment, etc. of the spectrum was performed with the help of Leco ChromaTOF software (St. Joseph MI, version 3.25) and XCMS (xcmsonline.scripps.edu). The assignment of the ion peaks was achieved by matching the library (NIST, Mainlib, Replib, Wiley and Feihn). The assignment of peaks was based on the value of m/z and the calculated RI. The qualification for most of the principal discriminators was confirmed by analyzing correspondent reference substances. For the case that several peaks correspond to one same metabolite, we retained the one with lower RSD and

higher ratio of signal and noise (S/N).

The recording of the area for each determined ion peak was regarded as the relative quantification for its corresponding metabolite. A data set recording the area for the ion peaks was therefore generated. The peaks that contained more than 20% null area in all the QC samples were excluded. Normalization of the peaks was then done. The relative standard deviation (RSD) for every normalized peak in the QC samples was also calculated. Those peaks whose RSDs were superior to 0.3 were also removed.

The principal component analysis (PCA) and the partial least square discriminant analysis (PLS-DA) were achieved by submitting the data set to the SIMCA-P software (version 11, Umetrics, Umeå, Sweden). Heat maps were displayed by the MultiExperiement Viewer (Mev, version 4.9.0, Dana-Farber Cancer Institute, MA, USA). Other statistical analyses were assumed by the SPSS statistics (version 19, IBM, Chicago, USA). The acquisition of spectra for some available reference substance was served to confirm the qualification of most of the discriminators.

To investigate the ability of prediction of the defined biomarker candidate of HCC recurrence, the validation of defined principal metabolites was performed by the feature selection of random forest (RF). The calculation was realized by the algorithm written in the C++ language. For the discrimination between the recurrent and non-recurrent HCV-HCC patients, two third of samples were utilized to be the training data while the remaining one third of the samples were acted as the validation set. Both the two RF analyses were run 100 times, the frequency of the present of a certain discriminator in all runs was obtained. Discriminator with a frequency of present superior to 50% was considered as a potential biomarker.

The binary logistic regression (BLR) with the method “condition: forward” was used to select the potential biomarkers in the discriminators. The data of the obtained

discriminators were again submitted to the BLR with the method “enter”. A probability representing the combination of the discriminators was calculated for each sample. And the probability was sent up to test the area under receiver operating characteristic curve (AUROC).

Results

For the samples in the training set, data pretreatment was started with the 16 QC samples. After the deconvolution and peak alignment for the QC samples, 459 peaks were initially detected. After removing the peaks with more than 20% null area, it was shown that 87% of the peaks were found stable with their RSD of area inferior to 30%, occupying 94% of total peak area. Other peaks with RSD superior to 30% were therefore excluded. To test the stability of the analytical sequence, an assessment by PCA for all the QC samples was performed (Figure S-1), a focalization of the QC samples was observed by comparing to all other real samples, which showed a good stability of the analytical sequence. Finally, 230 peaks which correspond to comprised compounds in the serum were obtained. Afterward, peaks in the real samples were qualified by the characterized peaks in QC samples and then quantified by the integration of their area. The information of peak area represents the relative concentration of corresponding compound in the serum. Finally, a data set for real samples containing peak area information for all their 230 defined peaks was therefore established, and analyzed in the following discriminatory analyses.

For the experiences with the samples in the validation set, the estimation of the RSD for the targeted peaks in the 9 QC samples were obtained, shown in the table S-3, the peaks with smaller RSD were selected and submitted to the tests of AUROC.

Baseline characteristic of patients.

85 samples from 46 patients fulfilling the inclusion criteria were ultimately included in the present study. Among the samples, 38 were included in the training set while 47 others were encompassed in the validation set. The distribution of all the samples was noted in Figure 1. The samples were regrouped by the sampling time (BT: before RFA therapy; AT: 2 months after RFA therapy) and recurrence (NR: non-recurrent patients; R: recurrent patients). e.g. R_{BT} means the sample obtained before RFA treatment from non-HCV infection HCC patient with recurrence; NR_{AT} means the sample drawn from HCV-infected patient without recurrence after RFA therapy. The baseline information for all the included patients is shown in Table 1. On the basis of the statistical data in the table, no significant variation ($p>0.05$) from the clinical assessments was found between the recurrent group and the non-recurrent group.

On the contrary, significant differences between HCV-HCC patients and non-viral HCC patients were found in the largest nodule size, the cholesterol, the blood sugar content and two transaminases. The results implied that the principal discrepancy among the patients corresponds to the fact whether the patient was affected by viral hepatitis, which has been determined in our previous study (23).

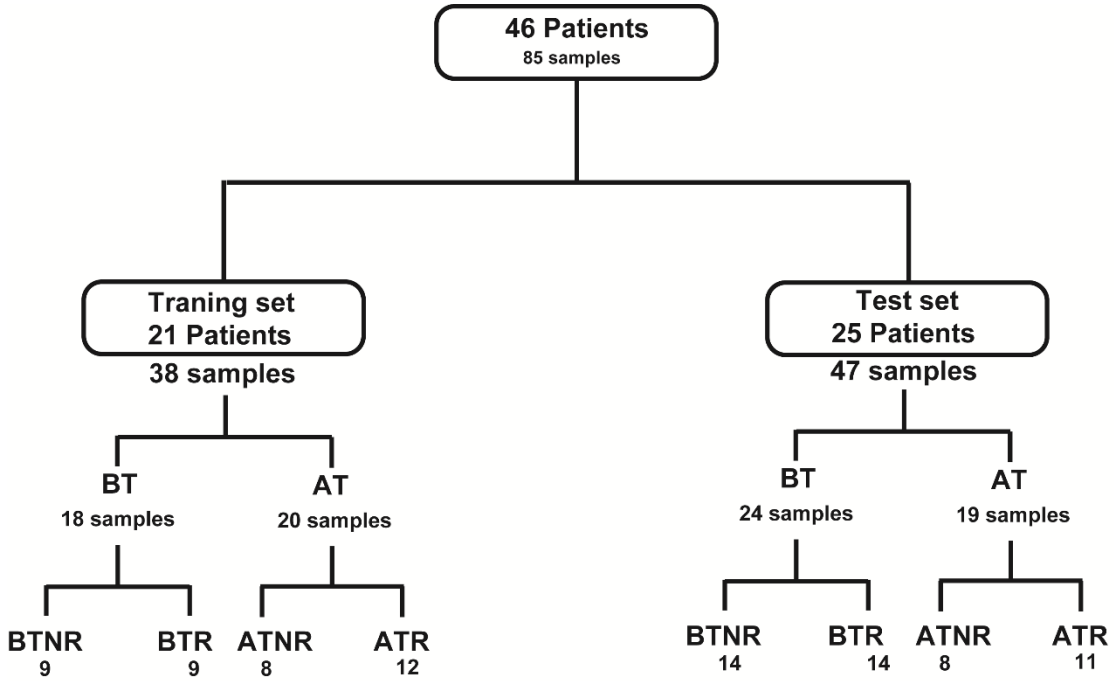

Figure 1. Flowchart of the distribution of patients and samples. BT: before RFA therapy, AT: after RFA therapy; NR: HCC patients without recurrence R: patients with recurrence.

Discriminatory analyses in the patients with HCV between the recurrent and the non-recurrent group

For the cohort of HCC patients infected with HCV, 18 samples collected before RFA treatment while 20 samples were collected 2 months after the treatment were available. PCA and PLS-DA were performed for the two cohorts respectively, shown in Figure 2. According to the multivariate analyses, clear separations between R_{BT} vs. NR_{BT} (Figure 2 A-B) and R_{AT} vs. NR_{AT} (Figure 2 C-D) were observed. Significant differences were shown between the recurrent patients and non-recurrent patients before and after RFA treatment. With 2 components, the Q2 for the two models were equal to 0.34 and 0.5 respectively. Cross validations for the two models demonstrated that they were not over-fitting (shown Figure S-2). As regard to the PLS-DA analyses, the contribution of each metabolite to the model was determined by the variable importance in the

projection (VIP). Metabolites with their VIP superior to 1 were all listed in the Table S1 accompanied by their P-value and fold change for the two model respectively. Heat maps showing their different variation directions and fold changes in each sample are present in Figure 2E-2F.

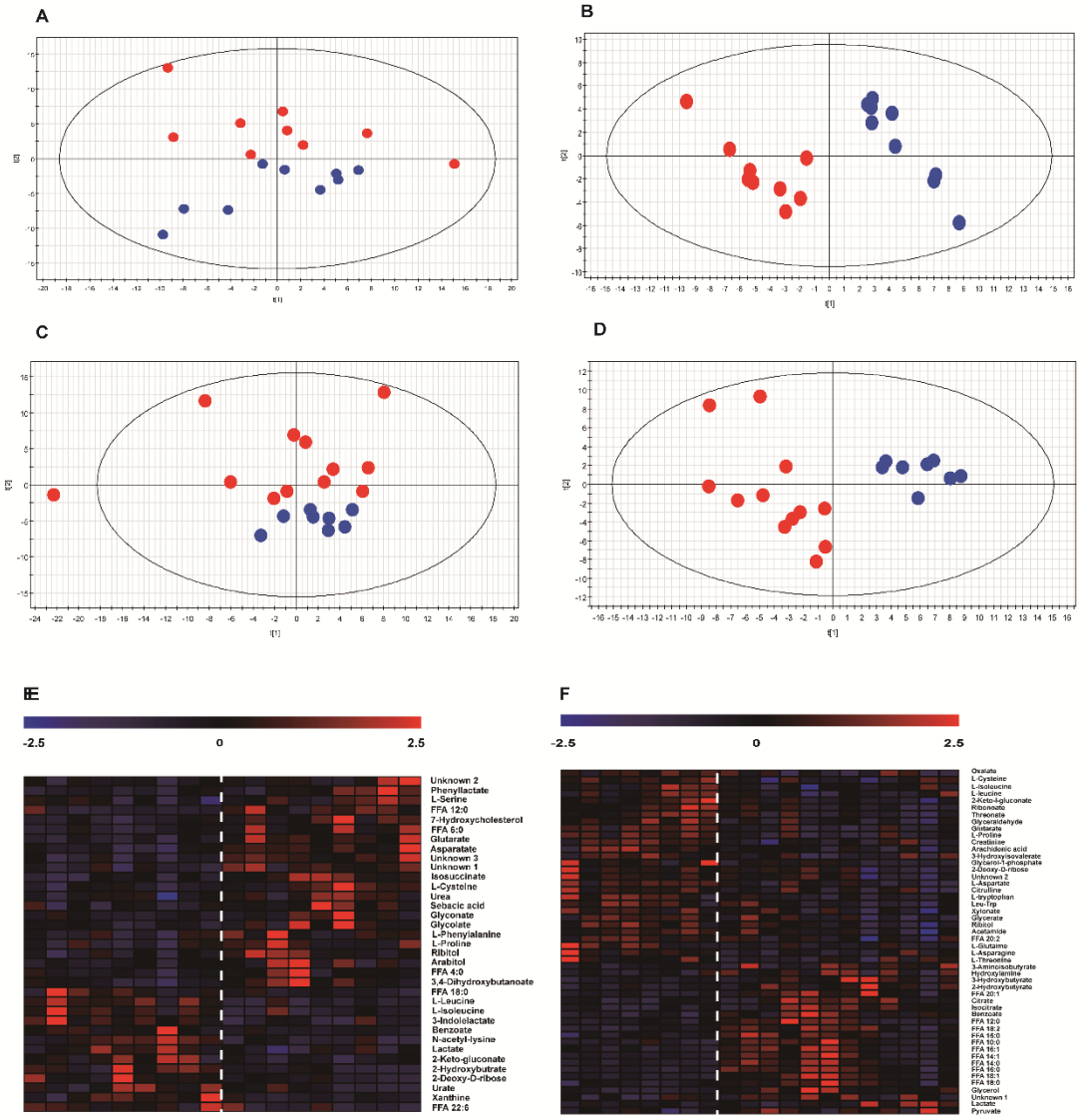

Figure 2. Multivariate analysis R_{BT} vs. NR_{BT}. and R_{AT} vs. R_{BT}. A-D: Score-plot of PCA and PLS-DA. Blue dots: non-recurrent patients; red dots: recurrent patients. A: PCA for the samples R_{BT} and NR_{BT}. B: PLS-DA for the separation between NR_{BT} and R_{BT}. C: PCA of the samples R_{AT} and NR_{AT}. D: PLS-DA for the separation between R_{AT} and

NR_{AT}. E-F: Heat map presenting the hierarchical clustering analysis for the two separation, on the left of the dotted line: non-recurrent patients; on the right of the dotted line: recurrent patients. E: heat map for R_{BT} vs. NR_{BT}; F: heat map for R_{AT} vs. NR_{AT}.

Metabolome differences between the recurrent and the non-recurrent groups before the RFA therapy (BT)

As it has been shown in Figure 2E, 35 metabolites were determined to be significant in the comparison between R_{BT} and NR_{BT}. Among the significant discriminators, we exhibited a general increased level of amino acids in the R_{BT}, compared with NR_{BT}. Concerning the free fatty acids in the serum, FFA 4:0 and FFA 12:0 were elevated in the R_{BT}s compared with those in NR_{BT}, while FFA 18:0 and FFA 22:6 (Docosahexaenoic acid, DHA) varied in the opposite direction. Besides, upregulation of two pentose phosphate pathway (PPP) involved metabolites such as ribitol and arabitol was observed. Being linked to the purine metabolism, xanthine and urate were down-regulated in the recurrent patients. Several energy-related organic acids such as lactic acid, glycolic acid, glutaric acid and sebacic acid were also shown to be responsible for the separation of R_{BT} vs. NR_{BT}. Other significant discriminators included indolelactate, benzeneacetate, benzoate and urea. A pathway showing the discriminations in involved metabolites between the R_{BT} and the NR_{BT} has been shown in Figure 3.

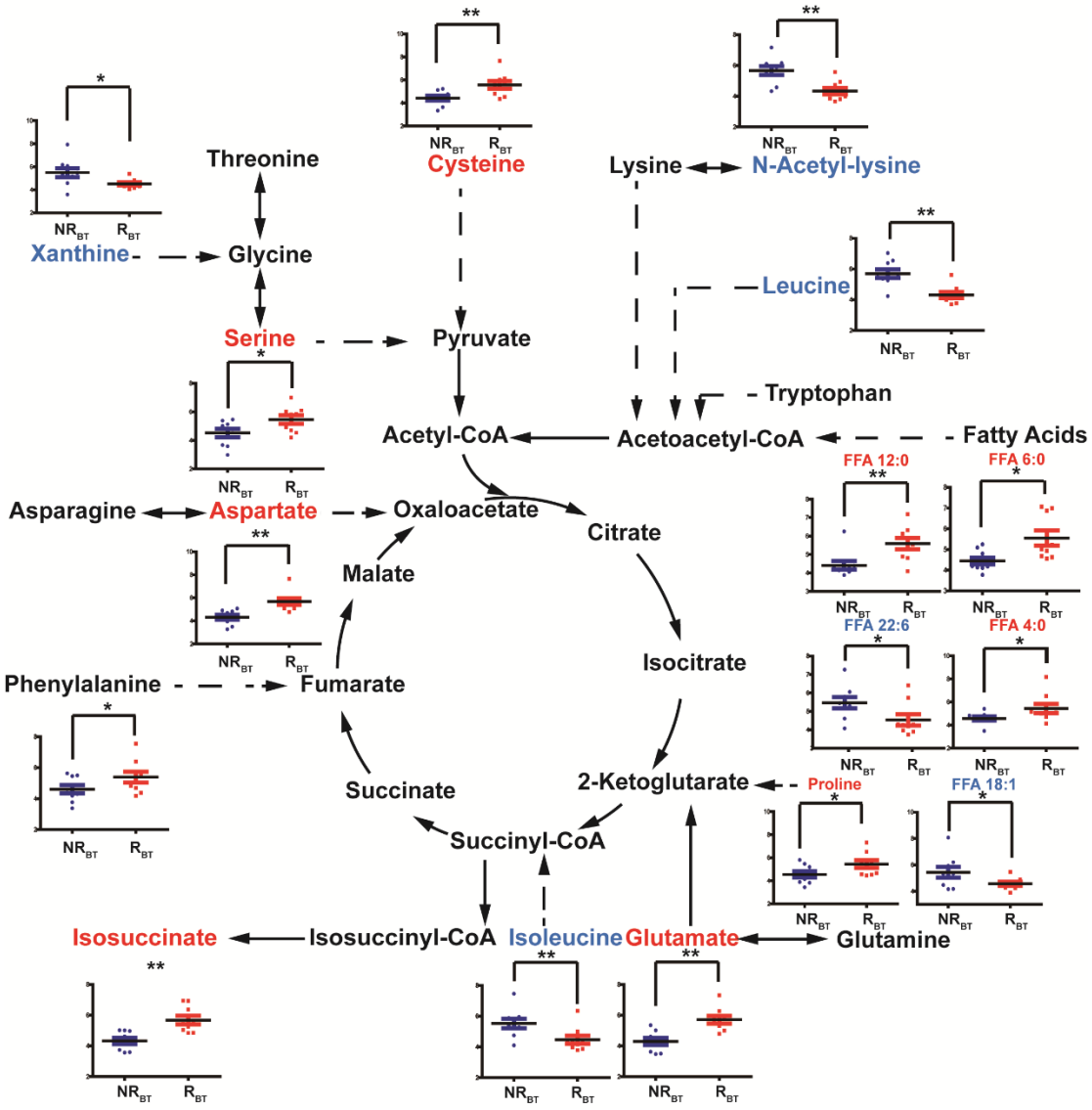

Figure 3. Discriminators with their relative quantification and their involving pathways of NR_{BT} (blue bars) vs. R_{BT} (red bars). *: $p<0.05$, **: $p<0.01$.

Metabolome differences between the recurrent and the non-recurrent patients after the RFA therapy (AT)

For the comparison between R_{AT} and NR_{AT}, 50 metabolites were shown significantly varied (shown Figure 2F). Among them, generally heightened fatty acids were found in the recurrent cases, except for arachidonic acid (ARA, FFA 20:4), which was similar to

the finding in the fatty acids with BT. But, we noticed kinds of metabolites such as amino acids, PPP involved metabolites and lactate altering adversely against the comparison in BT. Opposite variation directions of certain metabolites against their regularities observed with BT were otherwise true for metabolites such as benzoate and glutarate. Moreover, 2 metabolites involved in the TCA cycle, citrate and isocitrate, augmented in recurrent cases, which was not found in the comparison of R_{BT} vs. NR_{BT}. Other significant differences related to the post-operational recurrence were found in the metabolites such as creatinine, citrulline, threonate, 2-hydroxybutyrate, 3-aminoisobuyrate, etc. (Table S-4). Relative quantifications of some metabolite discriminators distinguishing the R_{AT} from the NR_{AT} have been shown within their involving pathways the Figure 4.

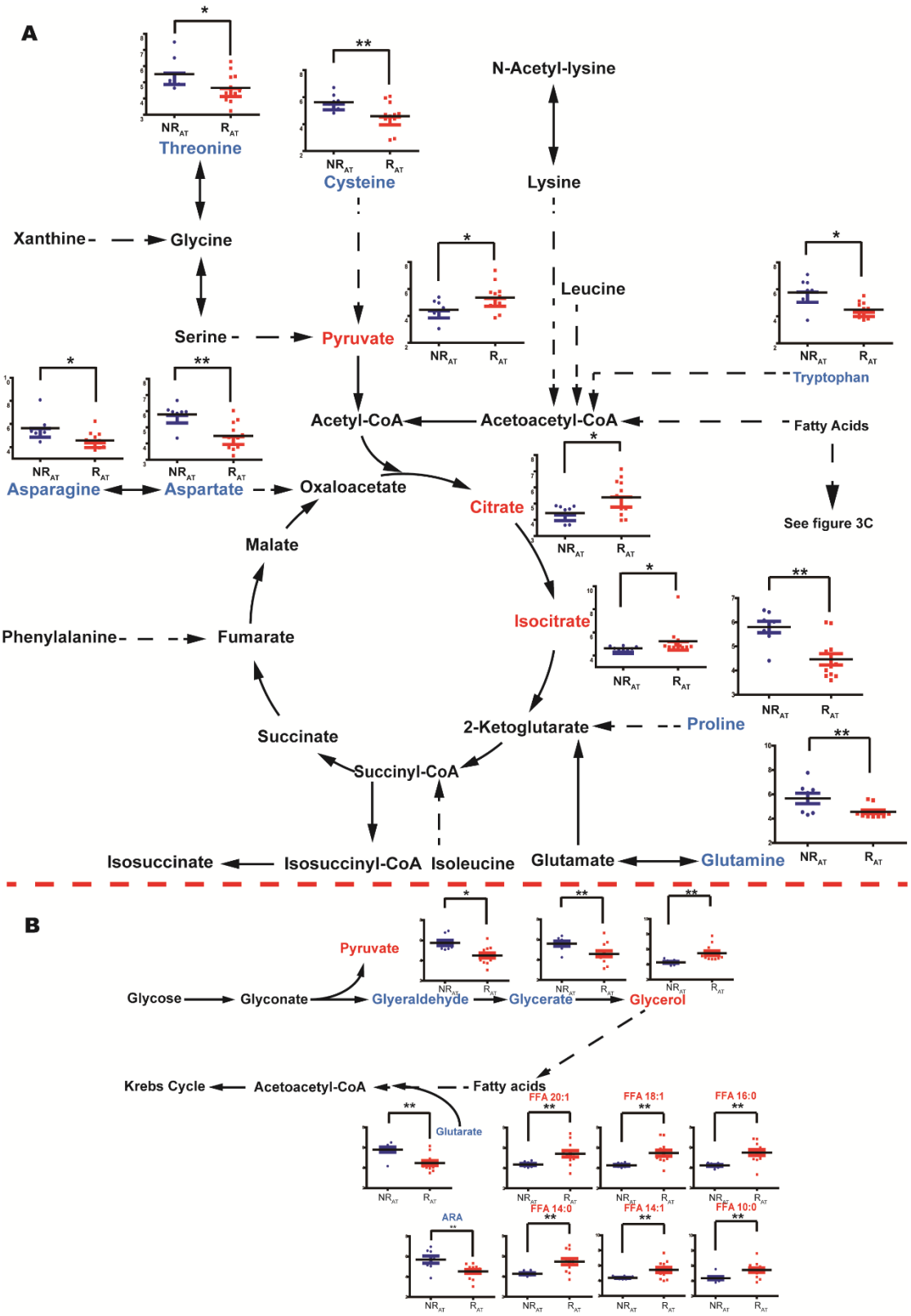

Figure 4. Discriminators with their relative quantification and their involving pathways. A: NR_{AT} (blue bars) vs. R_{AT} (red bars). B: Discriminators included in the glycerolipid metabolism and the fatty acids in the discrimination between NR_{AT} and R_{AT}s. *: $p<0.05$,

**: $p<0.01$.

Determination of potential biomarkers predicting HCC recurrence for the HCV-related patients

Further determination of key discriminators was achieved by the analysis of volcano plot (Figure 5). N-acetyl-lysine, glutamate and aspartate were defined for their acute variation in the R_{BT} vs. NR_{BT} comparison; aspartate, proline, glutarate, glycerol and FFA 14:0 were characterized as the metabolites highly correlated to the prediction of HCC relapse after the treatment. Area under receiver operating characteristic curve (AUROC) for each defined metabolite was subsequently calculated to affirm its reliability of recurrence prediction (shown in Table 2 and Figure 5C-D). Accordingly, apart from FFA 14:0, all the defined principal discriminators showed outstanding performances with their AUROC superior to 0.80.

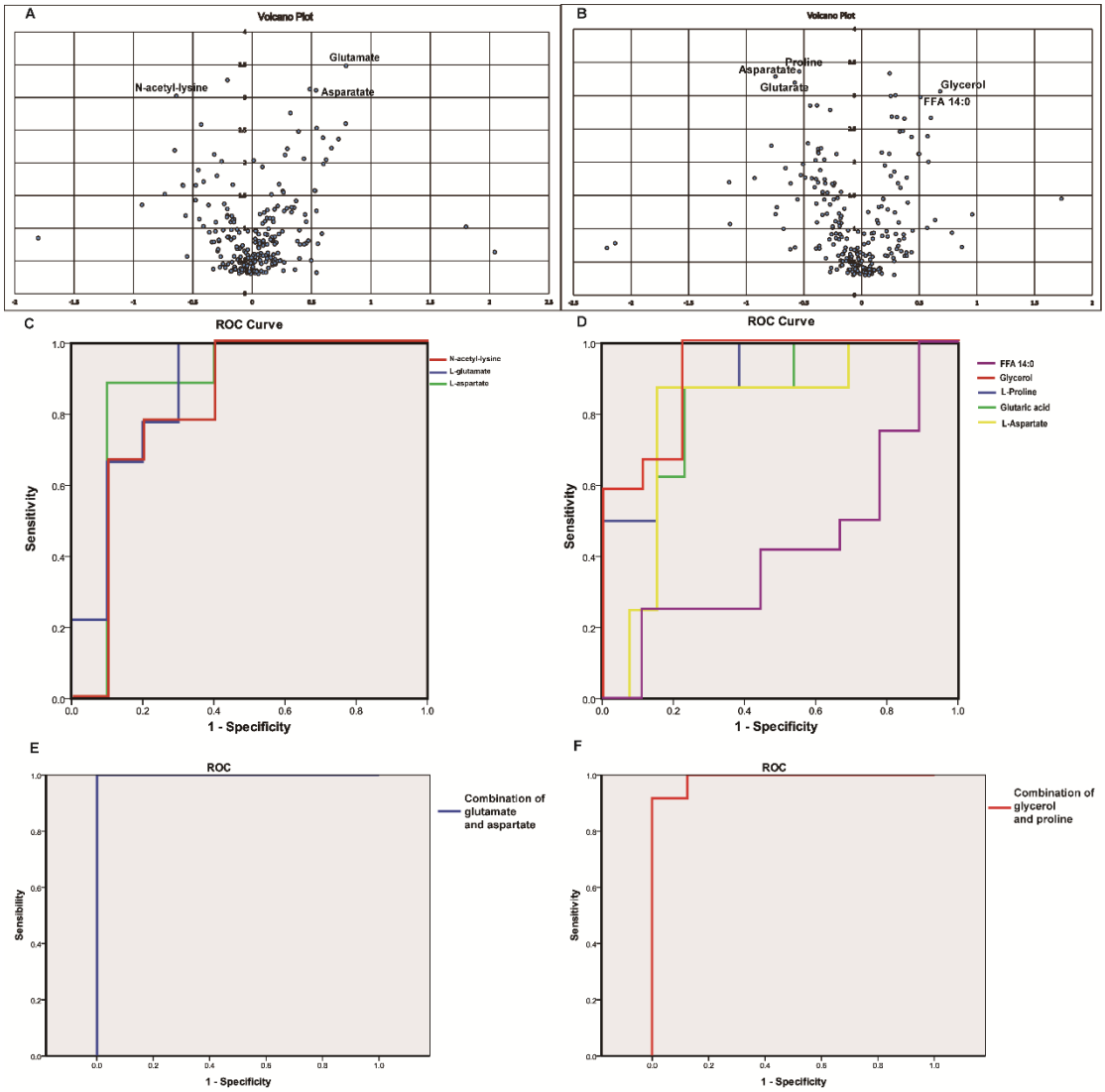

Figure 5. Determination of primary metabolite discriminators and potential combinational biomarkers of recurrence for HCV-related HCC patients. A-B Volcano plot for the determined metabolites. Axis x: $\log_2$ (fold change); axis y: $\log_{10}$ (P-value). A: R_{BT} vs. NR_{BT}; B: R_{AT} vs. NR_{AT}. C-D ROC for the obtained important discriminators from the volcano plot. C: R_{BT} vs. NR_{BT}; D: R_{AT} vs. NR_{AT}. E-F: ROC of the potential combinational biomarkers before and after RFA treatment. E: ROC of the combination of glutamate and aspartate separating R_{BT} from NR_{BT}; F: ROC of the combination of glycerol and proline separating R_{AT} from NR_{AT}.

Validation tests of the primary discriminators were performed by the random forest

(RF) during 100 runs. For the comparison by the recurrence prior to the treatment, the average accuracy rate on independent tests was 80.7%±7.6%; the result for the R_{AT} and NR_{AT} separation was 82.9%±8.0%. Table 2 displays the probability of presence of the discriminator in the 100 runs of RF models. It can be observed that N-acetyl-lysine and FFA 14:0 were present in less than half of the RF models, which should be rejected for being biomarker candidates. Other metabolites were proved to be more important for the two models.

Finally, after the exclusion of the two metabolites with poor performances in the RF models, the remaining metabolites were submitted to determine potential combinational biomarkers. For the model based on the samples obtained before the treatment (BT), the combination of aspartate and glutamate showed an accuracy of 100% in ROC (Figure 5E). For AT, glycerol and proline were the two crucial variables for the prediction. Their combination showed 99% accuracy of prediction for post-operative recurrence (Figure 5F).

Validation by the validation set

The predictability of recurrence of the two combinational biomarker candidates in the samples of validation set was verified by another ROCs. As shown in Figure 6, the combination of aspartate and glutamate presents an AUROC = 0.83 for the prediction of HCC recurrence in the BT. The AUROC was equal to 0.78 for the prediction of HCC recurrence in AT by the combination of glycerol and proline.

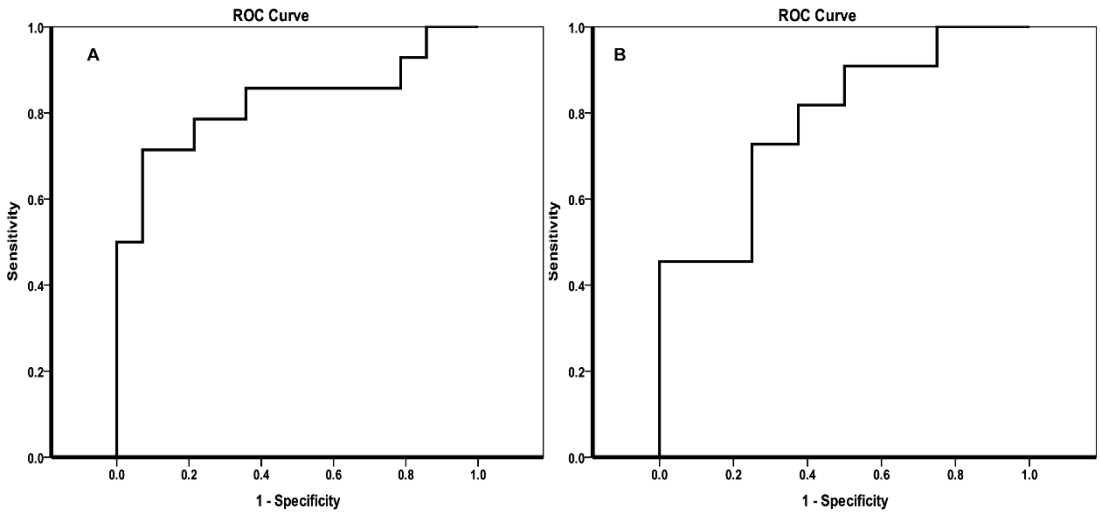

Figure 6. Validation of the combinational potential biomarkers predicting the recurrence of HCC in the patients with HCV by ROC curves. A. ROC curve for the prediction of recurrence in the BT; B. ROC curve for the prediction of recurrence in the AT.

Discussion

Until present, the causes of recurrence as well as the prevention of recurrence are still elusive and the recurrence of HCC remains a primary threat for the outcome. Metabolomics is powerful to reveal subtle physiological changes in the biological system, which may correspond to the stimulations of lesions and diseases, proved useful for predicting the recurrence of cancer (24,25). In the current work, obvious discrimination of recurrent samples against non-recurrent samples was revealed in the cohort with HCV infection before and after RFA therapy. From the point of view of metabolites, comprehensive alterations in the recurrent patients were detected, compared with the ones without HCC relapse.

Free fatty acids glycerolipid metabolism

Among the HCV-related HCC patients, it was notable that a comprehensive turnover of free fatty acids in the recurrent patients was found both before and after RFA treatment compared with those without recurrence. Even-carbon chain fatty acids including long-chain and medium-chain saturated fatty acids (SFAs) and monounsaturated fatty acids (MUFAs) were up-regulated in the comparison NR_{AT} vs. R_{AT}. Interestingly, short-chain and medium-chain fatty acids were determined up-regulated in R_{BT} compared to NR_{BT}. However, arachidonic acid (ARA, 20:4) and docosahexaenoic acid (DHA 22:6), which are long-chain polyunsaturated acids (PUFAs), were meanwhile down-regulated in R_{AT} and R_{BT} respectively (Shown in Figure 3, 4A). First, immune function like anti-inflammatory of PUFAs was well known (26). The depletion of PUFAs might refer to a poor prognosis owing to the hepatic viral infection. Second, HCV core protein causes insulin resistance which might be the direct origin of the wide increase of fatty acids in blood (27). It was also known as activating the liver X receptor alpha (LXRα), which modulated inflammatory genes and resulted in lipogensis (28). Being associated with the LXR, the raised level of 7-hydroxycholesterol ($P<0.05$) in recurrent patients also referred to a hypercholesterolemia and consequently cancer growth (29). Third, significant increased level in FFAs was found in the comparison between HCV infected cells and controls (30), a higher level in the HCC patients with HCV might imply a more activated HCV core protein. Finally, FFAs were demonstrated responsible for the cancer invasion and migration of HCC cancer cells (31). Taken together, both before and after RFA therapy, the deregulation of FFA in the serum of HCV infected HCC patients should account for the HCC recurrence.

Glycerolipid metabolism, TCA cycle and energy-related metabolism

Notable upregulation of glycerol ($p<0.01$), which is another precursor of triglyceride (TG) synthesis other than FFAs, was observed in R_{AT} compared with NR_{AT}. Meanwhile, as being two upstream metabolites for glycerol, glyceraldehyde ($p<0.05$) and glycerate ($p<0.01$) were down-regulated. It has been discussed that the HCV induced insulin resistance and inhibition of synthesis of TG, consistent with the accumulation of glycerol and FFAs in the patients with relapse, shown in Figure 4B.

On the other hand, enhanced lactate ($p<0.05$) synthesis from pyruvate ($p<0.05$) in the recurrent patients was observed. We ever reported upregulation of lactate as a potential biomarker for the HCC recurrence (32). This is due to a high energy demand from the HCC cell emergence (33). Notably, it was best known that the HCV core protein activates the hypoxia-inducible factor 1 (HIF1), which promotes hypoxic environment for the development of HCC (34)..

Increments of two metabolites in the TCA cycle, citrate ($p<0.05$) and isocitrate ($p<0.05$) were only found in recurrent patients after their treatment, which could be attributed to the growth of energy demand for generation of tumor.

Amino acids

According to our analyses before and after RFA therapy, the level of amino acids was of great importance for the separation between the recurrent and non-recurrent group (shown in Figure3 and 4A).

For the discriminatory analyses of recurrence in AT, the downregulation of various amino acids presented in Figure 4 had been widely reported as less optimist prognosis in HCC patients (14,18,20,35-38), which was primarily due to the comprehensive protein depletion after clinical treatment and the upregulation of anabolism prior to the relapse.

But, as a contrast to the results above in AT, except for two branched chain amino acids (BCCA), reverse variation trend was found in numbers of amino acids alteration emerged in NR_{BT} vs R_{BT}. As it has been documented, the up-regulated serine and threonine pathway was considered as an important signal of bad outcome of cancer (18,20). Upregulation of proline and cysteine pathway was otherwise observed along the proliferation and the cell cycle of HCC (39). The elevated level of glutamate and aspartate might be related to the deregulation of the aminotransferases such as GGC and AST in the case of HCC (40,41).

Pentose phosphate metabolism

Arabitol and ribitol, which were included in pentose phosphate pathway (PPP), were found significantly up-regulated in the comparison of R_{BT} to NR_{BT}. Being related to the synthesis of nucleoside, upregulation of pentose related pathway might be due to dynamic proliferation of DNA in the recurrent patients before RFA therapy. On the contrary, after the tumor was removed, significant declines not only in the two above metabolites but also in ribonic acid and xylonic acid in R_{AT} compared to NR_{AT}. Given that TCA cycle involved metabolites and lactate were found elevated in the recurrent group after RFA therapy, the decrement of the PPP metabolites might issue from a down-regulation of the energy supply from this pathway.

Other significantly varied metabolites in the recurrent patients

For the model NR_{BT} vs. R_{BT}, beyond discussed metabolites and pathways, other metabolites listed in the Table S1 were also significantly altered in R_{BT}. The decline of xanthine, accompanied by the decrease of urate might be subjected to the consumption of purine during the replication of DNA. Elevated methylmalonate was linked to the

up-regulated TCA cycle and the degradation of BCCAs. The acetylation of lysine was reported attenuated in another cancers (42), in accordance to our result. We previously reported heightened 2-hydroxybutyrate (2-HB) as a potential marker separating HCC patients and health controls (14), however, in this work, decline of 2-HB was exhibited in small HCC patients with relapse.

Metabolites such as citrulline and oxalate also contributed to the separation between NR_{AT} and R_{AT}. Citrulline is synthetized in liver, decreased citrulline indicated an altered liver function and a deprivation of synthesis citrulline from argininosuccinate (43). As for oxalate, it was also reported remarkably augmented in recurrent patients when compared with non-recurrent patients (32).

Determination of the combinational biomarkers of recurrence for the HCC patients with HCV

The primary discriminators related to the recurrence were defined, shown in Figure 5. Eventually, the combination of aspartate and glutamate shows potential to predict recurrence for the BT. As discussed above, previous studies have reported the predictability of HCC recurrence by AST and GGT, providing evidence that the two amino acids which are directly regulated by the two aminotransferases may be also significant indicators for recurrence before the clinical operation. On the other aspect, after the small HCC was removed by the RFA treatment, strikingly, the remarkable upregulation of glycerol, accompanied by the increment of various fatty acids should attribute to the HCV-induced insulin resistance which hindered the synthesis of TG. The combination of glycerol and proline was eventually shown powerful to predict HCC recurrence for the AT. Our experiences of validation with external test samples

showed the predictability of the determined combinational biomarker candidates were acceptable both before and after RFA therapy.

Conclusions

In our previous study, considerable metabolic differences were reported between HCC patients with and without hepatitis virus infections. In the present study, we contribute to investigate the metabolic differences between recurrent and non-recurrent HCC patients before and after their RFA therapy. In the HCC patients with HCV infection, clear separation by recurrence is found both before and after the RFA treatment. Further analysis concerning the patients shows a general increase of various fatty acids in the recurrent patients compared with the non-recurrent patients, which may indicate a dynamic activity of the HCV core protein in the recurrent patients. Whereas, inconsistent alterations regularity for the pathways of amino acids and PPP were otherwise revealed between pre-operation and post-operation. We suppose that specific metabolic variations before the suppression of tumor in the recurrent patients were linked to DNA replication and tumor proliferation. However, observed decline of amino acid and deregulation of energy-related metabolites, especially TCA cycle-involved metabolites, may be associated with the protein depletion after clinical operation and up-regulated anabolism for tumor genesis. With the confirmation of external validation, finally, we suggest that the combination of glutamate and aspartate and the combination of glycerol and proline are potential to be the combinational biomarkers for the prediction of HCC recurrence with HCV before and after RFA treatment respectively.

Acknowledgement

We first thank to Xin Huang for his programming and technic assistance on the random forest analysis, and to Corentine Goossense, Xianping Lin and Alexandre Baillard for their help of the preparation of samples. We need also express our thanks to Dr. Yang Liu, Dr. Yanni Zhao and Dr. Jieyu Zhao for their inspiring suggestions. The study has been supported by the key foundation (No. 21435006) from the National Natural Science Foundation of China.

References

1. Llovet JM, Burroughs A, Bruix J. Hepatocellular carcinoma. The Lancet **2003**;362(9399):1907-17.
2. Llovet JM, Bruix J. Novel advancements in the management of hepatocellular carcinoma in 2008. J Hepatol **2008**;48 Suppl 1:S20-37.
3. Wong LL, Limm WM, Severino R, Wong LM. Improved survival with screening for hepatocellular carcinoma. Liver transplantation : official publication of the American Association for the Study of Liver Diseases and the International Liver Transplantation Society **2000**;6(3):320-5.
4. Facciorusso A, Del Prete V, Antonino M, Neve V, Amoruso A, Crucinio N*, et al.* Conditional survival analysis of hepatocellular carcinoma patients treated with radiofrequency ablation. Hepatol Res **2015**;45(10):E62-72.
5. Livraghi T, Goldberg SN, Lazzaroni S, Meloni F, Solbiati L, Gazelle GS. Small hepatocellular carcinoma: Treatment with radio-frequency ablation versus ethanol injection. Radiology **1999**;210(3):655-61.
6. El-Serag HB. Epidemiology of viral hepatitis and hepatocellular carcinoma. Gastroenterology **2012**;142(6):1264-73 e1.
7. Levrero M. Viral hepatitis and liver cancer: the case of hepatitis C. Oncogene **2006**;25(27):3834-47.
8. Donato F, Tagger A, Gelatti U, Parrinello G, Boffetta P, Albertini A*, et al.* Alcohol and hepatocellular carcinoma: the effect of lifetime intake and hepatitis virus infections in men and women. Am J Epidemiol **2002**;155(4):323-31.
9. Buonfiglioli F, Conti F, Andreone P, Crespi C, Foschi F, Lenzi M*, et al.* Development of hepatocellular carcinoma in HCV cirrhotic patients treated with direct acting antivirals. J Hepatol **2016**;64(2):S215.
10. El-Serag HB, Marrero JA, Rudolph L, Reddy KR. Diagnosis and treatment of hepatocellular carcinoma. Gastroenterology **2008**;134(6):1752-63.
11. Mamas M, Dunn WB, Neyses L, Goodacre R. The role of metabolites and metabolomics in clinically applicable biomarkers of disease. Arch Toxicol **2011**;85(1):5-17.
12. Xia J, Broadhurst DI, Wilson M, Wishart DS. Translational biomarker discovery in clinical metabolomics: an introductory tutorial. Metabolomics **2013**;9(2):280-99.
13. Zhou L, Ding L, Yin P, Lu X, Wang X, Niu J*, et al.* Serum metabolic profiling study of hepatocellular carcinoma infected with hepatitis B or hepatitis C virus by using liquid chromatography-mass spectrometry. Journal of proteome research **2012**;11(11):5433-42.
14. Zeng J, Yin P, Tan Y, Dong L, Hu C, Huang Q*, et al.* Metabolomics study of hepatocellular carcinoma: discovery and validation of serum potential biomarkers by using capillary electrophoresis-mass spectrometry. Journal of proteome research **2014**;13(7):3420-31.
15. Nahon P, Amathieu R, Triba MN, Bouchemal N, Nault JC, Ziol M*, et al.* Identification of serum proton NMR metabolomic fingerprints associated with hepatocellular carcinoma in patients with alcoholic cirrhosis. Clin Cancer Res **2012**;18(24):6714-22.
16. Zhou L, Liao Y, Yin P, Zeng Z, Li J, Lu X*, et al.* Metabolic profiling study of early and late recurrence of hepatocellular carcinoma based on liquid chromatography-mass spectrometry. J Chromatogr B Analyt Technol Biomed Life Sci **2014**;966:163-70.

17. Nezami Ranjbar MR, Luo Y, Di Poto C, Varghese RS, Ferrarini A, Zhang C*, et al.* GC-MS Based Plasma Metabolomics for Identification of Candidate Biomarkers for Hepatocellular Carcinoma in Egyptian Cohort. PloS one **2015**;10(6):e0127299.
18. Fitian AI, Nelson DR, Liu C, Xu Y, Ararat M, Cabrera R. Integrated metabolomic profiling of hepatocellular carcinoma in hepatitis C cirrhosis through GC/MS and UPLC/MS-MS. Liver international : official journal of the International Association for the Study of the Liver **2014**;34(9):1428-44.
19. Budhu A, Roessler S, Zhao X, Yu Z, Forgues M, Ji J*, et al.* Integrated metabolite and gene expression profiles identify lipid biomarkers associated with progression of hepatocellular carcinoma and patient outcomes. Gastroenterology **2013**;144(5):1066-75 e1.
20. Chen T, Xie G, Wang X, Fan J, Qiu Y, Zheng X*, et al.* Serum and Urine Metabolite Profiling Reveals Potential Biomarkers of Human Hepatocellular Carcinoma. Molecular & Cellular Proteomics **2011**;10(7).
21. Patterson AD, Maurhofer O, Beyoglu D, Lanz C, Krausz KW, Pabst T*, et al.* Aberrant lipid metabolism in hepatocellular carcinoma revealed by plasma metabolomics and lipid profiling. Cancer Res **2011**;71(21):6590-600.
22. Wu H, Xue R, Dong L, Liu T, Deng C, Zeng H*, et al.* Metabolomic profiling of human urine in hepatocellular carcinoma patients using gas chromatography/mass spectrometry. Anal Chim Acta **2009**;648(1):98-104.
23. Goossens C, Nahon P, Le Moyec L, Triba MN, Bouchemal N, Amathieu R*, et al.* Sequential Serum Metabolomic Profiling after Radiofrequency Ablation of Hepatocellular Carcinoma Reveals Different Response Patterns According to Etiology. Journal of proteome research **2016**;15(5):1446-54.
24. Asiago VM, Alvarado LZ, Shanaiah N, Gowda GAN, Owusu-Sarfo K, Ballas RA*, et al.* Early Detection of Recurrent Breast Cancer Using Metabolite Profiling. Cancer Res **2010**;70(21):8309-18.
25. Cao MD, Sitter B, Bathen TF, Bofin A, Lonning PE, Lundgren S*, et al.* Predicting long-term survival and treatment response in breast cancer patients receiving neoadjuvant chemotherapy by MR metabolic profiling. Nmr Biomed **2012**;25(2):369-78.
26. Calder PC. Omega-3 fatty acids and inflammatory processes. Nutrients **2010**;2(3):355-74.
27. Li HC, Ma HC, Yang CH, Lo SY. Production and pathogenicity of hepatitis C virus core gene products. World J Gastroenterol **2014**;20(23):7104-22.
28. Lima-Cabello E, Garcia-Mediavilla MV, Miquilena-Colina ME, Vargas-Castrillon J, Lozano-Rodriguez T, Fernandez-Bermejo M*, et al.* Enhanced expression of pro-inflammatory mediators and liver X-receptor-regulated lipogenic genes in non-alcoholic fatty liver disease and hepatitis C. Clin Sci (Lond) **2011**;120(6):239-50.
29. Nelson ER, Wardell SE, Jasper JS, Park S, Suchindran S, Howe MK*, et al.* 27-Hydroxycholesterol Links Hypercholesterolemia and Breast Cancer Pathophysiology. Science **2013**;342(6162):1094-8.
30. Roe B, Kensicki E, Mohney R, Hall WW. Metabolomic Profile of Hepatitis C Virus-Infected Hepatocytes. PloS one **2011**;6(8):e23641.
31. Nath A, Li I, Roberts LR, Chan C. Elevated free fatty acid uptake via CD36 promotes epithelial-mesenchymal transition in hepatocellular carcinoma. Sci Rep **2015**;5:14752.
32. Ye G, Zhu B, Yao Z, Yin P, Lu X, Kong H*, et al.* Analysis of urinary metabolic signatures of early

hepatocellular carcinoma recurrence after surgical removal using gas chromatography-mass spectrometry. Journal of proteome research **2012**;11(8):4361-72.

33. Vander Heiden MG, Cantley LC, Thompson CB. Understanding the Warburg effect: the metabolic requirements of cell proliferation. Science (New York, NY) **2009**;324(5930):1029-33.
34. Arzumanyan A, Reis HM, Feitelson MA. Pathogenic mechanisms in HBV- and HCV-associated hepatocellular carcinoma. Nature reviews Cancer **2013**;13(2):123-35.
35. DeBerardinis RJ, Cheng T. Q's next: the diverse functions of glutamine in metabolism, cell biology and cancer. Oncogene **2010**;29(3):313-24.
36. Long J, Wang H, Lang Z, Wang T, Long M, Wang B. Expression level of glutamine synthetase is increased in hepatocellular carcinoma and liver tissue with cirrhosis and chronic hepatitis B. Hepatology international **2011**;5(2):698-706.
37. Zhang B, Dong LW, Tan YX, Zhang J, Pan YF, Yang C*, et al.* Asparagine synthetase is an independent predictor of surgical survival and a potential therapeutic target in hepatocellular carcinoma. Br J Cancer **2013**;109(1):14-23.
38. Loayza-Puch F, Rooijers K, Buil LC, Zijlstra J, Oude Vrielink JF, Lopes R*, et al.* Tumour-specific proline vulnerability uncovered by differential ribosome codon reading. Nature **2016**;530(7591):490-4.
39. De Giorgi V, Buonaguro L, Worschech A, Tornesello ML, Izzo F, Marincola FM*, et al.* Molecular Signatures Associated with HCV-Induced Hepatocellular Carcinoma and Liver Metastasis. PloS one **2013**;8(2):e56153.
40. Song P, Inagaki Y, Wang Z, Hasegawa K, Sakamoto Y, Arita J*, et al.* High Levels of Gamma-Glutamyl Transferase and Indocyanine Green Retention Rate at 15 min as Preoperative Predictors of Tumor Recurrence in Patients With Hepatocellular Carcinoma. Medicine (Baltimore) **2015**;94(21):e810.
41. Poon RT, Fan ST, Ng IO, Lo CM, Liu CL, Wong J. Different risk factors and prognosis for early and late intrahepatic recurrence after resection of hepatocellular carcinoma. Cancer **2000**;89(3):500-7.
42. Zhao D, Zou SW, Liu Y, Zhou X, Mo Y, Wang P*, et al.* Lysine-5 acetylation negatively regulates lactate dehydrogenase A and is decreased in pancreatic cancer. Cancer cell **2013**;23(4):464-76.
43. Wheatley DN, Kilfeather R, Stitt A, Campbell E. Integrity and stability of the citrulline-arginine pathway in normal and tumour cell lines. Cancer Lett **2005**;227(2):141-52.

Figure Legends

Figure 1. Flowchart of the distribution of patients and samples. BT: before RFA therapy, AT: after RFA therapy; NR: HCC patients without recurrence R: patients with recurrence.

Figure 2. Multivariate analysis R_{BT} vs. NR_{BT}. and R_{AT} vs. R_{BT}. A-D: Score-plot of PCA and PLS-DA. Blue dots: non-recurrent patients; red dots: recurrent patients. A: PCA for the samples R_{BT} and NR_{BT}. B: PLS-DA for the separation between NR_{BT} and R_{BT}. C: PCA of the samples R_{AT} and NR_{AT}. D: PLS-DA for the separation between R_{AT} and NR_{AT}. E-F: Heat map presenting the hierarchical clustering analysis for the two separation, on the left of the dotted line: non-recurrent patients; on the right of the dotted line: recurrent patients. E: heat map for R_{BT}s vs. NR_{BT}s; F: heat map for R_{AT} vs. NR_{AT}.

Figure 3. Discriminators with their relative quantification (y-axis) and their involving pathways of NR_{BT} (blue bars) vs. R_{BT} (red bars). *: $p<0.05$, **: $p<0.01$.

Figure 4. Discriminators with their relative quantification (y-axis) and their involving pathways. A: NR_{AT} (blue bars) vs. R_{AT} (red bars). B: Discriminators included in the glycerolipid metabolism and the fatty acids in the discrimination between NR_{AT} and R_{AT}. *: $p<0.05$, **: $p<0.01$.

Figure 5. Determination of primary metabolite discriminators and potential combinational biomarkers of recurrence for HCV-HCC patients. A-B Volcano plot for the determined metabolites. Axis x: $\log_2$ (fold change); axis y: $\log_{10}$ (P-value). A: R_{BT}

vs. NR_{BT}; B: R_{AT} vs. NR_{AT}. C-D ROC for the obtained important discriminators from the volcano plot. C: R_{BT} vs. NR_{BT}; D: R_{AT} vs. NR_{AT}. E-F: ROC of the potential combinational biomarkers before and after RFA treatment. E: ROC of the combination of glutamate and aspartate separating R_{BT} from NR_{BT}; F: ROC of the combination of glycerol and proline separating R_{AT} from NR_{AT}.

Figure 6. Validation of the combinational potential biomarkers predicting the recurrence of HCC in the patients with HCV by ROC curves. A. ROC curve for the prediction of recurrence in the BT; B. ROC curve for the prediction of recurrence in the AT.

Table 1. Baseline of the enrolled patients in the study. All the percentages were calculated by the proportion in all the enrolled patients. Uni-nodular: HCC patient who had only one nodule of tumor. AFP: alpha fetoprotein; TG: triglyceride; AST: aspartate aminotransferase; ALT: alanine aminotransferase; GGT: γ-glutamyl transpeptidase. P-value$_{Rec}$: P-value for the comparison between recurrent and non-recurrent HCC patients

	Traning Set				Test set			
	Total Training set	Patients with HCC recurrence	Patients without HCC recurrence	P-value$_{Rec}$	Total Test set	Patients with HCC recurrence	Patients without HCC recurrence	P-value$_{Rec}$
Number of patients	21	11 (52%)	10(45%)	NA	25	13(52%)	12(48%)	NA
Age (Average)	70.6±0.3	70.2±0.4	69.7±0.3	0.22	67.6±0.5	65.8±0.9	69.4±1.0	0.23
Gender (Male %)	18(86%)	9(82%)	9(90%)	NA	17 (68%)	8(61%)	9(75%)	NA
Uni-nodular HCC	16(76%)	9(81%)	7(70%)	NA	20(80%)	10(77%)	10(83%)	NA
Largest nodule size (mm)	28.2±0.2	28±0.4	28.4±0.4	0.44	24.4±0.4	27.6±0.8	21.0±0.7	0.04
AFP (ng/ml)	44.4±2.7	52.6±5.5	36.5±5.3	0.34	45.39±5.0	74±8.1	19.2±2.8	0.04
TG (g/L)	1.1±0.02	1.1±0.03	1.1±0.07	0.47	1.0±0.01	1.0±0.02	0.9±0.02	0.39
Cholesterol (g/L)	4.4±0.03	4.5±0.05	4.2±0.07	0.2	3.8±0.04	3.5±0.04	4.1±0.10	0.14
Glycemia (IU/L)	6.6±0.32	6.9±0.08	6.4±0.06	0.18	6.5±0.07	6.3±0.11	6.6±0.17	0.32
AST (IU/L)	58.4±1.1	64.3±3.1	53±0.9	0.26	68.9±1.6	87.8±3.3	50.1±2.3	0.01
ALT (IU/L)	49.5±0.7	50.3±1.7	48.8±1.1	0.45	57.7±1.6	72.9±3.3	42.5±2.3	0.03
GGT (IU/L)	123.2±1.9	140.0±4.7	107.7±3.5	0.13	141.5±5.1	177.4±7.0	105.6±12.7	0.09

Table 2. Determination of principal metabolites in the separation between the HCV-related HCC patients with recurrence and the patients without recurrence.

	Metabolite	m/z	RT (min)	VIP	P-value	Fold Change	AUROC	RF
BT	L-Glutamate	246	22.71	2.11	<0.001	2.3	0.87	54.3%
	L-Aspartate	232	20.31	2.01	<0.001	1.82	0.87	68.0%
	N-Acetyl-lysine	98	38.46	1.98	<0.001	0.56	0.82	43.3%
AT	Glycerol	205	13.89	1.78	<0.001	1.8	0.92	74.7%
	L-Proline	142	14.44	1.97	<0.001	0.6	0.89	51.7%
	L-Aspartate	232	20.31	1.94	<0.001	0.61	0.80	54.7%
	Glutaric acid	115	14.45	1.94	<0.001	0.58	0.80	50.7%
	FFA 14:0	285	27.73	1.76	0.001	1.76	0.43	44.0%

3.3.2 Conclusion to this part of experimental research

HCC is primary in liver cancer which leads to a high rate of recurrence and mortality. However, current prediction of HCC recurrence is not as reliable as expected. HCV infection is one of the primary causes of HCC. Our previous study has shown comprehensive differences of metabolome between the viral and non-viral HCC patients. Even though some studies concerning the recurrence of HCC has been performed before, to our known, the metabolome of the patients was not analyzed in the condition of a classification of the patients by the fact of virus infection.

In the present study, GC-MS-based metabolomics has been applied to analyze the differences of metabolome between the recurrent and non-recurrent HCC patients, especially in the patients who are affected by the HCV infection. We report that clear separations have been found with the metabolic profiles between the HCV-related recurrent and non-recurrent HCC patients, before and after their RFA therapies. Metabolites involved the pathways such as amino acids, fatty acids, glycerolipid metabolism, PPP accounted for the prediction of HCC recurrence in the HCV-HCC patients. With our validations of results, our eventually defined combinational biomarker candidates were shown to be potential for the prediction of HCC relapse before and after RFA treatment.

On the contrary, no clear separation about the HCC relapse was found when we compared the two groups of non-viral patients, same results were found with all the enrolled patients. Since variations in considerable kinds of lipids were revealed to be responsible to the HCC recurrence, next study should be performed with a systematic lipidomics which will provide further information of the variations of lipids and relevant pathways.

General conclusions and perspectives

The development of metabolomics makes it an important component in the system biology. It has been shown that the determination of the expression of certain metabolites was directly related to a physiological state. Therefore, its application in the field of clinical research is potential. One of the core tasks of metabolomics in the clinical applications is to find out novel and accurate biomarkers with which we are able to have a better understanding of individual physiological situation in time, to predict the outcome of disease and to perform targeted treatments.

In the first part of the study, we aimed to determine the biomarkers predicting the mortality of septic shock. Metabolic differences were uncovered by both LC-MS and 1D NMR spectroscopy between the septic survivors and the non-survivors before clinical intervention. Further, with the help of paired model by NMR-based approach, the evolution of metabolic profiles from the hospitalization to 24h later were investigated, and an apparent separation between the survivors and non-survivors was found again. Interestingly, according to the results found with the NMR experiences, variations of the metabolites such as energy-related metabolites and some amino acids in the non-survivors were in accord with those found with MS experiences. On the other hand, for example, variations in some urea cycle-involved metabolites and in glucose were only determined by the LC-MS-based method and by the NMR-based method respectively. According to the study using the both techniques, we figure out the method with LC-MS a better coverage of metabolites is achievable, but, an easier sample preparation and data analysis is proceeded with NMR than MS. Also, it is shown that both the MS and NMR-based metabolomics are useful for the clinical application and the two techniques are complementary. We claim that using meanwhile both the techniques will provide more information of the metabolome than using only one platform and the similar obtained findings from the two techniques can be a mutual confirmation for the two work.

In the second part of the work, biomarkers were sought for predicting HCC relapse in

the HCC patients who were also suffered from HCV infection. Serum samples from HCC patients before and after RFA treatment were studied separately by the fact of infectious hepatitis virus. GC-MS has been applied for the serum metabolome analyses. Accordingly, considerable differences of metabolic profiles have been exhibited between HCC recurrent patients and non-recurrent patients before and after RFA therapy. As regard to the obtained results, similar variation in the fatty acids, which may be related to the activity of HCV core protein, in the recurrent patients compared with the non-recurrent patients before and after RFA therapy. However, strikingly, opposite regularities in the pathways such as amino acids and PPP are found from the two discriminant models about HCC relapse. We suggest that the difference of variation directions in the involved pathways issue from the exclusion of tumor.

This study brings some imperfectness which might be accomplished in the following work. Above all, the number of samples was a remarkable limit in the both parts of the work. More other samples, especially some samples obtained from other hospitals should be tested to confirm the obtained results. Besides, we witnessed that there were a variety of variations in lipids along the study. Thus, to achieve a larger coverage of all kinds of lipids, lipidomics studies are suggested in the future work to detect concrete changes in certain lipids.

For the part concerning the septic shock, to better understand the exact mechanism from the septic shock to death in the non-survivors, the isotropic tracing technique is preferred to find out the origin of the variations in the discriminatory metabolites. Further, exhibited deregulation of urea cycle in the septic non-survivors implied severe kidney injury in these patients. A further metabolomic study using urine samples may be more direct and provide more information of alterations in kidney injury-related pathways.

For the study on HCC, as limited by the cohort, we principally worked on the recurrence in the patients with hepatitis C, but not in those with hepatitis B. It has been reported recently that the hepatitis B has become the main cause of HCC incidence, a following work may concentrate on determining the biomarkers predicting the recurrence in the HCC patients with hepatitis B.

Actually, the parts of the study are shared by our French and Chinese laboratory, but all the serum samples were taken in France. A validation of our results in the Chinese relevant patients in the future may make the results generally significant.

Finally, revealed metabolic variations in the non-survived patients of septic shock or in the HCC-HCV recurrent patients may indicate related alterations in the genome and proteome. Thus, studies applying other omics may provide a further understanding of the deregulation of relevant metabolic pathways and help to better understand the mechanisms for the patients with different outcomes.

Appendix

Appendix 1. Supporting information of the septic shock-related study 1

Table S1. Identified metabolites by the retained peaks following the pre-processing with the help of database. *: metabolites with VIP > 1; #: metabolites with p-value < 0.05; ^: metabolites confirmed by the MS/MS; metabolites identified by the database but rejected by the comparison to the result of MS/MS; &: significantly varied metabolites defined by both the positive and negative modes.

M/Z	Mode	Time	Attribution
80.0495	Positive	0.44	Pyridine
90.055	Positive	0.66	DL-Alanine
90.0551	Positive	0.91	L-Alanine?*#
90.0551	Positive	0.41	L-Alanine^
104.0706	Positive	0.44	Amino-isobutric acid*#
104.1073	Positive	0.4	Choline
105.0548	Positive	0.88	3,(4)-Hydroxybutryric acid*#
113.0348	Positive	2.86	Uracil*#
114.0661	Positive	0.69	Creatinine?*#
114.0665	Positive	0.42	Creatinine*#^
116.0709	Positive	0.96	DL-proline*#
116.0712	Positive	0.71	L-Proline*#^
117.0742	Positive	0.44	Betaine*#^
118.0862	Positive	0.44	L-Valine*#^
118.0863	Positive	0.72	L-Valine?*#
120.0655	Positive	0.44	L-Threonine
122.0965	Positive	3.1	Phenylethylamine*
130.0501	Positive	0.68	Pyroglutamic acid
130.0863	Positive	0.44	Pipecolic acid
132.077	Positive	0.43	Creatine*#^
132.077	Positive	0.71	Creatine?*#
132.1019	Positive	1.11	L-isoleucine*#^
132.1019	Positive	0.84	L-Leucine*#^
133.0973	Positive	0.35	Ornithine*#^
137.046	Positive	0.64	Hypoxanthine*#^
138.0551	Positive	2.52	Aminobenzoic acid*
139.0505	Positive	0.44	Urocanic acid
143.1069	Positive	4.85	Octenoic acid
144.102	Positive	0.71	Proline betaine*#
146.1174	Positive	2.15	Acetylcholine*

147.0767	Positive	0.71	DL-Glutamine?
147.0767	Positive	0.44	L-Glutamine*#^&
147.113	Positive	0.35	L-Lysine^
148.0604	Positive	0.44	L-Glutamate*#^
150.0586	Positive	0.62	Methionine^
152.0321	Positive	0.71	PhenylGlycine
152.0362	Positive	0.34	Methylcysteine sulfoxide^
153.041	Positive	0.67	Xanthine
162.1128	Positive	0.71	L-carnitine
166.0528	Positive	0.95	Methionine sulfoxide^
166.086	Positive	1.85	DL-Phenylalanine
166.0861	Positive	1.57	L-Phenylalanine*#^&
166.0864	Positive	1.32	DL-Phenylalanine?*#
169.036	Positive	0.59	Uric acid
176.0706	Positive	4.28	Indoleacetic Acid^
176.0708	Positive	4.7	Indoleacetic Acid?
176.1029	Positive	1.83	Citrulline*#^
176.1032	Positive	3.52	Citrulline?*#
176.1034	Positive	2.85	Citrulline?*#
180.0654	Positive	1.83	Hippuric acid*#^
181.072	Positive	2.56	Glucose
182.0811	Positive	2.28	L-Tyrosine?
182.0811	Positive	1.1	Tyrosine?*#
182.0815	Positive	0.71	L-Tyrosine*#^&
184.0948	Positive	0.41	Epinephrine
188.0707	Positive	2.43	L-Tryptophan*#
194.0816	Positive	3.36	2-Methylhippuric acid*#^
195.0875	Positive	3.07	Caffeine^
195.0878	Positive	3.56	Caffeine?
196.0604	Positive	2.96	Salicyluric acid
204.1234	Positive	0.62	Carnitine C2:0*#^
208.0971	Positive	4.31	N-acetyl-DL-Phenylalanine
218.1391	Positive	1.06	Carnitine C3:0
224.0915	Positive	1.99	N-acetyl-L-tyrosine*
229.1544	Positive	1.01	Ile-Pro*
229.1545	Positive	0.76	Pro-Leu
232.1548	Positive	2.33	Carnitine C4:0*#^
246.1703	Positive	3.05	Carnitine C5:0
247.1078	Positive	4.52	N-acetyl-DL-Tryptophan
252.1082	Positive	0.45	Deoxyadenosine
259.0929	Positive	0.68	Ribothymidine
260.1861	Positive	4.17	Carnitine C6:0?
260.1862	Positive	4.44	Carnitine C6:0*#^
261.145	Positive	2.76	Glu-Leu*

262.129	Positive	0.63	Epidermin
279.1702	Positive	4.28	Leucyl-Phe
280.1396	Positive	0.63	Glycated valine
284.186	Positive	2.98	α-Hydroxymetoprolol*#
286.2018	Positive	4.99	Carnitine C8:1*#
288.2172	Positive	5.16	Carnitine C8:0*#
288.2896	Positive	8	Sphinganine
294.1543	Positive	1.28	Glycated Isoleucine
294.155	Positive	0.98	Glycated leucine
300.2899	Positive	11.8	Sphingosine
314.1578	Positive	4.5	Phe-Phe
314.2328	Positive	6.37	Carinitine C10:1
316.248	Positive	6.86	Carnitine C10:0*#^
328.1025	Positive	1.32	p-Acetamidophenyl glucuronide
331.2847	Positive	12.33	MG 16:0*
339.1547	Positive	4.72	Nicotine glucuronide*
342.264	Positive	7.47	Carnitine C12:1
344.279	Positive	7.93	Carnitine C12:0*#^
359.3156	Positive	13.81	MG 18:0^
368.2795	Positive	7.91	Carnitine C14:2
370.2948	Positive	8.44	Carnitine C14:1
371.1699	Positive	5.16	4-Hydroxy-3,5-bis(1-methylethyl)phenyl glucuronide
372.3109	Positive	8.97	Carnitine C14:0^
388.1969	Positive	5.83	Terazosin
398.3262	Positive	9.32	Carnitine C16:1*
400.3421	Positive	9.91	Carnitine C16:0*#^
401.3415	Positive	14.4	7-Ketocholesterol
401.3457	Positive	9.91	Calcifediol
426.358	Positive	10.16	Carnitine C18:1
428.3735	Positive	10.77	Carnitine C18:0*#^
73.0293	Negative	0.74	Propionic acid*
89.0241	Negative	0.61	L-Lactic acid*#^
89.0241	Negative	1.75	DL-Lactic acid?*#
89.0242	Negative	1.21	DL-Lactic acid?*#
101.0244	Negative	0.4	2-Oxobutanoate
103.0398	Negative	1.04	Hydroxybutyric acid
103.0398	Negative	1.54	Hydroxyisobutyric acid
105.0193	Negative	0.43	Glyceric acid
117.0189	Negative	0.76	Succinic acid*#^
117.0552	Negative	2.31	Hydroxyvaleric acid*#
121.0291	Negative	3.19	Benzoic acid
128.0348	Negative	0.68	DL-Glutamate*
130.0868	Negative	0.78	DL-Leucine/Isoleucine

133.014	Negative	0.41	Malic acid*#^
135.0296	Negative	0.43	Threonic acid*
137.0238	Negative	4.48	Salicylic acid
145.05	Negative	2.32	Adipic acid
145.0617	Negative	0.4	L-Glutamine*#^&
145.0866	Negative	4.78	2-Hydroxy enanthoic acid
146.0456	Negative	0.43	L-Glutamate
147.0293	Negative	0.79	alpha-Ketoglutarate*#^
147.0444	Negative	3.85	Cinnamic acid*#
149.0451	Negative	0.43	Ribose
150.0554	Negative	2.94	2-Phenylglycine
151.0258	Negative	0.77	Xanthine*
151.0395	Negative	3.54	p-Hydroxyphenylacetic acid
157.0498	Negative	2.5	Succinylacetone*#
158.0814	Negative	3.5	N-isovalerylglycine
164.0709	Negative	1.89	L-Phenylalanine*#^&
172.9904	Negative	2.2	Phenol sulfate*#
179.0558	Negative	0.4	Allo-Inostiol*
180.0659	Negative	0.74	L-Tyrosine*#^&
183.1381	Negative	7.12	FFA C11:1
185.1175	Negative	6.94	OH-FFA C11:1*
187.0059	Negative	3.38	p-Cresol sulfate
187.0968	Negative	4.7	Nonanedioic acid
191.0193	Negative	0.65	Citric acid*#^
191.0557	Negative	0.43	Quinic acid
201.1121	Negative	5.44	Sebacic acid*
202.1076	Negative	0.76	Acetylcarnitine
203.0816	Negative	4.14	3-Hydroxymethylantipyrine
203.0816	Negative	2.43	L-Tryptophan
204.0656	Negative	4.12	Indolelactic acid*#^
207.0763	Negative	3.55	Kynurenine
208.0605	Negative	3.53	Hydroxyphenylacetylglycine
212.0013	Negative	2.49	Indoxy sulfate*#^
213.0215	Negative	4.95	Methylthiobenzoic acid
215.164	Negative	8.62	Hydroxydodecanoic acid*#
222.0761	Negative	1.72	Acetyl-L-tyrosine*^
222.0762	Negative	2.64	Acetyl-L-tyrosine?*#
227.1275	Negative	6.34	Traumatic acid
229.1432	Negative	6.81	Dodecanedioic acid
230.0116	Negative	1.47	Norepinephrine sulfate
243.1701	Negative	3.53	Leu-Iso
246.0735	Negative	5.51	Asp-Asp
255.2313	Negative	9.82	FFA 16:0*#^
263.1018	Negative	3.18	Phe-Gln

269.2106	Negative	10.63	FFA 17:0
283.2628	Negative	11.08	FFA 18:0*#^
289.1277	Negative	3.2	Argininosuccinate*#^
327.2161	Negative	7.17	FFA 22:6
367.1557	Negative	6.36	Etiocholanolone sulfate
369.1717	Negative	5.78	DHAS
369.172	Negative	6.83	ANDS
391.2831	Negative	9.27	UDCA*#^
391.2834	Negative	12	CDCA
407.2778	Negative	7.84	CA^
409.2335	Negative	11.1	LPC 16:0^
433.2335	Negative	10.69	LPC 18:2
448.3033	Negative	7.92	GUDCA*#^
448.3035	Negative	6.99	GCDCA*#^
452.2758	Negative	8.92	LPE 16:0
464.2994	Negative	5.91	GCA*#^
466.3047	Negative	7	LPC 14:0*#^
476.2757	Negative	9.64	LPE 18:2*#^
478.2911	Negative	10.31	LPE 18:1
480.3064	Negative	11.08	LPE 18:0*#^
498.26	Negative	9.15	LPE 20:5*#^
498.2858	Negative	6.31	TCDCA
500.2753	Negative	9.7	LPE 20:4*#^
502.2917	Negative	10.08	LPE 20:3*#
514.2804	Negative	6.4	TCA
528.2595	Negative	6.8	GUDCS*#^

Table S2. Discriminating metabolites in the comparison between septic survivors and non-survivors. The fold change is calculated by the report of concentration non-survivor/ survivor, thereby values which are inferior to 1 are for decreased metabolites in dead patients and increased metabolites possess values which are superior to 1

Identified Metabolites	Mode	m/z	tR (Min)	P-Value	Fold change
L-Lactic acid	Negative	89.0241	0.61	1.53E-02	1.51
Creatinine	Positive	114.0665	0.42	6.13E-03	1.69
L-Proline	Positive	116.0712	0.71	1.47E-04	2.64
Succinic acid	Negative	117.0189	0.76	1.52E-02	2.66
Betaine	Positive	117.0742	0.44	1.62E-05	5.18
L-Valine	Positive	118.0862	0.44	1.00E-08	4.30
Creatine	Positive	132.077	0.43	8.84E-04	3.04
L-Leucine	Positive	132.1019	0.84	7.39E-09	6.04
L-Isoleucine	Positive	132.1019	1.11	6.21E-08	15.77

Malic acid	Negative	133.014	0.41	8.80E-04	3.83
Ornithine	Positive	133.0973	0.35	1.06E-02	0.18
Hypoxanthine	Positive	137.046	0.64	1.18E-03	0.36
L-Glutamine	Negative	145.0617	0.40	2.40E-02	2.28
alpha-KG	Negative	147.0293	0.79	6.41E-04	2.17
L-Glutamate	Positive	148.0604	0.44	5.00E-02	1.89
L-Phenylalanine	Positive	166.0861	1.57	6.88E-04	1.92
Citrulline	Positive	176.1029	1.83	3.95E-08	0.13
Hippuric acid	Positive	180.0654	1.84	3.57E-03	0.17
L-Tyrosine	Positive	182.0815	0.71	1.23E-02	2.44
Citric acid	Negative	191.0193	0.65	2.29E-03	2.23
2-Methylhippuric acid	Positive	194.0816	3.36	8.70E-03	0.18
Indolelactic acid	Negative	204.0656	4.12	1.58E-03	2.59
Carnitine C2:0	Positive	204.1234	0.62	8.93E-09	0.18
Indoxy sulfate	Negative	212.0013	2.49	2.85E-03	3.14
Carnitine C4:0	Positive	232.1548	2.33	7.11E-03	6.06
FFA 16:0	Negative	255.2313	9.82	1.15E-06	0.70
Carnitine C6:0	Positive	260.1862	4.44	3.07E-02	2.60
FFA 18:0	Negative	283.2628	11.08	5.30E-04	0.57
Argininosuccinate	Negative	289.1277	3.2	1.00E-02	0.70
Carnitine C10:0	Positive	316.248	6.86	2.46E-03	1.72
Carnitine C12:0	Positive	344.279	7.93	5.52E-03	4.33
UDCA	Negative	391.2831	9.27	1.25E-02	4.75
Carnitine C16:0	Positive	400.3421	9.91	1.97E-03	0.52
Carnitine C18:0	Positive	428.3735	10.77	1.25E-02	0.55
GUDCA	Negative	448.3033	7.92	8.19E-04	3.87
GCDCA	Negative	448.3035	6.99	3.83E-02	3.23
GCA	Negative	464.2994	5.91	1.50E-03	4.32
LPC 14:0	Negative	466.3047	7.00	7.33E-04	4.91
LPE 18:2	Negative	476.2757	9.64	4.96E-03	0.56
LPE 18:0	Negative	480.3064	11.08	7.91E-03	0.48
LPE 20:5	Negative	498.26	9.15	5.33E-03	0.60
LPE 20:4	Negative	500.2753	9.70	8.70E-03	0.57
GUDCS	Negative	528.2595	6.80	1.89E-03	3.35

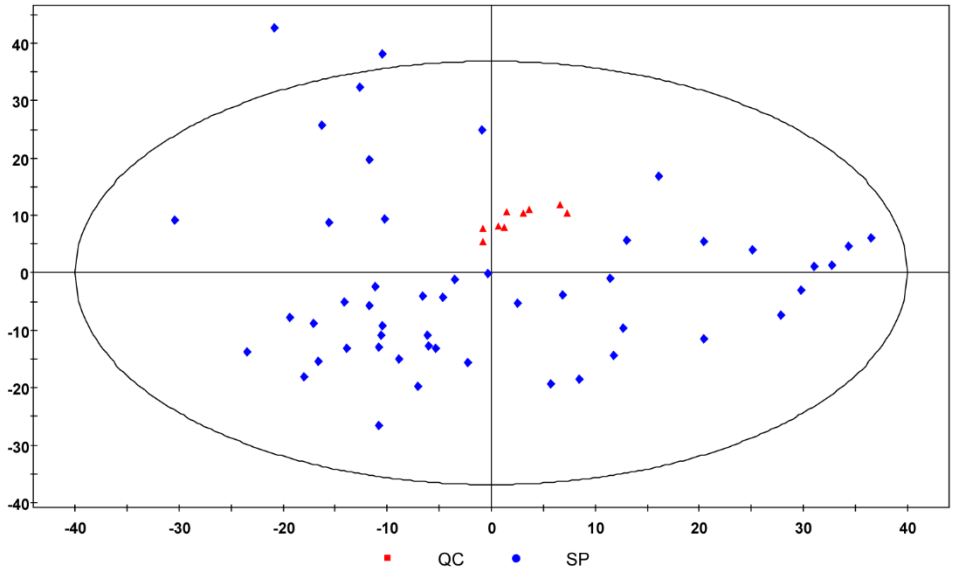

Figure S1. The PCA score plot for all the real samples and QC samples. Red triangles: QC samples; blue squares : real samples.

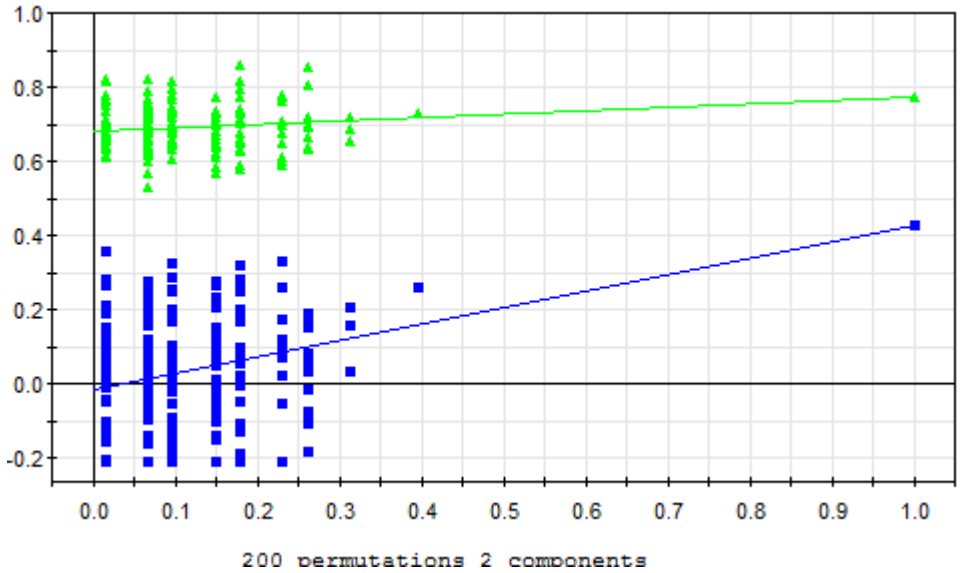

Figure S2. Validation of the PLS-DA model revealing that the model is not over-fitting. The samples were permutated into a different order from that in the established model for 200 times. The green triangles stand for the obtained R^2 value and the blue squares stand for the obtained Q^2 value by the 200 permutations.

Appendix 2: Supporting information of the HCC-related study.

S1. Chemical reference substance used in the study.

2-Hydroxybutyrate, 3-Hydroxybutyrate, 3-aminoisobutyrate, 7-hydroxycholesterol, benzoate, citrate, isocitrate, gluconate, glyceraldehyde, glycerate, glycerol, glycolate, hydroxyisovalerate, hydroxylamine, isosuccinate, lactate, threonate, oxalate, urate, xanthine, citrulline, L- asparagine, L-aspartate, L-cysteine, L-glutamine, L-glutamate, L-isoleucine, L-leucine, L-proline, L-threonine, L-serine, L-tryptophan and N-acetyl-L-lysine were purchased from Sigma-Aldrich China Inc. (Shanghai, China); D-arabitol, D-ribitol, butanoic acid (FFA 4:0), hexanoic acid (FFA 6:0), decanoic acid (FFA 10:0), dodecanoic acid (FFA 12:0), pentadecanoic acid (FFA 15:0), palmitic acid (FFA 16:0), octadecanoic acid (FFA 18:0), 11-Eicosenoic acid (FFA 20:1), Arachidonic acid (FFA 20:4) and Docosahexaenoic acid (FFA 22:6) were offered by the J&K Scientific Ltd. (Beijing, China).

Table S-1 Definition of the characteristic ions for the targeted metabolites. The information was obtained by analyzing the corresponding standards.

Metabolites	**Retention time (min)**	**m/z**
Aspartate	18.16 20.63	160 232
Proline	11.3 14.75 20.04	70 142 142
Glutamate	20.91 23.02	84 246
Glycerol	14.21	205
L-Norvaline	9.64 13.35	72 144

Table S-2. Targeted scan period and ions for the validation experience. The listed ions are the ions characterize the metabolites norvaline (targeted ion: 72/144), glutamate (84/246), aspartate (160,232), proline (70,142) and glycerol (205).

Scan time (min)	Targeted Ions (m/z)
9～12	72，70
12～16	144,205,142
17～19	160
19～21	232,84
21～24	142,246

Table S-3. Relative standard deviation (RSD) for all the detected characteristic ions. For the peak normalization by the internal standard, 2 characteristic ions for L-norvaline (m/z = 72, m/z = 144) were detected. The ion m/z = 144 was ultimately chosen as the reference of peak normalization because it brought a RSD = 0.17, which was calculated by the peak area in all the 9 QC samples, lower than that for m/z = 72 (RSD = 0.25). After all the peak areas were normalized, RSD for the targeted ions in each QC sample were obtained as shown. For one metabolite with two detected characteristic ions, the ion with a lower RSD than the other (presented in bold) was chosen for the following analyses.

Metabolites	**m/z**	**Retention time (min)**	**RSD**
L-Norvaline 1	72	9.34	0.255
L-Proline 1	70	11	0.359
L-Norvaline 2	144	13.05	0.000
Glycerol	**205**	**13.93**	**0.230**
L-Proline 2	**142**	**14.48**	**0.196**
Aspartate 1	**160**	**17.86**	**0.139**
Aspartate 1	232	20.33	0.361
Glutamate 1	**84**	**20.61**	**0.290**
Glutamate 2	246	22.72	0.761

Table S-4. Significant altered metabolites in discrimination between recurrent HCV-HCC patients and non-recurrent HCV-HCC patients. BT: before RFA therapy; AT: after RFA therapy. TR: time of retention. FC: fold change, calculated by the ratio of R/NR. *: metabolites confirmed by the standard reference substance.

Subgroup	TR	QN	Metabolites	P-value	FC
BT	7.95	117	Lactate*	0.021	0.81
	8.32	173	FFA 6:0*	0.009	1.76
	8.39	147	Glycolic acid*	0.027	1.3
	9.74	131	2-Hydroxybutyrate*	0.006	0.55
	10.60	86	L-Leucine*	0.001	0.59
	11.17	86	L-isoleucine*	0.009	0.63
	13.29	177	Urea	0.028	1.26
	13.39	132	L-Serine*	0.021	1.37
	14.53	164	Benzeneacetate	0.010	1.65
	15.01	147	Isosuccinate*	0.001	1.47
	17.47	147	Unknown 3	0.006	1.98
	17.51	373	Sebacic acid	0.030	1.31
	17.59	103	FFA 4:0	0.038	1.44
	18.14	189	(R,S)-3,4-Dihydroxybutanoate	0.006	1.41
	20.31	232	L-Aspartate*	0.001	1.82
	20.41	230	L-Proline*	0.027	1.75
	21.11	246	L-Cysteine*	0.006	1.83
	21.71	110	Unknown 1	0.002	1.56
	22.71	246	L-Glutamate*	0.000	2.3
	22.74	192	L-Phenylalanine*	0.049	1.34
	23.47	257	FFA 12:0*	0.004	1.86
	24.89	217	Arabitol*	0.048	1.37
	24.99	217	Ribitol*	0.009	1.38
	30.58	333	D-Gluconic acid*	0.048	1.57
	30.95	173	Benzoate	0.044	0.49
	31.03	353	Xanthine*	0.022	0.58
	32.44	437	2-Keto-d-gluconic acid	0.013	0.67
	32.58	456	Urate*	0.030	0.52
	34.33	202	3-indolelactic acid	0.003	0.62
	35.50	232	Unknown 2	0.046	1.24
	36.83	70	2-Deoxy-D-ribose	0.022	0.68
	38.46	98	N-alpha-acetyl-L-lysine*	0.001	0.56
	38.73	98	FFA 18:0	0.037	0.67
	40.26	91	FFA 22:6*	0.022	0.61

	47.97	456	7-Hydroxycholesterol*	0.004	2.24
AT	7.95	117	Lactate*	0.036	1.2
	8.67	147	Pyruvate*	0.017	1.28
	9.29	146	Hydroxylamine*	0.035	1.26
	9.74	131	2-Hydroxybutyric acid*	0.010	1.62
	10.15	147	Oxalate*	0.021	0.79
	10.71	233	3-Hydroxybutyric acid*	0.007	1.86
	12.08	131	Hydroxyisovalericacid*	0.043	0.77
	12.41	73	Glyceraldehyde*	0.001	0.66
	13.13	179	Benzoate*	0.001	1.38
	13.79	158	L-leucine*	0.028	0.81
	13.89	205	Glycerol*	0.001	1.8
	14.37	158	L-Isoleucine*	0.022	0.79
	14.39	130	L-Threonine*	0.036	0.78
	14.44	142	L-Proline*	0.000	0.6
	14.45	115	Glutaric acid*	0.001	0.58
	15.41	189	glycerate*	0.008	0.81
	18.66	248	3-Aminoisobutyrate*	0.035	2.03
	18.79	229	FFA 10:0*	0.003	1.66
	20.31	232	L-Aspartate*	0.001	0.61
	20.84	292	L-Threonate*	0.002	0.77
	20.99	115	Creatinine*	0.001	0.66
	21.11	246	L-Cysteine*	0.005	0.65
	21.71	110	Unknown 1	0.051	1.3
	23.47	257	FFA 12:0*	0.021	1.52
	23.81	116	L-asparagine*	0.016	0.57
	25.83	292	Ribonic acid	0.006	0.67
	25.85	357	Glycerol 1-phosphate	0.021	0.6
	26.10	156	L-glutamine*	0.020	0.27
	26.20	292	2-Keto-l-gluconic acid	0.009	0.67
	27.05	273	Citric acid*	0.008	1.7
	27.12	245	Isocitric acid*	0.002	2
	27.19	157	Citrulline*	0.017	0.65
	27.47	283	Myristoleicacid 14:1	0.004	2.51
	27.73	285	Myristic acid 14:0*	0.001	1.76
	29.72	299	FFA 15:0*	0.007	1.29
	29.76	175	Acetamide	0.007	0.73
	31.21	311	Palmitelaidic acid FFA 16:1*	0.004	2.11
	31.63	313	FFA 16:0*	0.000	1.27

	33.59	217	Ribitol	0.006	0.76
	34.54	202	L-Tryptophan*	0.006	0.49
	34.85	117	FFA 18:1	0.001	1.54
	35.22	117	FFA 18:0*	0.007	1.23
	35.49	82	FFA 18:2	0.002	1.54
	35.50	232	Unknown 2	0.018	0.78
	35.82	232	2-Deoxy-D-ribose	0.029	0.79
	36.27	56	11,14-Eicosadienoic acid	0.020	0.77
	37.26	80	FFA 20:4*	0.007	0.71
	37.37	158	Xylonic acid	0.018	0.73
	38.09	367	11-Eicosenoic acid*	0.003	1.52
	49.14	202	Leu-Trp	0.012	0.59

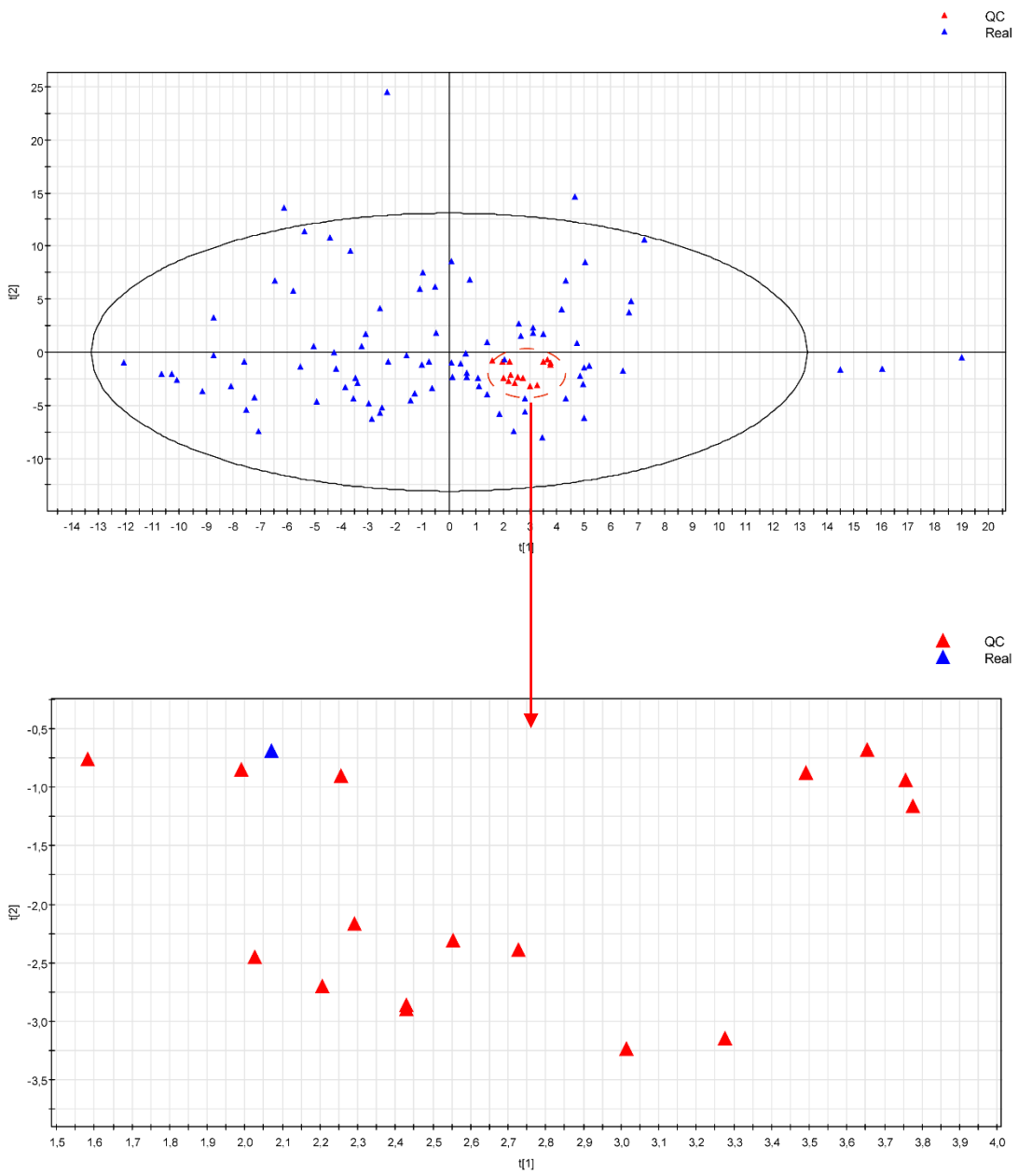

Figure S-1 Score plot of PCA presenting the comparison between the QC samples (red and circled triangles) and the real samples (blue triangles).

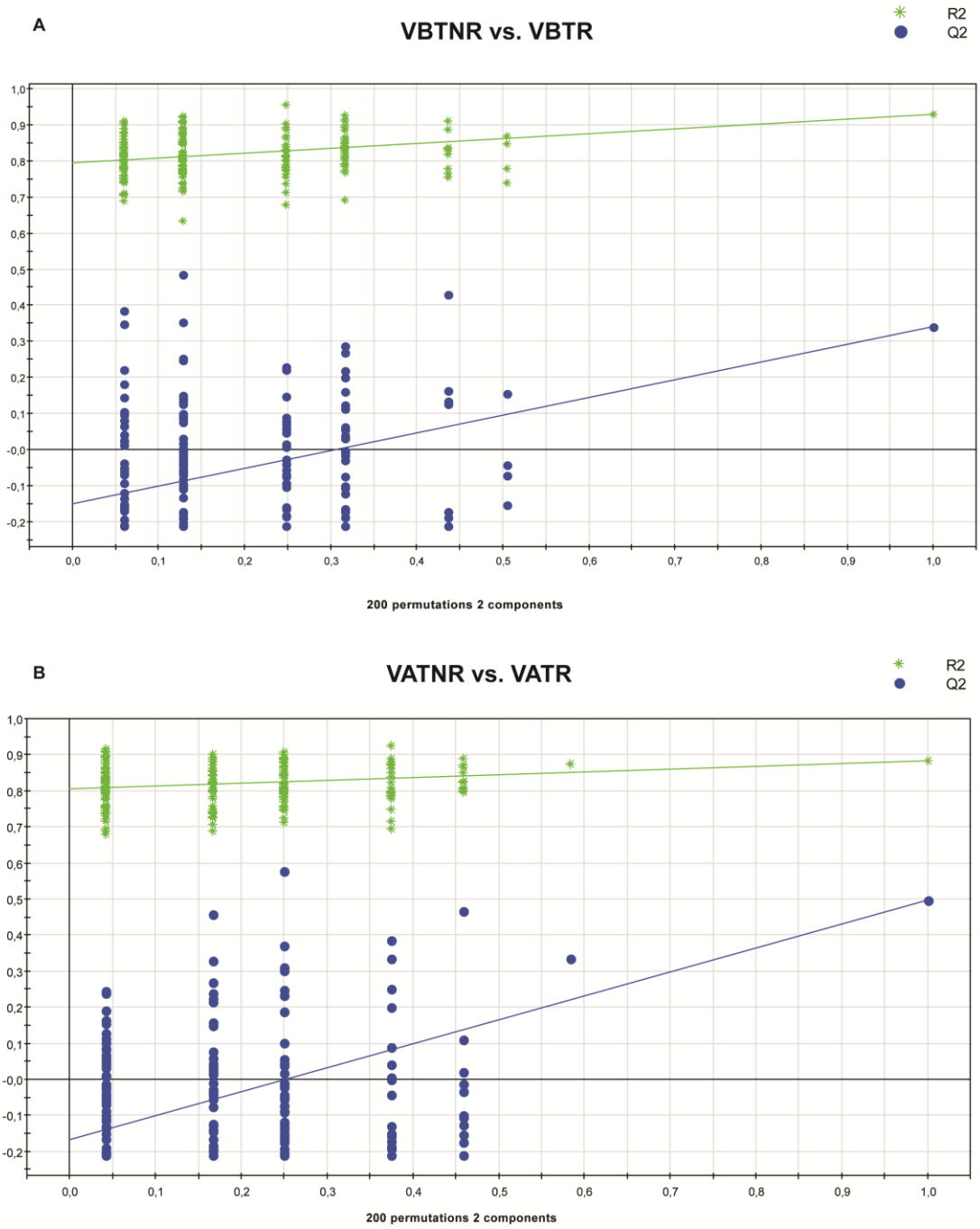

Figure S-2. Cross-validation for the two PLS-DA models separating the recurrent and the non-recurrent HCC patients with HCV. A: Model validation for NR_{BT} vs R_{BT} B: Model validation for NR_{AT} vs R_{AT}. The samples were permutated into a different order from that in the established model for 200 times. The green triangles stand for the obtained R^2 value and the blue squares stand for the obtained Q^2 value by the 200 permutations. The Y-axis represents R^2 and Q^2 value for every model while the X-axis represents the correlation coefficient between original and permuted response data.

References

1. Nicholson JK, Lindon JC, Holmes E. 'Metabonomics': understanding the metabolic responses of living systems to pathophysiological stimuli via multivariate statistical analysis of biological NMR spectroscopic data. Xenobiotica. 1999;29(11):1181-9.
2. Fiehn O. Metabolomics–the link between genotypes and phenotypes. Plant Mol Biol. 2002;48(1-2):155-71.
3. Nicholson JK, Lindon JC. Systems biology: metabonomics. Nature. 2008;455(7216):1054-6.
4. Rochfort S. Metabolomics reviewed: a new “omics” platform technology for systems biology and implications for natural products research. J Nat Prod. 2005;68(12):1813-20.
5. Dettmer K, Aronov PA, Hammock BD. Mass spectrometry-based metabolomics. Mass Spectrom Rev. 2007;26(1):51-78.
6. Madsen R, Lundstedt T, Trygg J. Chemometrics in metabolomics—a review in human disease diagnosis. Anal Chim Acta. 2010;659(1):23-33.
7. Mamas M, Dunn WB, Neyses L, Goodacre R. The role of metabolites and metabolomics in clinically applicable biomarkers of disease. Arch Toxicol. 2011;85(1):5-17.
8. Gowda GN, Zhang S, Gu H, Asiago V, Shanaiah N, Raftery D. Metabolomics-based methods for early disease diagnostics. Expert review of molecular diagnostics. 2008;8(5):617-33.
9. Gill SR, Pop M, DeBoy RT, Eckburg PB, Turnbaugh PJ, Samuel BS et al. Metagenomic analysis of the human distal gut microbiome. Science. 2006;312(5778):1355-9.
10. Bundy JG, Davey MP, Viant MR. Environmental metabolomics: a critical review and future perspectives. Metabolomics. 2009;5(1):3-21.
11. Sumner LW, Mendes P, Dixon RA. Plant metabolomics: large-scale phytochemistry in the functional genomics era. Phytochemistry. 2003;62(6):817-36.
12. Shyur L-F, Yang N-S. Metabolomics for phytomedicine research and drug development. Curr Opin Chem Biol. 2008;12(1):66-71.
13. Gibney MJ, Walsh M, Brennan L, Roche HM, German B, Van Ommen B. Metabolomics in human nutrition: opportunities and challenges. The American journal of clinical nutrition. 2005;82(3):497-503.
14. Cevallos-Cevallos JM, Reyes-De-Corcuera JI, Etxeberria E, Danyluk MD, Rodrick GE. Metabolomic analysis in food science: a review. Trends Food Sci Tech. 2009;20(11):557-66.
15. Cifuentes A. Food analysis and foodomics. J Chromatogr A. 2009;1216(43):7109.
16. Collins FS, Varmus H. A new initiative on precision medicine. N Engl J Med. 2015;372(9):793-5.
17. Biomedical F. NIH definition of biomarker. Clin Pharmacol Ther. 2001;69:89-95.
18. Epstein LH. The direct effects of compliance on health outcome. Health Psychology. 1984;3(4):385.
19. Dunn WB, Broadhurst D, Begley P, Zelena E, Francis-McIntyre S, Anderson N et al. Procedures for large-scale metabolic profiling of serum and plasma using gas chromatography and liquid chromatography coupled to mass spectrometry. Nat Protoc. 2011;6(7):1060-83.
20. Pan Z, Raftery D. Comparing and combining NMR spectroscopy and mass spectrometry in metabolomics. Analytical and bioanalytical chemistry. 2007;387(2):525-7.
21. Nicholson JK, Lindon JC, Holmes E. 'Metabonomics': understanding the metabolic responses of living systems to pathophysiological stimuli via multivariate statistical analysis of biological NMR

spectroscopic data. Xenobiotica. 1999;29(11):1181-9.
22. Fiehn O. Metabolomics--the link between genotypes and phenotypes. Plant Mol Biol. 2002;48(1-2):155-71.
23. Dettmer K, Hammock BD. Metabolomics--a new exciting field within the" omics" sciences. Environ Health Persp. 2004;112(7):A396.
24. Want EJ, Wilson ID, Gika H, Theodoridis G, Plumb RS, Shockcor J et al. Global metabolic profiling procedures for urine using UPLC-MS. Nat Protoc. 2010;5(6):1005-18.
25. Beckonert O, Keun HC, Ebbels TM, Bundy J, Holmes E, Lindon JC et al. Metabolic profiling, metabolomic and metabonomic procedures for NMR spectroscopy of urine, plasma, serum and tissue extracts. Nat Protoc. 2007;2(11):2692-703.
26. Dunn WB, Wilson ID, Nicholls AW, Broadhurst D. The importance of experimental design and QC samples in large-scale and MS-driven untargeted metabolomic studies of humans. Bioanalysis. 2012;4(18):2249-64.
27. Rocke DM, editor. Design and analysis of experiments with high throughput biological assay data. Seminars in cell & developmental biology; 2004: Elsevier.
28. Metabolomics: Current analytical platforms and methodologies. TrAC Trends in Analytical Chemistry. 2005;24(4):285-94.
29. Sykes BD. Urine stability for metabolomic studies: effects of preparation and storage. Metabolomics. 2007;3(1):19-27.
30. Fernández-Peralbo MA, Luque de Castro MD. Preparation of urine samples prior to targeted or untargeted metabolomics mass-spectrometry analysis. TrAC Trends in Analytical Chemistry. 2012;41:75-85.
31. Yin P, Peter A, Franken H, Zhao X, Neukamm SS, Rosenbaum L et al. Preanalytical aspects and sample quality assessment in metabolomics studies of human blood. Clin Chem. 2013;59(5):833-45.
32. Andrew ER. Nuclear magnetic resonance. Nuclear Magnetic Resonance, by ER Andrew, Cambridge, UK: Cambridge University Press, 2009. 2009;1.
33. Koutcher JA, Burt CT. Principles of nuclear magnetic resonance. J Nucl Med. 1984;25(1):101-11.
34. Becker ED. High resolution NMR: theory and chemical applications. Academic Press; 1999.
35. Brewer RG, Shoemaker R. Optical free induction decay. Physical Review A. 1972;6(6):2001.
36. Yamamoto H, Saitoh K, Hasegawa H, Ochi H. NMR spectrometer and NMR probe. Google Patents; 2006.
37. Defernez M, Colquhoun IJ. Factors affecting the robustness of metabolite fingerprinting using 1H NMR spectra. Phytochemistry. 2003;62(6):1009-17.
38. Shimizu A, Ikeguchi M, Sugai S. APPROPRIATENESS OF DSS AND TSP AS INTERNAL REFERENCES FOR H-1-NMR STUDIES OF MOLTEN GLOBULE PROTEINS IN AQUEOUS-MEDIA. J Biomol NMR. 1994;4(6):859-62.
39. Vandegans J, de Kersabiec A-M. Spectrométrie d'absorption atomique. Ed. Techniques Ingénieur; 1997.
40. Hoffmann E. Mass spectrometry. Wiley Online Library; 1996.
41. Munson MS, Field F-H. Chemical ionization mass spectrometry. I. General introduction. J Am Chem Soc. 1966;88(12):2621-30.
42. Barber M, Bordoli RS, Sedgwick RD, Tyler AN. Fast atom bombardment of solids (FAB): A new ion source for mass spectrometry. Journal of the Chemical Society, Chemical Communications. 1981(7):325-7.

43. Andrade FJ, Shelley JT, Wetzel WC, Webb MR, Gamez G, Ray SJ et al. Atmospheric pressure chemical ionization source. 1. Ionization of compounds in the gas phase. Anal Chem. 2008;80(8):2646-53.
44. Hillenkamp F, Karas M, Beavis RC, Chait BT. Matrix-assisted laser desorption/ionization mass spectrometry of biopolymers. Anal Chem. 1991;63(24):1193A-203A.
45. Dawson P. Quadrupole mass analyzers: performance, design and some recent applications. Mass Spectrom Rev. 1986;5(1):1-37.
46. Balcerzak M. An overview of analytical applications of time of flight-mass spectrometric (TOF-MS) analyzers and an inductively coupled plasma-TOF-MS technique. Anal Sci. 2003;19(7):979-89.
47. Makarov A, Denisov E, Kholomeev A, Balschun W, Lange O, Strupat K et al. Performance evaluation of a hybrid linear ion trap/orbitrap mass spectrometer. Anal Chem. 2006;78(7):2113-20.
48. Hu Q, Noll RJ, Li H, Makarov A, Hardman M, Graham Cooks R. The Orbitrap: a new mass spectrometer. J Mass Spectrom. 2005;40(4):430-43.
49. Marshall AG, Hendrickson CL, Jackson GS. Fourier transform ion cyclotron resonance mass spectrometry: a primer. Mass Spectrom Rev. 1998;17(1):1-35.
50. McLuckey SA, Glish GL, Van Berkel GJ. Charge determination of product ions formed from collision-induced dissociation of multiply protonated molecules via ion/molecule reactions. Anal Chem. 1991;63(18):1971-8.
51. Hu Q, Noll RJ, Li H, Makarov A, Hardman M, Graham Cooks R. The Orbitrap: a new mass spectrometer. J Mass Spectrom. 2005;40(4):430-43.
52. Bachmann S, Bressan A, Ropelewski L, Sauli F, Sharma A, Mörmann D. Charge amplification and transfer processes in the gas electron multiplier. Nuclear Instruments and Methods in Physics Research Section A: Accelerators, Spectrometers, Detectors and Associated Equipment. 1999;438(2):376-408.
53. Patel R, Roy M, Dutta G. Mass spectrometry-A review. Veterinary World. 2012;5(3):185-92.
54. McLafferty FW. Tandem mass spectrometry. Science. 1981;214(4518):280-7.
55. Giddings JC. Dynamics of chromatography: principles and theory. CRC Press; 2002.
56. Smith R, Haken J, Wainwright M. Evaluation of mathematical procedures for the calculation of dead-time. J Chromatogr A. 1978;147:65-73.
57. Christie WW. Gas chromatography and lipids. Oily Press Ayr; 1989.
58. Cooper JR, Bowater IC, Wilkins CL. Gas chromatography/Fourier transform infrared/mass spectrometry using a mass selective detector. Anal Chem. 1986;58(13):2791-6.
59. Knapp DR. Handbook of analytical derivatization reactions. John Wiley & Sons; 1979.
60. Petrovic M, Barcelo D. Liquid chromatography-tandem mass spectrometry. Analytical and bioanalytical chemistry. 2013;405(18):5857-8.
61. Majors RE, Przybyciel M. Columns for reversed-phase LC separations in highly aqueous mobile phases. Lc Gc N Am. 2002;20(7):584-93.
62. Cubbon S, Antonio C, Wilson J, Thomas‐Oates J. Metabolomic applications of hilic‐lc‐ms. Mass Spectrom Rev. 2010;29(5):671-84.
63. Swartz ME. UPLC™: an introduction and review. J Liq Chromatogr R T. 2005;28(7-8):1253-63.
64. Ramautar R, Somsen GW, de Jong GJ. CE‐MS in metabolomics. Electrophoresis. 2009;30(1):276-91.
65. Ramautar R, Mayboroda OA, Somsen GW, de Jong GJ. CE‐MS for metabolomics: Developments and applications in the period 2008–2010. Electrophoresis. 2011;32(1):52-65.
66. Shevchenko A, Simons K. Lipidomics: coming to grips with lipid diversity. Nat Rev Mol Cell Bio. 2010;11(8):593-8.

67. Hochrein J, Zacharias HU, Taruttis F, Samol C, Engelmann JC, Spang R et al. Data Normalization of (1)H NMR Metabolite Fingerprinting Data Sets in the Presence of Unbalanced Metabolite Regulation. J Proteome Res. 2015;14(8):3217-28.
68. Dieterle F, Ross A, Schlotterbeck G, Senn H. Probabilistic quotient normalization as robust method to account for dilution of complex biological mixtures. Application in H-1 NMR metabonomics. Anal Chem. 2006;78(13):4281-90.
69. Lee J, Park J, Lim MS, Seong SJ, Seo JJ, Park SM et al. Quantile Normalization Approach for Liquid Chromatography-Mass Spectrometry-based Metabolomic Data from Healthy Human Volunteers. Anal Sci. 2012;28(8):801-5.
70. Gallon S, Loubes JM, Maza E. Statistical properties of the quantile normalization method for density curve alignment. Math Biosci. 2013;242(2):129-42.
71. van den Berg RA, Hoefsloot HC, Westerhuis JA, Smilde AK, van der Werf MJ. Centering, scaling, and transformations: improving the biological information content of metabolomics data. BMC genomics. 2006;7:142.
72. De Meyer T, Sinnaeve D, Van Gasse B, Rietzschel ER, De Buyzere ML, Langlois MR et al. Evaluation of standard and advanced preprocessing methods for the univariate analysis of blood serum H-1-NMR spectra. Analytical and Bioanalytical Chemistry. 2010;398(4):1781-90.
73. Gibbons JD, Chakraborti S. Nonparametric statistical inference. Springer; 2011.
74. Kaempf U. The binomial test: a simple tool to identify process problems. IEEE T Semiconduct M. 1995;8(2):160-6.
75. Norusis MJ. SPSS: Statistical data analysis. SPSS; 1990.
76. Miller Jr RG. Beyond ANOVA: basics of applied statistics. CRC Press; 1997.
77. Estivill-Castro V. Why so many clustering algorithms: a position paper. ACM SIGKDD explorations newsletter. 2002;4(1):65-75.
78. Bridges CC. Hierarchical cluster analysis. Psychological reports. 1966;18(3):851-4.
79. Saghatelian A, Trauger SA, Want EJ, Hawkins EG, Siuzdak G, Cravatt BF. Assignment of endogenous substrates to enzymes by global metabolite profiling. Biochemistry. 2004;43(45):14332-9.
80. Jolliffe I. Principal component analysis. Wiley Online Library; 2002.
81. Wold S, Esbensen K, Geladi P. Principal component analysis. Chemometr Intell Lab. 1987;2(1-3):37-52.
82. Abdi H, Williams LJ. Principal component analysis. Wiley Interdisciplinary Reviews: Computational Statistics. 2010;2(4):433-59.
83. Wold S, Sjöström M, Eriksson L. PLS-regression: a basic tool of chemometrics. Chemometr Intell Lab. 2001;58(2):109-30.
84. Bylesjö M, Rantalainen M, Cloarec O, Nicholson JK, Holmes E, Trygg J. OPLS discriminant analysis: combining the strengths of PLS‐DA and SIMCA classification. J Chemometr. 2006;20(8‐10):341-51.
85. Worley B, Powers R. Multivariate analysis in metabolomics. Current Metabolomics. 2013;1(1):92-107.
86. Lu B, Castillo I, Chiang L, Edgar TF. Industrial PLS model variable selection using moving window variable importance in projection. Chemometr Intell Lab. 2014;135:90-109.
87. Bewick V, Cheek L, Ball J. Statistics review 13: Receiver operating characteristic curves. Critical Care. 2004;8(6):508.
88. Westerhuis JA, van Velzen EJ, Hoefsloot HC, Smilde AK. Multivariate paired data analysis: multilevel PLSDA versus OPLSDA. Metabolomics. 2010;6(1):119-28.

89. Bijlsma S, Bobeldijk I, Verheij ER, Ramaker R, Kochhar S, Macdonald IA et al. Large-scale human metabolomics studies: a strategy for data (pre-) processing and validation. Anal Chem. 2006;78(2):567-74.
90. Serkova NJ, Niemann CU. Pattern recognition and biomarker validation using quantitative 1H-NMR-based metabolomics. Expert review of molecular diagnostics. 2006;6(5):717-31.
91. Triba MN, Le Moyec L, Amathieu R, Goossens C, Bouchemal N, Nahon P et al. PLS/OPLS models in metabolomics: the impact of permutation of dataset rows on the K-fold cross-validation quality parameters. Molecular bioSystems. 2015;11(1):13-9.
92. Westerhuis JA, Hoefsloot HCJ, Smit S, Vis DJ, Smilde AK, van Velzen EJJ et al. Assessment of PLSDA cross validation. Metabolomics. 2008;4(1):81-9.
93. Lindgren F, Hansen B, Karcher W, Sjöström M, Eriksson L. Model validation by permutation tests: Applications to variable selection. J Chemometr. 1996;10(5‐6):521-32.
94. Ke C, Li A, Hou Y, Sun M, Yang K, Cheng J et al. Metabolic phenotyping for monitoring ovarian cancer patients. Scientific reports. 2016;6.
95. Hanley JA, McNeil BJ. The meaning and use of the area under a receiver operating characteristic (ROC) curve. Radiology. 1982;143(1):29-36.
96. Kanehisa M, Araki M, Goto S, Hattori M, Hirakawa M, Itoh M et al. KEGG for linking genomes to life and the environment. Nucleic Acids Res. 2008;36(suppl 1):D480-D4.
97. Kanehisa M, Goto S, Hattori M, Aoki-Kinoshita KF, Itoh M, Kawashima S et al. From genomics to chemical genomics: new developments in KEGG. Nucleic Acids Res. 2006;34(suppl 1):D354-D7.
98. Wishart DS, Tzur D, Knox C, Eisner R, Guo AC, Young N et al. HMDB: the human metabolome database. Nucleic Acids Res. 2007;35(suppl 1):D521-D6.
99. Xia J, Sinelnikov IV, Han B, Wishart DS. MetaboAnalyst 3.0—making metabolomics more meaningful. Nucleic Acids Res. 2015;43(W1):W251-W7.
100. Karp PD, Ouzounis CA, Moore-Kochlacs C, Goldovsky L, Kaipa P, Ahrén D et al. Expansion of the BioCyc collection of pathway/genome databases to 160 genomes. Nucleic Acids Res. 2005;33(19):6083-9.
101. Puchades-Carrasco L, Palomino-Schatzlein M, Perez-Rambla C, Pineda-Lucena A. Bioinformatics tools for the analysis of NMR metabolomics studies focused on the identification of clinically relevant biomarkers. Briefings in bioinformatics. 2016;17(3):541-52.
102. Pan Z, Raftery D. Comparing and combining NMR spectroscopy and mass spectrometry in metabolomics. Analytical and bioanalytical chemistry. 2007;387(2):525-7.
103. Foxall PJ, Spraul M, Farrant RD, Lindon LC, Neild GH, Nicholson JK. 750 MHz 1H-NMR spectroscopy of human blood plasma. J Pharm Biomed Anal. 1993;11(4-5):267-76.
104. Schauer N, Steinhauser D, Strelkov S, Schomburg D, Allison G, Moritz T et al. GC-MS libraries for the rapid identification of metabolites in complex biological samples. Febs Lett. 2005;579(6):1332-7.
105. Theodoridis G, Gika HG, Wilson ID. LC-MS-based methodology for global metabolite profiling in metabonomics/metabolomics. TrAC Trends in Analytical Chemistry. 2008;27(3):251-60.
106. Crockford DJ, Holmes E, Lindon JC, Plumb RS, Zirah S, Bruce SJ et al. Statistical heterospectroscopy, an approach to the integrated analysis of NMR and UPLC-MS data sets: application in metabonomic toxicology studies. Anal Chem. 2006;78(2):363-71.
107. Crockford DJ, Maher AD, Ahmadi KR, Barrett A, Plumb RS, Wilson ID et al. 1H NMR and UPLC-MSE statistical heterospectroscopy: characterization of drug metabolites (xenometabolome) in epidemiological studies. Anal Chem. 2008;80(18):6835-44.

108. Wu H, Southam AD, Hines A, Viant MR. High-throughput tissue extraction protocol for NMR- and MS-based metabolomics. Anal Biochem. 2008;372(2):204-12.
109. Bingol K, Bruschweiler-Li L, Yu C, Somogyi A, Zhang F, Brüschweiler R. Metabolomics beyond spectroscopic databases: a combined MS/NMR strategy for the rapid identification of new metabolites in complex mixtures. Anal Chem. 2015;87(7):3864-70.
110. Bone RC, Balk RA, Cerra FB, Dellinger RP, Fein AM, Knaus WA et al. Definitions for sepsis and organ failure and guidelines for the use of innovative therapies in sepsis. Chest. 1992;101(6):1644-55.
111. Dellinger RP, Levy MM, Rhodes A, Annane D, Gerlach H, Opal SM et al. Surviving Sepsis Campaign: international guidelines for management of severe sepsis and septic shock, 2012. Intens Care Med. 2013;39(2):165-228.
112. Dellinger RL, MM ; Carlet, JM ; Bion, J; Parker, MM ; Jaeschke, R; Reinhart, K ; Angus, DC; Brun-Buisson, C; Beale, R Surviving Sepsis Campaign: International guidelines for management of severe sepsis and septic shock: 2008. CRITICAL CARE MEDICINE. 2008;36: 296-327.
113. Balk RA. Systemic inflammatory response syndrome (SIRS): where did it come from and is it still relevant today? Virulence. 2014;5(1):20-6.
114. Martin-Loeches I, Levy MM, Artigas A. Management of severe sepsis: advances, challenges, and current status. Drug design, development and therapy. 2015;9:2079-88.
115. Singer M, De Santis V, Vitale D, Jeffcoate W. Multiorgan failure is an adaptive, endocrine-mediated, metabolic response to overwhelming systemic inflammation. The Lancet. 2004;364(9433):545-8.
116. Angus DC, van der Poll T. Severe sepsis and septic shock. N Engl J Med. 2013;369(9):840-51.
117. Cao Z, Robinson RA. The role of proteomics in understanding biological mechanisms of sepsis. Proteomics Clin Appl. 2014;8(1-2):35-52.
118. Haase N, Wetterslev J, Winkel P, Perner A. Bleeding and risk of death with hydroxyethyl starch in severe sepsis: post hoc analyses of a randomized clinical trial. Intensive care medicine. 2013;39(12):2126-34.
119. Semeraro N, Ammollo CT, Semeraro F, Colucci M. Sepsis, thrombosis and organ dysfunction. Thromb Res. 2012;129(3):290-5.
120. Tsao CM, Ho ST, Wu CC. Coagulation abnormalities in sepsis. Acta anaesthesiologica Taiwanica : official journal of the Taiwan Society of Anesthesiologists. 2015;53(1):16-22.
121. Janigan DT, Morris J, Hirsch D. ACUTE SKIN AND FAT NECROSIS DURING SEPSIS IN A PATIENT WITH CHRONIC-RENAL-FAILURE AND SUBCUTANEOUS ARTERIAL CALCIFICATION. Am J Kidney Dis. 1992;20(6):643-6.
122. Jean-Baptiste E. Cellular mechanisms in sepsis. J Intensive Care Med. 2007;22(2):63-72.
123. Ramachandran G. Gram-positive and gram-negative bacterial toxins in sepsis: a brief review. Virulence. 2014;5(1):213-8.
124. Ferrer R, Martin-Loeches I, Phillips G, Osborn TM, Townsend S, Dellinger RP et al. Empiric antibiotic treatment reduces mortality in severe sepsis and septic shock from the first hour: results from a guideline-based performance improvement program. Critical care medicine. 2014;42(8):1749-55.
125. EMANUEL RIVERS MD, M.P.H., BRYANT NGUYEN, M.D., SUZANNEH,AVSTAD, M.A., J ULIERSSLER, B.S.,A LEXANDRIA MUZZIN, B.S., BERNHARD. EARLY GOAL-DIRECTED THERAPY IN THE TREATMENT OF SEVERE SEPSIS AND SEPTIC SHOCK. The New England Journal of Medicine. 2001;345:1368-77.
126. Shane AL, Stoll BJ. Neonatal sepsis: progress towards improved outcomes. J Infect. 2014;68 Suppl 1:S24-32.
127. Wichterman KA, Baue AE, Chaudry IH. SEPSIS AND SEPTIC SHOCK - A REVIEW OF LABORATORY

MODELS AND A PROPOSAL. J Surg Res. 1980;29(2):189-201.
128. Zhao X, Chen YX, Li CS. Predictive value of the complement system for sepsis-induced disseminated intravascular coagulation in septic patients in emergency department. J Crit Care. 2015;30(2):290-5.
129. Cho SY, Choi JH. Biomarkers of sepsis. Infect Chemother. 2014;46(1):1-12.
130. Henriquez-Camacho C, Losa J. Biomarkers for sepsis. Biomed Res Int. 2014;2014:547818.
131. Sweet MJ, Hume DA. Endotoxin signal transduction in macrophages. J Leukocyte Biol. 1996;60(1):8-26.
132. Yu DH, Nho DH, Song RH, Kim SH, Lee MJ, Nemzek JA et al. High-mobility group box 1 as a surrogate prognostic marker in dogs with systemic inflammatory response syndrome. J Vet Emerg Crit Care (San Antonio). 2010;20(3):298-302.
133. Kitchens RL, Thompson PA. Impact of sepsis-induced changes in plasma on LPS interactions with monocytes and plasma lipoproteins: roles of soluble CD14, LBP, and acute phase lipoproteins. J Endotoxin Res. 2003;9(2):113-8.
134. Frevert CW, Matute-Bello G, Skerrett SJ, Goodman RB, Kajikawa O, Sittipunt C et al. Effect of CD14 Blockade in Rabbits with Escherichia coli Pneumonia and Sepsis. The Journal of Immunology. 2000;164(10):5439-45.
135. Clyne B, Olshaker JS. The C-reactive protein. J Emerg Med. 1999;17(6):1019-25.
136. Louis E, Franchimont D, Piron A, Gevaert Y, Schaaf-Lafontaine N, Roland S et al. Tumour necrosis factor (TNF) gene polymorphism influences TNF-alpha production in lipopolysaccharide (LPS)-stimulated whole blood cell culture in healthy humans. Clin Exp Immunol. 1998;113(3):401-6.
137. Yoshimura T, Matsushima K, Oppenheim JJ, Leonard EJ. NEUTROPHIL CHEMOTACTIC FACTOR PRODUCED BY LIPOPOLYSACCHARIDE (LPS)-STIMULATED HUMAN-BLOOD MONONUCLEAR LEUKOCYTES - PARTIAL CHARACTERIZATION AND SEPARATION FROM INTERLEUKIN-1 (IL-1). J Immunol. 1987;139(3):788-93.
138. Berg DJ, Kuhn R, Rajewsky K, Muller W, Menon S, Davidson N et al. INTERLEUKIN-10 IS A CENTRAL REGULATOR OF THE RESPONSE TO LPS IN MURINE MODELS OF ENDOTOXIC-SHOCK AND THE SHWARTZMAN REACTION BUT NOT ENDOTOXIN TOLERANCE. J Clin Invest. 1995;96(5):2339-47.
139. Hoerr V, Zbytnuik L, Leger C, Tam PP, Kubes P, Vogel HJ. Gram-negative and Gram-positive bacterial infections give rise to a different metabolic response in a mouse model. Journal of proteome research. 2012;11(6):3231-45.
140. Su L, Huang Y, Zhu Y, Xia L, Wang R, Xiao K et al. Discrimination of sepsis stage metabolic profiles with an LC/MS-MS-based metabolomics approach. BMJ open respiratory research. 2014;1(1):e000056.
141. Izquierdo-Garcia JL, Nin N, Ruiz-Cabello J, Rojas Y, de Paula M, Lopez-Cuenca S et al. A metabolomic approach for diagnosis of experimental sepsis. Intensive Care Med. 2011;37(12):2023-32.
142. Mickiewicz B, Vogel HJ, Wong HR, Winston BW. Metabolomics as a novel approach for early diagnosis of pediatric septic shock and its mortality. Am J Respir Crit Care Med. 2013;187(9):967-76.
143. Fanos V, Caboni P, Corsello G, Stronati M, Gazzolo D, Noto A et al. Urinary 1 H-NMR and GC-MS metabolomics predicts early and late onset neonatal sepsis. Early human development. 2014;90:S78-S83.
144. Schmerler D, Neugebauer S, Ludewig K, Bremer-Streck S, Brunkhorst FM, Kiehntopf M. Targeted metabolomics for discrimination of systemic inflammatory disorders in critically ill patients. Journal of lipid research. 2012:jlr. P023309.
145. Hubbard WJ, Choudhry M, Schwacha MG, Kerby JD, Rue III LW, Bland KI et al. Cecal ligation and puncture. Shock. 2005;24:52-7.

146. Lin ZY, Xu PB, Yan SK, Meng HB, Yang GJ, Dai WX et al. A metabonomic approach to early prognostic evaluation of experimental sepsis by (1)H NMR and pattern recognition. Nmr Biomed. 2009;22(6):601-8.
147. Xu PB, Lin ZY, Meng HB, Yan SK, Yang Y, Liu XR et al. A metabonomic approach to early prognostic evaluation of experimental sepsis. J Infect. 2008;56(6):474-81.
148. Garcia-Simon M, Morales JM, Modesto-Alapont V, Gonzalez-Marrachelli V, Vento-Rehues R, Jorda-Miñana A et al. Prognosis Biomarkers of Severe Sepsis and Septic Shock by 1 H NMR Urine Metabolomics in the Intensive Care Unit. PloS one. 2015;10(11):e0140993.
149. Mickiewicz B, Tam P, Jenne CN, Leger C, Wong J, Winston BW et al. Integration of metabolic and inflammatory mediator profiles as a potential prognostic approach for septic shock in the intensive care unit. Crit Care. 2015;19:11.
150. Langley RJ, Tsalik EL, van Velkinburgh JC, Glickman SW, Rice BJ, Wang C et al. An integrated clinico-metabolomic model improves prediction of death in sepsis. Science translational medicine. 2013;5(195):195ra95.
151. Wasmuth HE, Kunz D, Yagmur E, Timmer-Stranghoner A, Vidacek D, Siewert E et al. Patients with acute on chronic liver failure display "sepsis-like" immune paralysis. J Hepatol. 2005;42(2):195-201.
152. Abraham E, Singer M. Mechanisms of sepsis-induced organ dysfunction. Critical care medicine. 2007;35(10):2408-16.
153. Schrier RW, Wang W. Acute renal failure and sepsis. New Engl J Med. 2004;351(2):159-69.
154. Vincent M. Consensus conference definitions for sepsis, septic shock, acute lung injury, and acute respiratory distress syndrome: time for a reevaluation. Critical care medicine. 2000;28(1):232-5.
155. Hasper D, Hummel M, Kleber F, Reindl I, Volk H-D. Systemic inflammation in patients with heart failure. Eur Heart J. 1998;19(5):761-5.
156. Marquardt DJ, Knatz NL, Wetterau LA, Wewers MD, Hall MW. Failure to recover somatotropic axis function is associated with mortality from pediatric sepsis-induced multiple organ dysfunction syndrome. Pediatric critical care medicine : a journal of the Society of Critical Care Medicine and the World Federation of Pediatric Intensive and Critical Care Societies. 2010;11(1):18-25.
157. Kathleen A. Stringer NJS, 2,3,4* Alla Karnovsky,5 Kenneth Guire,6 Robert Paine III and Theodore J. Standiford. Metabolic consequences of sepsis-induced acute lung injury revealed by plasma 1H-nuclear magnetic resonance quantitative metabolomics and computational analysis. AJP-Lung Cell Mol Physiol. 2011;300:L4-L11.
158. Recknagel P, Gonnert FA, Westermann M, Lambeck S, Lupp A, Rudiger A et al. Liver dysfunction and phosphatidylinositol-3-kinase signalling in early sepsis: experimental studies in rodent models of peritonitis. PLoS medicine. 2012;9(11):e1001338.
159. Liu Y, Yan S, Ji C, Dai W, Hu W, Zhang W et al. Metabolomic changes and protective effect of (L)-carnitine in rat kidney ischemia/reperfusion injury. Kidney Blood Press Res. 2012;35(5):373-81.
160. Hinkelbein J, Kalenka A, Schubert C, Peterka A, Feldmann J, Robert E. Proteome and metabolome alterations in heart and liver indicate compromised energy production during sepsis. Protein Peptide Lett. 2010;17(1):18-31.
161. Stringer KA, Younger JG, McHugh C, Yeomans L, Finkel MA, Puskarich MA et al. Whole Blood Reveals More Metabolic Detail of the Human Metabolome Than Serum as Measured by 1H-NMR Spectroscopy: Implications for Sepsis Metabolomics. Shock. 2015.
162. Cao Z, Yende S, Kellum JA, Angus DC, Robinson RA. Proteomics reveals age-related differences in the host immune response to sepsis. Journal of proteome research. 2014;13(2):422-32.

163. Wu W, Zhao S. Metabolic changes in cancer: beyond the Warburg effect. Acta Bioch Bioph Sin. 2013;45(1):18-26.
164. Leithead JA, Hayes PC, Ferguson JW. Review article: advances in the management of patients with cirrhosis and portal hypertension-related renal dysfunction. Aliment Pharmacol Ther. 2014;39(7):699-711.
165. Sauneuf B, Champigneulle B, Soummer A, Mongardon N, Charpentier J, Cariou A et al. Increased survival of cirrhotic patients with septic shock. Crit Care. 2013;17(2):10.
166. Go AS, Chertow GM, Fan D, McCulloch CE, Hsu C-y. Chronic kidney disease and the risks of death, cardiovascular events, and hospitalization. New Engl J Med. 2004;351(13):1296-305.
167. Zhang A, Sun H, Wang X. Serum metabolomics as a novel diagnostic approach for disease: a systematic review. Analytical and bioanalytical chemistry. 2012;404(4):1239-45.
168. Llovet JM, Burroughs A, Bruix J. Hepatocellular carcinoma. The Lancet. 2003;362(9399):1907-17.
169. O'Connor S, Ward J, Watson M, Momin B, Richardson L. Hepatocellular carcinoma-United States, 2001-2006. Morbidity and Mortality Weekly Report. 2010;59(17):517-20.
170. El-Serag HB. Epidemiology of viral hepatitis and hepatocellular carcinoma. Gastroenterology. 2012;142(6):1264-73 e1.
171. Donato F, Tagger A, Gelatti U, Parrinello G, Boffetta P, Albertini A et al. Alcohol and hepatocellular carcinoma: the effect of lifetime intake and hepatitis virus infections in men and women. American journal of epidemiology. 2002;155(4):323-31.
172. Kew MC. Aflatoxins as a cause of hepatocellular carcinoma. J Gastrointestin Liver Dis. 2013;22(3):305-10.
173. Page JM, Harrison SA. Nash and HCC. Clinics in liver disease. 2009;13(4):631-47.
174. Younossi ZM, Otgonsuren M, Henry L, Venkatesan C, Mishra A, Erario M et al. Association of nonalcoholic fatty liver disease (NAFLD) with hepatocellular carcinoma (HCC) in the United States from 2004 to 2009. Hepatology. 2015;62(6):1723-30.
175. Bialecki ES, Di Bisceglie AM. Diagnosis of hepatocellular carcinoma. HPB : the official journal of the International Hepato Pancreato Biliary Association. 2005;7(1):26-34.
176. Pons F, Varela M, Llovet JM. Staging systems in hepatocellular carcinoma. HPB : the official journal of the International Hepato Pancreato Biliary Association. 2005;7(1):35-41.
177. Wiesner RH, Freeman RB, Mulligan DC. Liver transplantation for hepatocellular cancer: the impact of the MELD allocation policy. Gastroenterology. 2004;127(5):S261-S7.
178. Hu R-H, Lee P-H, Yu S-C, Dai H-C, Sheu J-C, Lai M-Y et al. Surgical resection for recurrent hepatocellular carcinoma: prognosis and analysis of risk factors. Surgery. 1996;120(1):23-9.
179. Lin S, Lin C, Lin C, Hsu C, Chen Y. Randomised controlled trial comparing percutaneous radiofrequency thermal ablation, percutaneous ethanol injection, and percutaneous acetic acid injection to treat hepatocellular carcinoma of 3 cm or less. Gut. 2005;54(8):1151-6.
180. Livraghi T, Solbiati L, Meloni MF, Gazelle GS, Halpern EF, Goldberg SN. Treatment of focal liver tumors with percutaneous radio-frequency ablation: Complications encountered in a multicenter study 1. Radiology. 2003;226(2):441-51.
181. Livraghi T, Goldberg SN, Lazzaroni S, Meloni F, Solbiati L, Gazelle GS. Small hepatocellular carcinoma: treatment with radio-frequency ablation versus ethanol injection. Radiology. 1999;210(3):655-61.
182. Johnstone RW, Ruefli AA, Lowe SW. Apoptosis: a link between cancer genetics and chemotherapy. Cell. 2002;108(2):153-64.
183. Altekruse SF, McGlynn KA, Reichman ME. Hepatocellular Carcinoma Incidence, Mortality, and

Survival Trends in the United States From 1975 to 2005. J Clin Oncol. 2009;27(9):1485-91.
184. Forner A, Vilana R, Ayuso C, Bianchi L, Solé M, Ayuso JR et al. Diagnosis of hepatic nodules 20 mm or smaller in cirrhosis: prospective validation of the noninvasive diagnostic criteria for hepatocellular carcinoma. Hepatology. 2008;47(1):97-104.
185. Tan Y, Yin P, Tang L, Xing W, Huang Q, Cao D et al. Metabolomics study of stepwise hepatocarcinogenesis from the model rats to patients: potential biomarkers effective for small hepatocellular carcinoma diagnosis. Molecular & cellular proteomics : MCP. 2012;11(2):M111 010694.
186. Liu Y, Hong Z, Tan G, Dong X, Yang G, Zhao L et al. NMR and LC/MS-based global metabolomics to identify serum biomarkers differentiating hepatocellular carcinoma from liver cirrhosis. Int J Cancer. 2014;135(3):658-68.
187. Fages A, Duarte-Salles T, Stepien M, Ferrari P, Fedirko V, Pontoizeau C et al. Metabolomic profiles of hepatocellular carcinoma in a European prospective cohort. BMC medicine. 2015;13:242.
188. Zhou L, Wang Q, Yin P, Xing W, Wu Z, Chen S et al. Serum metabolomics reveals the deregulation of fatty acids metabolism in hepatocellular carcinoma and chronic liver diseases. Analytical and bioanalytical chemistry. 2012;403(1):203-13.
189. Nahon P, Amathieu R, Triba MN, Bouchemal N, Nault JC, Ziol M et al. Identification of serum proton NMR metabolomic fingerprints associated with hepatocellular carcinoma in patients with alcoholic cirrhosis. Clin Cancer Res. 2012;18(24):6714-22.
190. Chen T, Xie G, Wang X, Fan J, Qiu Y, Zheng X et al. Serum and Urine Metabolite Profiling Reveals Potential Biomarkers of Human Hepatocellular Carcinoma. Molecular & Cellular Proteomics. 2011;10(7).
191. Huang Q, Tan Y, Yin P, Ye G, Gao P, Lu X et al. Metabolic characterization of hepatocellular carcinoma using nontargeted tissue metabolomics. Cancer Res. 2013;73(16):4992-5002.
192. Ye G, Zhu B, Yao Z, Yin P, Lu X, Kong H et al. Analysis of urinary metabolic signatures of early hepatocellular carcinoma recurrence after surgical removal using gas chromatography-mass spectrometry. Journal of proteome research. 2012;11(8):4361-72.
193. Zhou L, Liao Y, Yin P, Zeng Z, Li J, Lu X et al. Metabolic profiling study of early and late recurrence of hepatocellular carcinoma based on liquid chromatography-mass spectrometry. J Chromatogr B Analyt Technol Biomed Life Sci. 2014;966:163-70.
194. Wang J, Zhang S, Li Z, Yang J, Huang C, Liang R et al. (1)H-NMR-based metabolomics of tumor tissue for the metabolic characterization of rat hepatocellular carcinoma formation and metastasis. Tumour biology : the journal of the International Society for Oncodevelopmental Biology and Medicine. 2011;32(1):223-31.
195. Takano S, Yokosuka O, Imazeki F, Tagawa M, Omata M. INCIDENCE OF HEPATOCELLULAR-CARCINOMA IN CHRONIC HEPATITIS-B AND HEPATITIS-C - A PROSPECTIVE-STUDY OF 251 PATIENTS. Hepatology. 1995;21(3):650-5.
196. Perz JF, Armstrong GL, Farrington LA, Hutin YJ, Bell BP. The contributions of hepatitis B virus and hepatitis C virus infections to cirrhosis and primary liver cancer worldwide. J Hepatol. 2006;45(4):529-38.
197. Morgan TR, Mandayam S, Jamal MM. Alcohol and hepatocellular carcinoma. Gastroenterology. 2004;127(5):S87-S96.
198. Caldwell SH, Crespo DM, Kang HS, Al-Osaimi AMS. Obesity and hepatocellular carcinoma. Gastroenterology. 2004;127(5):S97-S103.
199. Goossens C, Nahon P, Le Moyec L, Triba MN, Bouchemal N, Amathieu R et al. Sequential Serum Metabolomic Profiling after Radiofrequency Ablation of Hepatocellular Carcinoma Reveals Different

Response Patterns According to Etiology. Journal of proteome research. 2016;15(5):1446-54.
200. Gao R, Cheng J, Fan C, Shi X, Cao Y, Sun B et al. Serum Metabolomics to Identify the Liver Disease-Specific Biomarkers for the Progression of Hepatitis to Hepatocellular Carcinoma. Sci Rep. 2015;5:18175.
201. Lu Y, Huang C, Gao L, Xu Y-J, Chia SE, Chen S et al. Identification of serum biomarkers associated with hepatitis B virus-related hepatocellular carcinoma and liver cirrhosis using mass-spectrometry-based metabolomics. Metabolomics. 2015;11(6):1526-38.
202. Fitian AI, Nelson DR, Liu C, Xu Y, Ararat M, Cabrera R. Integrated metabolomic profiling of hepatocellular carcinoma in hepatitis C cirrhosis through GC/MS and UPLC/MS-MS. Liver international : official journal of the International Association for the Study of the Liver. 2014;34(9):1428-44.
203. Li S, Liu H, Jin Y, Lin S, Cai Z, Jiang Y. Metabolomics study of alcohol-induced liver injury and hepatocellular carcinoma xenografts in mice. J Chromatogr B. 2011;879(24):2369-75.
204. Clarke JD, Novak P, Lake AD, Shipkova P, Aranibar N, Robertson D et al. Characterization of hepatocellular carcinoma related genes and metabolites in human nonalcoholic fatty liver disease. Dig Dis Sci. 2014;59(2):365-74.
205. Safaei A, Oskouie AA, Mohebbi SR, Rezaei-Tavirani M, Mahboubi M, Peyvandi M et al. Metabolomic analysis of human cirrhosis, hepatocellular carcinoma, non-alcoholic fatty liver disease and non-alcoholic steatohepatitis diseases. Gastroenterology and Hepatology from bed to bench. 2016;9(3):158.
206. Ryder SD. Guidelines for the diagnosis and treatment of hepatocellular carcinoma (HCC) in adults. Gut. 2003;52(suppl 3):iii1-iii8.
207. Ikeda K, Saitoh S, Tsubota A, Arase Y, Chayama K, Kumada H et al. Risk factors for tumor recurrence and prognosis after curative resection of hepatocellular carcinoma. Cancer. 1993;71(1):19-25.
208. Imamura H, Matsuyama Y, Tanaka E, Ohkubo T, Hasegawa K, Miyagawa S et al. Risk factors contributing to early and date phase intrahepatic recurrence of hepatocellular carcinoma after hepatectomy. J Hepatol. 2003;38(2):200-7.
209. Qin LX, Tang ZY. Recent progress in predictive biomarkers for metastatic recurrence of human hepatocellular carcinoma: a review of the literature. J Cancer Res Clin Oncol. 2004;130(9):497-513.

Abstract

A cascade of metabolomic studies have been developed in the recent decade. The application of metabolomics in the clinical field has been shown to be promising since even subtle physiological changes can be revealed by a metabolomic study which determines variations in the metabolome. Personalized clinical care is currently proposed for almost all the diseases, however, it is still difficult to be executed for the scarce of clinical biomarkers. This thesis work concerns the applications of both ^{1}H NMR-based and MS-based metabolomics in the determination of potential serum biomarkers which help to improve personalized diagnosis and prognosis. It is composed by two principal parts. The first part of the work aims to find out metabolite biomarkers predicting the mortality of septic shock before clinical intervention and first 12 hours after hospitalization using NMR-based and LC-MS-based metabolomic methods respectively. The goal of the second part of the work is to seek potential biomarkers predicting the recurrence of HCC before and after RFA treatment. Our findings not only show that both the two applied techniques were useful for the discovery of novel clinical biomarkers, but also show that the two techniques are complementary.

Key words: Metabolomics, ^{1}H NMR spectroscopy, Mass spectrometry, biomarkers, septic shock, Hepatocellular carcinoma.

Résumé

De nombreuses études métabolomiques a été développée au cours de la dernière dizaine année. L'application de la métabolomique dans le traitement clinique s'est révélée prometteuse puisque même des faibles modifications physiologiques peuvent être révélées par une étude métabolomique. Des soins cliniques personnalisés sont actuellement proposés pour presque toutes les maladies, mais il est encore difficile de les réaliser à cause du manque de biomarqueurs cliniques. Ce travail de thèse a pour le but de la détermination de biomarqueurs cliniques par la spectroscopie RMN et par la spectrométrie de masse. Il est composé de deux parties : la première partie du travail vise à déterminer les biomarqueurs des métabolites prédisant la mortalité du choc septique avant l'intervention clinique et les 12 premières heures après l'hospitalisation en utilisant respectivement des méthodes métaboliques basées sur la RMN et la LC-MS. L'objectif de la deuxième partie du travail est de rechercher des biomarqueurs potentiels prédisant la récidive du CHC avant et après le traitement RFA. Nos résultats montrent non seulement que les deux techniques appliquées ont été utiles pour la découverte de nouveaux biomarqueurs cliniques, mais montrent également que les deux techniques sont complémentaires.

Mots clés : Métabolomique, ^{1}H résonance magnétique nucléaire, spectrométrie de masse, biomarqueur, choc septique, carcinome hépatocellulaire